UNIVERSITÀ DEGLI STUDI DI MILANO

SCUOLA DI DOTTORATO IN SCIENZE BIOLOGICHE E MOLECOLARI

DIPARTIMENTO DI BIOLOGIA

DOTTORATO DI RICERCA IN BIOLOGIA CELLULARE E MOLECOLARE

XXIV CICLO

ccdc80 and *ccdc80-l1*: Identification and Functional Analysis of Two Novel Genes Involved in Zebrafish (*Danio rerio*) Development

settori scientifico/disciplinari: BIO/06; BIO/11

Tesi di dottorato di
Chiara Brusegan
R08215

TUTOR: prof. Franco Cotelli

COORDINATORE DEL DOTTORATO: prof. Martino Bolognesi

A.A.
2010/2011

Index

Part I

Part I

Abstract

1. Abstract

The *ccdc80* and *ccdc80-like1* (*ccdc80-l1*) genes were isolated in zebrafish *in silico,* on the basis of their high aminoacidic sequence identity with the human CCDC80 protein (coiled-coil domain containing 80). In human, *CCDC80* is involved in several carcinomas, and during recent years it has been proposed as an onco-suppressor gene, increasing the interest in the comprehension of its functions. During my Ph.D., I have been studying the expression patterns and the functions of its zebrafish homologs, in order to gain insights into the processes and the molecular mechanisms in which they are involved. I took advantage of zebrafish as a model system allowing the application of common genetic and biological experimental assays such as PCR, whole mount *in situ* hybridization and microinjection technique. I investigated *ccdc80* and *ccdc80-l1* functions during zebrafish embryonic development, finding that they show very different expression patterns and roles. *ccdc80* is expressed in the notochord during somitogenesis up to 48 hour post fertilization (hpf). At this stage, it is expressed also in the heart. Instead, at the same developmental stages, *ccdc80-l1* is expressed in cranial ganglia, adaxial cells, muscle pioneers and dorsal dermis. These patterns are suggestive of different roles, in fact, the genes are involved in distinct developmental processes, such as somitogenesis and axonal pathfinding, respectively. Functional analysis were obtained performing loss- and gain-of-function experiments. The results clearly demonstrated that manipulation of Ccdc80 protein levels during embryonic development, both increasing and decreasing them, leads to a severe impairment of somites, metameric structures from which several tissues derive, such as muscle. Nevertheless, this phenotype seemed to be recovered at 24 hpf, since at this stage somites no longer showed the same morphological alterations observed previously. By converse, notwithstanding its expression in muscular tissues, loss-of-*ccdc80-l1* does not impair somites formation, leading instead to motoneurons axonal migrations defects, capable to affect embryonic motility. Given the external development of the zebrafish embryo, motility is required very soon for prey and escaping predators, and muscle and motoneurons are equally required for a proper motor behavior. Communication and interactions between these two tissues are fundamental for proper muscles innervation and transmission of nervous inputs to be translated in muscular contractions. *ccdc80* and *ccdc80-l1* may derive from an ancestor gene involved in these processes and, during evolution, may have developed different functions, but still bound to a key process for embryonic viability in the external environment.

State of the art

2.1 Motility of the zebrafish embryo

Motility is a key determinant of evolutionary success and vertebrates survival, for instance allowing animals to prey and escape predators. In zebrafish, the fertilization of the eggs is external, and adult zebrafish does not display any parental care. Thus, embryos are released in the environment right after the fertilization, having just a thin protective membrane (chorion) and a yolk to be nourished on for a few days. Hence, zebrafish embryos need to develop early motor activity. In fact, they exhibit three distinct motor behaviors during embryogenesis: spontaneous coiling, touch-evoked escape contractions and swimming (Hirata *et al*., 2009). Spontaneous coiling appears after 17 hours post fertilization (hpf) and consists of side-to-side alternating contractions of the axial muscles in the trunk and tail (Downes and Granato, 2006; Pietri *et al*., 2009; Saint-Amant and Drapeau, 1998). After 21 hpf, zebrafish embryos respond to touch with escape contractions that typically consists of two to three rapid, alternating contractions of the tail, to turn the embryo away from the stimulus (Saint-Amant and Drapeau, 1998). By 28 hpf, tactile stimulation initiates swimming (Fig. 2.1) (Saint-Amant and Drapeau, 1998).

Motility requires the coordination of both muscle and nervous system. Mutants for the former or the latter anatomical structure show similar phenotype (Granato *et al*., 1996; Haffter *et al*., 1996), resulting in abnormal motor behavior. Typically, motor defects can be easily observed after tactile stimulation, and consist of absence of contractions or a characteristic circular swimming, rather than a fast escape in the opposite direction of the stimulus (Granato et al., 1996; Haffter *et al*., 1996).

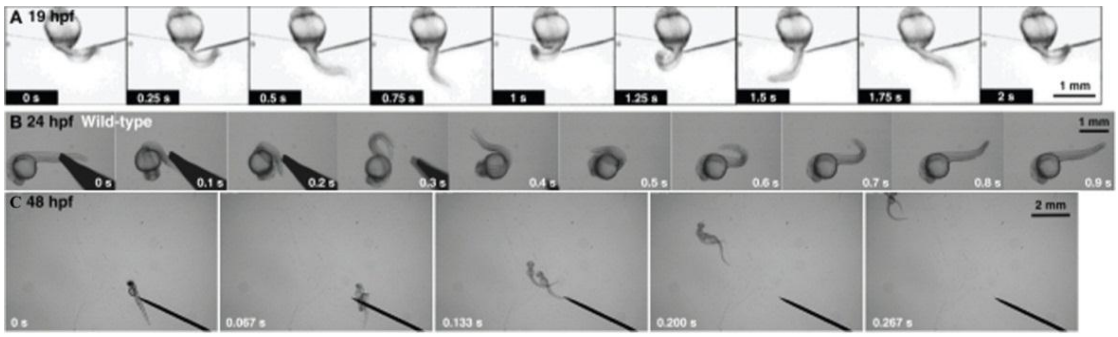

Figure 2.1: Zebrafish embryos display three early behaviors. *(A)* A 19 hpf embryos exhibits spontaneous coiling. *(B)* At 24 hpf, embryos responds to mechanosensory stimulation with fast and alternating contractions. *(C)* At 48 hpf, embryos swim away following tactile stimulation (modified from Hirata *et al*., 2010).

2.2 Muscle formation

Muscles arise prior to nervous system, and, in all vertebrates, develop from somites. The somites are mesodermal segments that form in bilateral pairs flanking the notochord, that is an embryonic midline structure common to all members of the phylum Chordata (Stemple, 2005). Somitogenesis occurs between 10.5 hpf and 24 hpf (Stickney *et al*., 2000), and somites are created sequentially in an anterior to posterior sequence concomitant with the posterior growth of the trunk and tail (Fig. 2.2.A) (Holley, 2007). Cells in the presomitic mesoderm (PSM) alter their adhesive properties and undergo mesenchymal to epithelial transitions, forming epithelia around loosely organized mesenchymal cells. Additional somites are produced in a similar fashion at 20-30 min intervals until a total of about 30 somite (Stickney *et al*., 2000). A molecular clock has been proposed to account for the precise regulation of this reiterative process. The clock causes cells in the PSM to undergo cyclical activation and repression of several Notch pathway genes, such as *her* genes, a family of transcriptional repressors (Fig. 2.2.B and Fig.2.3.A) (Echeverri and Oates, 2007; Oates *et al*., 2005). Each cell in the PSM periodically makes and degrades the products of these genes, in a synchronous manner with its neighbors. There is a translational delay while *her* mRNAs are converted into protein products, which form homo- or heterodimers and then inhibit their own transcription in a negative feedback loop. Her proteins are predicted to have short lifespans, so while protein levels recede, transcription of the her genes resumes and the oscillation starts a new cycle. Positive feedback is provided by the Notch ligand *deltaC*, which oscillates in phase with the *her* genes (Mara and Holley, 2007). The first functional evidence for the role of Notch signaling in zebrafish segmentation came from gain-of-function studies. Ectopic expression of an activated form of Notch, perturbs the normal pattern of *her1* expression, segment polarity, and morphological somite formation (Takke and Campos-Ortega, 1999). Soon after segmentation, the creation of morphologically distinct somites occurs via the generation of a boundary between anterior and posterior somite halves. Not surprisingly, mutations that affect clock function also perturb segment polarity, with markers of anterior and posterior- half somites generally expressed in a disorganized manner throughout the somitic mesoderm (Durbin *et al*., 2000; van Eeden *et al*., 1996). Two bHLH (basic-helix-loop-helix) transcription factors in the zebrafish Mesp family, Mesp-a and Mesp-b, are required for the specification of anterior and posterior identity within each segment. *mesp-b* is expressed in the anterior halves of the three most anterior presumptive somites and seems to confer anterior identity (Sawada *et al*., 2000). The expression pattern of *mesp-a* does not persist as long as *mesp-b*, so only two bands of expression are observed, and the more posterior *mesp-a*-expressing band occupies the entire somite primordium rather than just the

anterior half (Fig. 2.3.B-C) (Durbin *et al*., 2000; Sawada *et al*., 2000). Ectopic expression of *mesp-a* causes a defect in gastrulation precluding an analysis of its effect on segmentation. Ectopic expression of *mesp-b* blocks somite formation, inhibits the expression of *myod*, which is normally expressed in the posterior of each somite (Fig. 2.3.D), and expands the expression of several markers which are normally expressed in the anterior half of each somite (Sawada *et al*., 2000).

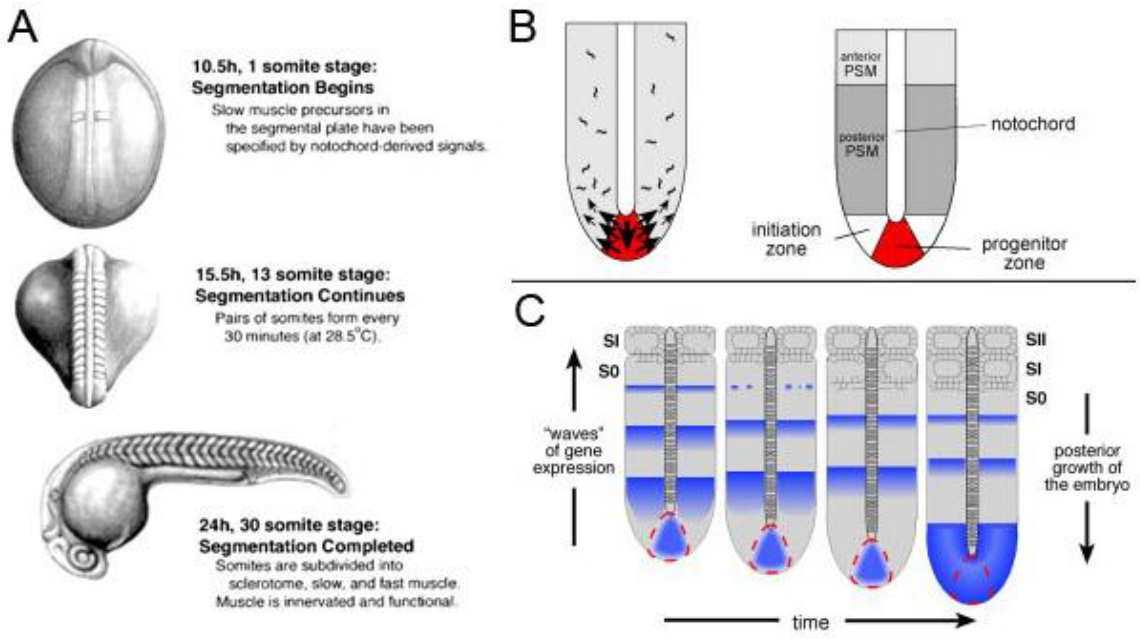

Figure 2.2: Overview of zebrafish somitogenesis. *(A)* These drawings show the stages of embryogenesis during which segmentation and patterning of the paraxial mesoderm takes place. Significant events in each stage are indicated. *(B)* Dorsal views of the tail bud. The progenitors of the posterior somites exit the progenitor zone laterally (small arrows) to enter the initiation zone as the tail extends posteriorly (large arrow). Cells attenuate their movement and are relatively sessile in the PSM. The PSM is bilaterally symmetric and flanks the notochord and neural tube (not shown). *(C)* A time series representing a single somite cycle, in which the posterior displacement of the progenitor zone (red) occurs as the tail extends. Oscillating gene expression (blue) sweeps from posterior to anterior. These oscillations cease in the anterior PSM, and expression of the gene disappears as morphological somite formation occurs. Note that the most-recently formed somite is called the SI while the region in the anterior PSM that will give rise to the next somite is the S0. As the S0 becomes the SI, the old SI becomes the SII (modified from Holley, 2007 and Stickney *et al*., 2000).

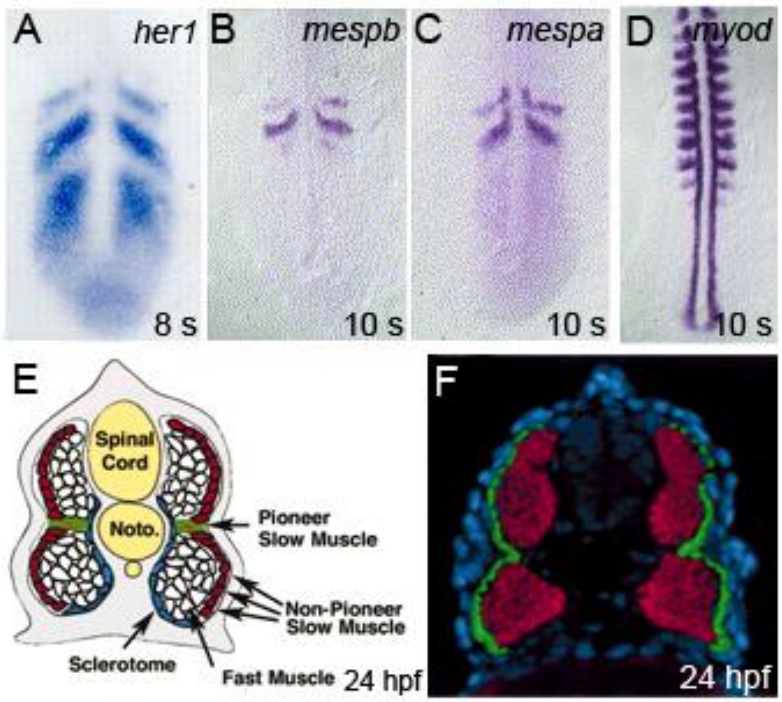

Figure 2.3: Somitogenesis markers and somite organization at the end of segmentation. *(A-D)* Dorsal view of the tail; expression patterns of *her1*, *mespb*, *mespa* and *myod*, respectively. *(E)* Schematic cross-section through a 24 hpf zebrafish embryo, showing the positions of the four characterized cell types: pioneer slow muscle, non-pioneer slow muscle, fast muscle and sclerotome. *(F)* Cross-sections of zebrafish embryos at 24 hpf. Slow muscle cells (green) form a superficial monolayer whereas fast muscle cells (red) remain deep (modified from Oates *et al*., 2005; Stickney *et al*., 2000 and Zhang *et al*., 2008).

As somite polarity is established, morphological segmentation occurs. Somite maturation implies the differentiation between myotome and sclerotome that give rise to skeletal muscle of the trunk and axial skeleton, respectively. Fish somite is predominantly myotome, and the sclerotome is a relatively minor component resulting in a cluster of cells on the ventromedial surface of the somite (Fig. 2.3.E) (Stickney et al., 2000). During somitogenesis, slow muscle precursors are specified in the segmental plate immediately adjacent to the notochord (Devoto *et al*., 1996). These cells, which were named adaxial cells by virtue of their position, demonstrate a myogenic identity very early, as indicated by their expression of *myod* and *myog* (*myogenin*). Conversely, The more lateral paraxial mesoderm does not express detectable levels of *myod* and *myog* transcripts until the time of somite formation (Fig. 2.3.D) (Devoto *et al*., 1996). Adaxial cells migrate toward the external somite and, reaching the surface, differentiate into mononucleated slow twitch muscle fibres, each of which spans the somite, forming a superficial monolayer of around 20 fibres (Fig. 2.3.F) (Ingham and Kim, 2005). Conversely , fast muscle fibers are found in the deep portion of the myotome (Fig. 2.3.E-F) (Devoto *et al*., 1996). Slow fibers have low-force, long-duration contractions because they express myosin isoforms that are specialized for slow contraction and an oxidative

metabolism. Fast fibers have distinct fast myosins and glycolytic metabolism, ideal for high-force, short-duration contractions (Blagden *et al*., 1997). Another population of slow muscle fibers, that do not migrate, remains located at the level of the myoseptum, corresponding to a subset of two to six cells for each somite, which are named muscle pioneers (MP) (Fig. 2.3.E-F) (Felsenfeld *et al*., 1991; Wolff *et al*., 2003). MP are distinguished also by their morphology and their high levels of Engrailed expression (Hatta *et al*., 1991).

It has been demonstrated that adaxial cells and muscle pioneers fate is finely regulated by a molecule secreted by the nothocord: Sonic hedgehog (*shh*), a vertebrate homologue of the *Drosophila* segment polarity protein Hedgehog (Hh). In particular, the differentiation of these cell populations depends upon the levels and range of *shh* signaling within the myotome (Wolff *et al*., 2003). Indeed, the notochord patterns surrounding tissues in vertebrates through the secretion of this molecule, that is thus required for both muscle and motoneurons induction (Blagden *et al*., 1997; Lewis *et al*., 1999; Lewis and Eisen, 2001). The first evidences of *shh* inducing slow muscle fates came from the observation of the expansion of the MP population at the expense of other muscle fibres after microinjection of Hh encoding mRNAs. Moreover, most of the remaining muscle cells exhibit characteristics of the slow twitch lineage (reviewed by Ingham and Kim, 2005). Further support for this hypothesis came from the characterization of three mutants, *floating head* (*flh*), *no tail* (*ntl*), and *bozozok* (*boz*). In addition to the loss of notochord, these mutant embryos have variable deficiencies in early adaxial *myod* expression, muscle pioneers, and horizontal myoseptum. Furthermore, muscle pioneers are rescued in mutant embryos containing transplanted wild-type notochord cells (reviewed by Stickney *et al*., 2000).

2.3 Neural differentiation

At embryonic stages, the nervous system is a complex network of growing axons, whose growth cones navigate in response to guidance cues. Their targets could be neural or non-neuronal tissues, such as skeletal muscle, where they form synaptic contacts (Beattie, 2000). The movements displayed by embryos at early stages are due to early-developing primary motoneurons (PMNs), that innervate the myotome with non-overlapping arbors. In zebrafish, PMNs are present in each somitic hemisegment and are identified by their specific axonal pathway and soma position within the spinal cord: caudal primary motoneurons, middle primary motoneurons and rostral primary motoneurons (CaP, MiP and RoP, respectively) (Eisen, 1999; Liu and Westerfield, 1990; Westerfield *et al*., 1986). As in other vertebrates, zebrafish motoneurons express *islet1* and *islet2* (*isl1* and *isl2*), two members of

the LIM homeodomain (LIM-HD) protein family known to play a role in several aspects of motoneuron development, including initial specification and adoption of a particular subtype identity (Eisen, 1999; Hutchinson and Eisen, 2006; Pfaff and Kintner, 1998; Pfaff *et al*., 1996). *isl1* is expressed in all PMNs around the time they exit the cell cycle. MiPs transiently downregulate and then reinitiate its expression prior to axogenesis. These cells do not express *isl2*. By contrast, prior to axogenesis, CaPs initiate expression of *isl2* and then downregulate expression of *isl1* (Hutchinson and Eisen, 2006). The end result of this dynamic pattern of *islet* genes expression is that by the time of axon extension, MiPs express exclusively *isl1* and CaPs express exclusively *isl2* (Fig. 2.4.A). PMNs extend their axons out of the spinal cord at about 16-17 hpf following a common pathway. Their growth cones project ventrally along the medial surface of the myotome and pause at the horizontal myoseptum, which separates dorsal and ventral myotomes. Here, they specifically interact with muscle pioneers (Fig. 2.4.B) (Eisen, 1991; Melancon *et al*., 1997).

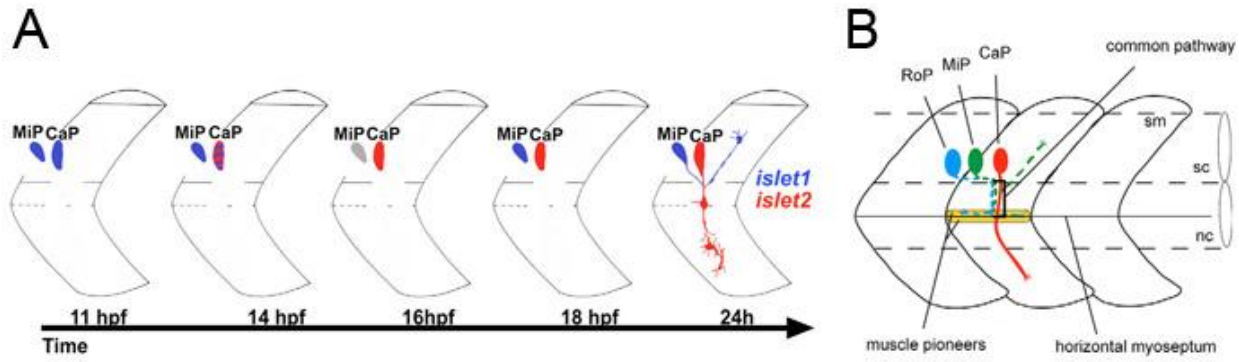

Figure 2.4: Expression pattern of *islet* genes in the developing PMNs. *(A)* Schematic 8-12 segment region of whole-mount embryos with rostral towards the left and dorsal towards the top, showing the dynamic expression of *isl1* (blue) and *isl2* (red) in CaP and MiP between 11 and 24 hpf. Blue and red stripes indicate co-expression of *isl1* and *isl2*; grey indicates downregulation of *isl1*. *(B)* Schematic representation of the different soma positions and axonal projections of CaP, RoP and MiP. CaP axons are projected first to establish the common pathway. The common pathway ends at the muscle pioneers located at the horizontal myoseptum. This point is a choice point where the three axons diverge and follow cell specific pathways to innervate the ventral (CaPs), dorsal (MiPs) and horizontal myoseptal (RoPs) myotomes. Sc: spinal cord; nc: notochord; sm: somite (modified from Hutchinson and Eisen, 2006 and Sato-Maeda *et al*., 2006).

CaPs are responsible for pioneering the common pathway before projecting the axons that innervate the ventral myotome (Sato-Maeda *et al*., 2006). Amongst PMNs, they show the largest and most extensive branching pattern (Westerfield *et al*., 1986). MiPs sprout a collateral axon to innervate dorsal myotome, while the first ventral process extending along

the common pathway is retracted by 48 hpf (Melancon *et al*., 1997). RoPs innervate the middle region of the muscle segment, sprouting laterally after pausing at the myoseptum (Eisen, 1991). Therefore, muscle pioneers represent a choice point from which motoneurons select their specific pathway, though the ablation of this cell population leads to abnormal motor axonal extension without altering the target choice (Melancon *et al*., 1997). Secondary motoneurons (SMNs) growth cones extend later from spinal cord, beginning at 22 hpf and following the paths pioneered by the primary axons (Myers *et al*., 1986; Pike *et al*., 1992). SMNs and PMNs differ also in soma position, morphology and number per hemisegment, since SMNs are more numerous.

Axonal pathfinding is dependent on attractive and repulsive stimuli coming from both nervous and non-nervous surrounding tissues (Beattie, 2000; Tessier-Lavigne and Goodman, 1996). For instance, besides playing a pivotal role in muscle differentiation, the hedgehog pathway is known to pattern also neural development and axonal migration. Both primary and secondary motoneurons specification depends on *shh* induction by notochord and floorplate (Beattie *et al*., 1997). In particular, PMNs number and distribution are alterated in mutants lacking both the notochord and the floorplate (Beattie *et al*., 1997). Further evidences of *shh* involvement in the induction of motoneurons differentiation were provided by blocking *shh* activity *in vitro* with specific antibodies against its biologically active amino-terminal fragment. This treatment led indeed to the loss of *isl1/islt2* motoneurons (Ericson *et al*., 1996). Also muscular tissues can pattern axonal migration: muscular adaxial cells are able to rescue motor axon defects in *diwanka* mutants (Zeller and Granato, 1999), showing that this myotomal population plays a pivotal role in axonal migration. Moreover, the semaphorin proteins Z1b and Sema3A1 are expressed in the somites, and are both involved in repelling axonal guidance in the zebrafish embryo (Fig. 2.5.A-F) (Roos *et al*., 1999; Sato-Maeda *et al*., 2006). Netrin-1a protein is present both in nervous tissue (ventral spinal cord) and in adaxial cells and muscle pioneers, and seems to guide axonal growth through a chemoattractive function (Fig. 2.5.G-I) (Lauderdale *et al*., 1997). The manipulation of the proper expression of these molecules, both knocking-down and inducing ectopic expression, induces axons to follow aberrant pathways, branch excessively or stall. For instance, overexpression of *z1b* leads to severely stunted or missing ventral motor nerves (Fig. 2.5.B-C) (Roos *et al*., 1999), whereas aberrant branching axons are observed after loss-of- *sema3A1*-function (Fig. 2.5.E-F) (Sato-Maeda *et al*., 2006). *netrin1A* expression is disrupted in *flh* mutants, such as it is no longer uniformly expressed but results in islands of expression; in this case, axons tend to extend toward the nearest patch of cells expressing *netrin-1a* (Fig. 2.5.I) (Lauderdale *et al*., 1997).

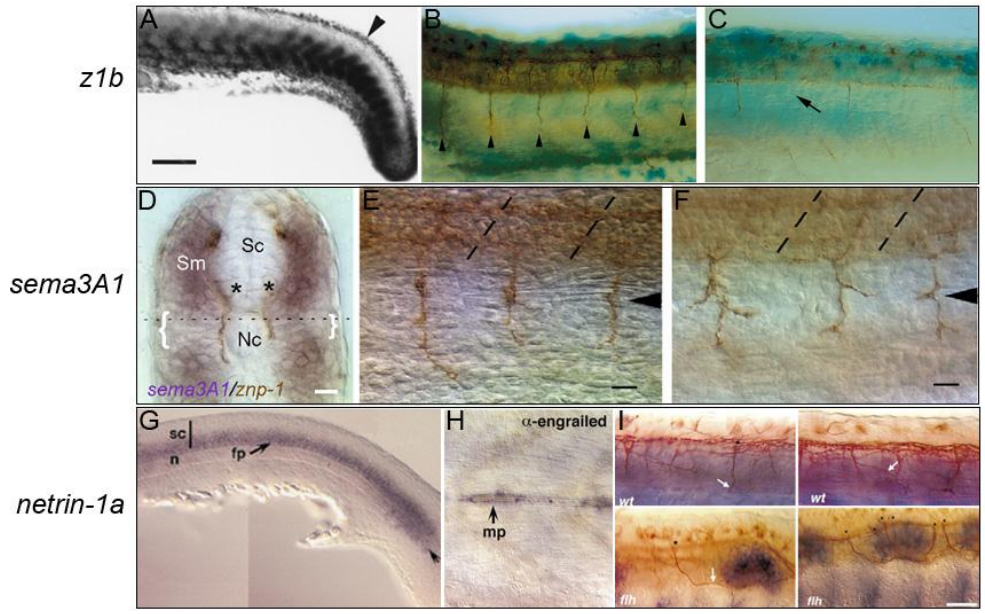

Figure 2.5: *z1b*, *sema3a1* and *netrin-1a* are involved in axonal migration. Unless otherwise noted, embryos are oriented with rostral leftwards and dorsal upwards. *(A-C)* At 24 hpf, *z1b* is expressed in the somites (arrow-head in *A*) and injection of *z1b* mRNA leads to severely stunted or missing ventral motor nerves (arrow in *C*) in comparison to control embryos (arrow-heads in *B*). (D) A transverse section of the trunk of a 24 hpf embryo (dorsal upwards) showing that *sema3a1* is expressed in the dorsal and ventral regions of the myotome and less so in the horizontal myoseptal region (brackets). Asterisks indicate CaPs whose axons extend along the medial surface of the myotome. Sm, somite; Nc, notochord; Sc, spinal cord. *(E-F)* CaP axons often branch aberrantly in an antisense *sema3a1*-MO-injected embryo (24 hpf) (arrow-head in *E*), with respect to control embryos (arrow-head in *F*). *(G-H)* At 18 hpf, *netrin-1a* is expressed in: ventral spinal cord (sc), floor plate (fp), adaxial cells in the tailbud region (arrow in *G*) and in the muscle pioneers (arrow in *H*). *(I)* Axons extend within an apparently uniform field of *netrin-1a* expression (arrows in the upper section *I*). In *floating head* mutants (lower section of *I*), *netrin-1a* expression in the caudal spinal cord is disrupted such that islands of expression are separated by regions of the cord in which it is not expressed; neurons located at the edges of or in between islands of *netrin-1a* expression tend to extend their axons toward the nearest patch of cells expressing *netrin-1a* (arrow) (modified from Roos *et al*., 1999; Sato-Maeda *et al*., 2006 and Lauderdale *et al*., 1997).

2.4 Identification of zebrafish *ccdc80* genes

The *Coiled-Coil-Domain Containing 80* (*Ccdc80*) gene, also named *DRO1* in human (*Down-Regulated by Oncogene 1*), *URB* in mouse (*Up-Regulated in BRS-3 deficient mice*), *CL2* in rat (*Clone 2*), and *equarin* in chicken, has been recently suggested to be involved in different functions amongst vertebrates. *Ccdc80* was first isolated in mice (Aoki *et al*., 2002), where it is up-regulated in adipose tissue of obese BRS-3-deficient animals. Thus, it was suggested to play a role in the regulation of body weight and energy metabolism. Moreover, *Ccdc80* is highly expressed in mice white adipose tissue and its silencing inhibit adipocytes differentiation (Tremblay *et al*., 2009). *Ccdc80* expression was also investigated during mice embryonic development. Northern blot analysis performed on developing embryos showed

that the gene is expressed from 7 days post coitum (dpc) up to 17 dpc (Visconti *et al*., 2003). Moreover, Liu and colleagues (2004) described an abundant expression of *Ccdc80* gene and protein in the developing cartilage, suggesting a role during skeletogenesis. In chickens, two alternative splicing forms of *ccdc80* are described: *S*- and *L-equarin*. During embryogenesis, both transcripts are detected in the developing lens, with a high dorsal to ventral gradient. Microinjection of *equarin* mRNAs into Xenopus embryos induced abnormal eye development, suggesting that it is involved in eye formation (Mu *et al*., 2003). Human *CCDC80* is almost ubiquitously expressed, with the highest levels in heart and skeletal muscle (Visconti *et al*., 2003). Further studies of expression profiling show that *CCDC80* is highly expressed in skeletal myotubes during normal differentiation of skeletal muscles (Raymond *et al*., 2010) and in muscles from patients with Duchenne dystrophy (Haslett *et al*., 2003; Tseng *et al*., 2002). In skeletal myotubes, its expression is elicited by pyruvate (Wilson *et al*., 2007) and suppressed by starvation (Stevenson *et al*., 2005). Overall, these *data* suggest a possible role of *CCDC80* as a cell differentiation protein both in cultured cells and muscle tissues undergoing regeneration or remodelling. Furthermore, human *CCDC80* can be considered a potential tumor suppressor gene (Visconti *et al*., 2003). In fact, it is strikingly down-regulated in thyroid neoplastic cell lines and tissues, as well as in colon and pancreatic cancer cell lines and in most colorectal cancer specimens (Bommer *et al*., 2005). Ectopic expression of *CCDC80* in colorectal and pancreatic cancer cell lines resulted in substantial inhibition of growth properties. Further evidences of its involvement in tumors came from observation of *CCDC80* significant down-regulation in transgenic mouse mammary epithelial cells overexpressing the oncogene AIB1 (Ferragud *et al*., 2011).

The encoded CCDC80 protein is highly conserved among vertebrates, and contains multiple signals of cellular compartmentalization and post-translational modifications. In particular, it has a N-terminus leader peptide for extracellular export and many nuclear localization signals (Visconti *et al*., 2003). In different studies, the CCDC80 protein has been identified in a N-glycosylated secreted form and was suggested to be secreted. To verify the cellular localization of Ccdc80, Visconti and colleagues (2003) transfected COS7 cells with an expression vector containing the entire ORF of rat *Ccdc80* fused in-frame with the EGFP (Enhanced Green Fluorescent Protein) gene. Expression of EGFP-Ccdc80 resulted in two different sub-cellular localization patterns: in most cells the fluorescent signal was juxtanuclear, indicating a Golgian localization, suggestive of secretion; nevertheless, in the 5-10% of cells the signal was nuclear-cytoplasmic (Visconti *et al*., 2003). Mouse Ccdc80 and chicken equarin were described as secreted proteins (Liu *et al*., 2004; Mu *et al*., 2003), whereas immunofluorescence studies revealed cytosolic localization of human CCDC80 and

only partial overlap with markers for the endoplasmic reticulum and Golgi stack was seen (Bommer *et al*., 2005). However, further studies confirmed CCDC80 as a secreted protein, given its presence in the Golgi apparatus and in the cell medium (Ferragud *et al*., 2011).

Human CCDC80 show high sequence identity with its homologs in rat (84%), mouse (83%), and chicken (66%). In all species, the protein is highly basic and show a lysine-reach region and a threonine-rich region. Moreover, three P-DUDES domains are present (Procaryotes-*DRO1*-*URB*-*DRS*-*Equarin*-*SRPUL*). In human, P-DUDES are correlated with a tumor suppressor role and are found in single copy also in SRPX and SRPX2 protein, which are involved in tumor suppression and progression, respectively (Pawlowsky *et al*., 2010).

In silico analysis of the genomic *Danio rerio* database using the human CCDC80 aminoacidic sequence as a virtual probe, led to the identification of three homolog sequences. The first isolated sequence (named *ccdc80*) was 2604 bp long and corresponded to one ORF. The final zebrafish *ccdc80* mRNA sequence (2926bp) has been deposited in the Genbank database with the Accession Number EU269066 (GI:166831573). Northern Blot analysis on poli(A)$^+$ RNA from adult fish revealed two alternative forms of the *ccdc80* transcript, 4.7 kb (more abundant) and 3.6 kb, respectively (Fig. 2.6) (Della Noce, Ph.D. thesis, 2009).

In silico translation of the *ccdc80* cDNA produced a protein of 867 amino acids long. Its physical and chemical properties appeared similar to those shown by the ortholog proteins. In fact, zebrafish Ccdc80 is a highly basic protein (pI 9.68) and has a predicted molecular mass of 99.92 kDa. Sequence analysis showed a putative signal peptide and multiple nuclear localization signals. Moreover, it showed a putative endoplasmic reticulum retention signal at N-terminus (RARY), putative N-glycosylation sites and several mucin type O-glycosylation sites in the threonine-rich region. A lysine-rich region is also present (Fig. 2.7). Zebrafish *ccdc80*, as its orthologs in other vertebrates, show three P-DUDES domains (Fig. 2.7) (Della Noce, Ph.D. thesis, 2009; Pawlowski *et al*., 2010). The entire zebrafish Ccdc80-encoded protein shares high sequence homology with human DRO1 (56% identity, 69% similarity), mouse URB (55% identity, 68% similarity), rat CL2 (54% identity, 68% similarity), and chicken L-Equarin (59% identity, 71% similarity) (Della Noce, Ph.D. thesis, 2009).

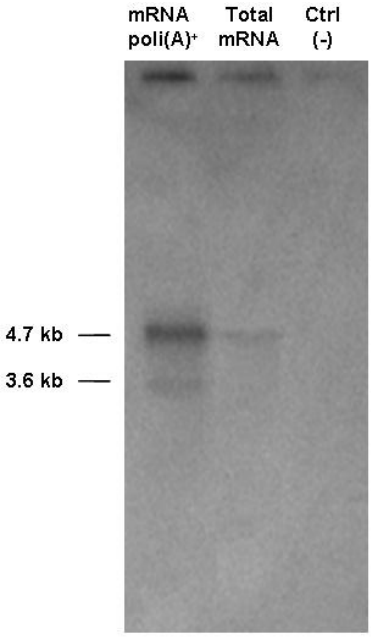

Figure 2.6: Northern blot analysis of the *ccdc80* transcript. Two bands are visible in the zebrafish mRNApoli(A)$^+$ lane, one band is visible in the zebrafish total RNA lane, and no bands are detectable in the negative control lane (Della Noce, Ph.D. thesis, 2009).

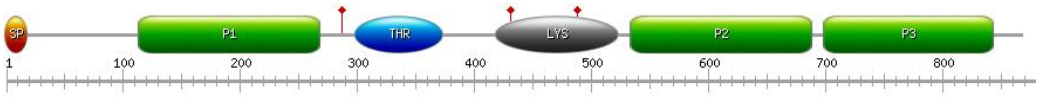

Figure 2.7: Zebrafish Ccdc80 protein structure. Domains boundaries were defined by the protein sequence properties and on the basis of the Ccdc80 motifs alignment with other known protein sequences (human SPRX, human DRO1, mouse Urb, chicken L-Equarin, and rat CL2). The image is displayed with the software PROSITE tool MyDomains - Image Creator (Sigrist et al., 2002). SP: signal peptide; : nuclear localization signal; P1, P2, P3: P-DUDES domains; Thr: threonine-rich region; Lys: lysine-rich region (Della Noce, Ph.D. thesis, 2009).

Aim of the project

3. Aim of the project

The aim of this project was the spatial and functional characterization of two zebrafish *ccdc80* homolgs showing the highest level of identity with human *CCDC80*: *ccdc80* and *ccdc80-like1* (*ccdc80-l1).* The third zebrafish *CCDC80*-homolog, annotated as wu:fb92b05 in Ensemble and which we named *ccdc80-l2*, showed the lowest levels of identity and similarity with other *Ccdc80* genes sequences, and has not been studied yet.

The expression profiling of *ccdc80* and *ccdc80-l1* was examined by means of RT-PCR (Reverse Transcription Polymerase Chain Reaction) on cDNA from adult tissues and embryos at different developmental stages. Spatial analysis were obtained through whole mount *in situ* hybridization (WISH) on embryos at various developmental stages. Functional analysis was conducted performing loss- and gain-of-function assays. Loss of function is commonly obtained in zebrafish embryos microinjecting specific morpholinos, that are small, specific oligonucleotides that bind to the transcript start site. The resulting steric block prevents the protein translation, leading to the knock-down of its function. Gain-of-function experiments are conducted microinjecting synthetic mRNA encoding the protein of interest. Microinjections are performed at very early stages of development, before the second blastomeres division. Thus, morpholinos or mRNAs spread uniformly in the yolk, and then in all cells. Investigation on up-stream regulation was also conducted, whereas only preliminary *data* on potential targets are available.

ccdc80 and *ccdc80-l1* are both maternally and zygotically expressed, but show different expression patterns and functions. *ccdc80* is expressed in the notochord and plays a role in somitogenesis, as evidenced by both loss- and gain-of-function experiments. *ccdc80-l1* is expressed in muscular territories such as muscle pioneers and adaxial cells, but its loss-of-function leads to axonal migration defects. The investigation of up-stream regulation evidenced that the transcriptional activation of both genes is regulated by the hedgehog pathway; in particular, *shh* specifically regulates *ccdc80* and *ccdc80-l1* transcription. The potential synergy between the two genes was also investigated through the simultaneous silencing of both genes. The results indicate that *ccdc80* and *ccdc80-l1* do not cooperate during embryonic development, despite the high conservation between the two sequences.

Materials and methods

4.1 Zebrafish lines and maintenance

The following Zebrafish (*Danio rerio*) strains were used: AB obtained from the Zebrafish International Research Center, Oregon US, and from Wilson lab, University College London. Zebrafish were raised and maintained according to established techniques (Westerfield M., 2000. The Zebrafish Book. A guide for the laboratory use of zebrafish (*Danio rerio*). Eugene: University of Oregon Press), approved by the veterinarian (OVSAC) and the animal use committee (IACUC) at the University of Oregon, in agreement with local and national sanitary regulations. Adult fish were maintained at 28.5 C, 14 hours light/10 hours dark cycle, in a recirculating fresh water system (Fig. 4.1). Fish were fed every day with brineshrimps, Artemia salina, (living or frozen) and Small Granular feed from Zebrafish Management Ltd.,Embryos were collected by natural spawning, staged according to Kimmel (Kimmel *et al.*, 1995), and raised at 28°C in fish water (Instant Ocean, 0.1% methylene blue) in Petri dishes (Haffter and Nusslein-Volhard, 1996).

Stock solution for fish water: 34 g of Instant Ocean Sea Salt dissolved in 1 l of deionised H_2O.

Fish water: 50 ml of stock solution in 10 l of deionised H_2O.

Figure 4.1: System for fish maintenance.

4.2 Sequence analysis

Zebrafish chromosome 6 region hosting the *ccdc80-l1* gene were identified through *in silico* search of the ENSEMBL zebrafish assembly version 9 (Zv9) using zebrafish Ccdc80 protein

sequence as a bait. The alignments between sequences were performed with the software program LALIGN version 2.2u (Myers and Miller, 1988). Analysis on synteny was performed with the program Genomicus v57.01. Physical-chemical properties of the proteins were deducted *in silico* by the analysis of the amino acidic sequence with the software program Compute pI / Mw (Gasteiger *et al.*, 2005). The putative sub-cellular localization of the proteins was predicted using the software program WoLF PSORT (Nakai *et al.*, 1999). The presence of common motifs in the proteins was analyzed with the software program MEME (Timothy *et al.*, 1994), and the software program Motif Alignment and Search Tool analysis (MAST) (Timothy *et al.*, 1998**)**.

4.3 RT-PCR

Total RNA from 11 samples (an average of 30 embryos per sample) corresponding to 9 different developmental stage embryos (2-4 cells, 64-1000 cells, 30% epiboly, 60%-70% epiboly, somitogenesis, 24 and 72 hpf) and 2 adult organs (ovary and muscle) was extracted with the TOTALLY RNA isolation kit (Ambion), treated with RQ1 RNase-Free DNase (Promega) and oligo (dT)-reverse transcribed using Super- Script II RT (Invitrogen), according to manufacturers' instructions:

Cycles for ccdc80-l1 and ccdc80 amplification:

- 1st cycle:
  - 3 min at 95°C (denaturing)
- 2nd cycle up to 35th:
  - 30 sec at 95°C (denaturing)
  - 30 sec at 55°C (annealing)
  - 30 sec at 72°C (elongation)
- the last cycle:
  - 10 min at 72°C (final incubation)

Cycles for β-actin amplification:

- 1st cycle:
  - 3 min at 95°C (denaturing)
- 2nd cycle up to 35th:
  - 30 sec at 95°C (denaturing)
  - 30 sec at 55°C (annealing)
  - 30 sec at 72°C (elongation)
- the last cycle:
  - 10 min at 72°C (final incubation)

Then the RT-PCR products were run on a 1% agarose gel and acquired with the Epson 1200 scanner.

The following primers were used for PCR reactions:

ccdc80 FF 5’ AGCAGTGCTATGAGGGCACGG 3’ (Ta 63°C)

ccdc80 REV	5′ GGCATGCGGGACACTCTGGC 3′	(Ta 63°C)
ccdc80-l1 FF	5′ ACCACAATGGAGCAAACACA 3′	(Ta 55°C)
ccdc80-l1 REV	5′ GGTTTAGCTCTCCCCTTTGG 3′	(Ta 55°C)
β-actina FF	5′ TGTTTTCCCCTCCATTGTTGG 3′	(Ta 57°C)
β-actina REV	5′ TTCTCCTTGATGTCACGGAC 3′	(Ta 55°C)

All primers are synthesised by Invitrogen Life Technologies.

4.4. Synthesis of probes for whole mount *in situ* hybridization (WISH)

To perform an *in situ* hybridization assay we synthesised two probes: a RNA antisense probe and a control RNA sense probe that is identical to endogenous transcript and consequently should not bind to the mRNA during the hybridization. The control probe is necessary to verify the specificity of the RNA–antisense probe.

In order to synthesise the probes for *ccdc80* and *ccdc80-l1* we used the same primers we designed for the RT-PCR, thus amplifying a region corresponding to the first 300 base pairs of *ccdc80* and *ccdc80-l1* coding sequence. The probes of all the markers we used in loss- and gain-of-function experiments were already present in our laboratory as common markers of embryonic structures.

Cloning and transformation reaction

The RT-PCR products were cloned in the pCR®II-TOPO® vector following manufacturer's instructions of TOPO TA Cloning® kit (Invitrogen), that provide for the cloning of PCR product in the plasmidic vector and then its bacteric transformation using E. Coli TOP 10 chem. Competent.Th cells. pCR®II-TOPO® vector has two promoters Sp6 and T7 in order to synthesise the antisense and sense probes.

Isolation of plasmid DNA

Recombinant colonies were screened and preparation of plasmid was performed using PureYeld™ Plasmid Midiprep System (Promega) according to the manufacturer's instructions.

The extracted plasmidic DNA was run on 1% agarose gel. The preparation was verified by DNA sequencing on both strands in order to understand the insert orientation. The cDNA-containing plasmids were then linearized with restriction enzymes as follows:

digestion mixture:

- 10 μg of plasmidic DNA in water solution
- at least 10 U of restriction enzyme
- 10 μl of buffer 10X
- 10 μl BSA 10X, when required
- sterile water up to a final volume of 100 μl

- incubate the mixture at least for 2 h at the optimum temperature for each used enzyme
- cool the digestion mixture in ice
- extract twice with an equal volume of Phenol: Chloroform: Isoamyl alcohol (25:24:1)
- recover aqueous phase and precipitate over night at –20°C by adding 2,5 volumes of ethanol and 1/10 volume of Sodium Acetate 3M, pH 5.2
- wash the pellet of DNA with 70% ethanol
- melt the pellet in 12 µl of sterile water

Probes labelling and synthesis

The linearized plasmids were then used as templates for antisense and sense digoxigenin-UTP labelling and for *in vitro* riboprobe synthesis following the DIG RNA Labeling Kit (SP6/T7; Roche) manufacturer's instructions.

4.5 Whole-mount *in situ* hybridization

Whole-mount *in situ* hybridizations were carried out as described (Thisse *et al.*, 1993) on embryos fixed for 2 hours in 4% paraformaldehyde in PBS, then rinsed with PBS-Tween (PBT), dehydrated in 100% methanol and stored at –20°C until processed (Jowett and Lettice, 1994).

4.6 Immunohistochemistry

Embryos were fixed as already described. After re-hydration and permeabilization with 0,005% Pronase treatment, primary antibody incubation was overnight at 4°C, followed by several washes in PBT and incubation of secondary antibody for 1 hour at room temperature. Primary antibodies are MF20 (mouse anti-sarcomeric) and 4D9 (mouse anti-engrailed/invected) purchased from Developmental Studies Hybridoma Bank; znp1 (mouse anti-*syt2b*) purchased from Zebrafish International Resource Center (ZIRC); zn5 (mouse anti-Alcam) kindly provided by Paolo Sordino. Secondary antibody is EnVision+ System- HRP Labelled Polymer anti-mouse (Dako). Embryos were observed under the Leica MZ16F stereomicroscope and images were acquired with the Leica DFC 480 digital camera using the IM500 software (Leica Microsystems). Images were processed using the Adobe Photoshop software.

4.7 Histological sections

After hybridization and immunohistochemistry experiments, stained embryos were re-fixed in 4% paraformaldehyde, dehydrated and stored in methanol, wax embedded, and sectioned (5–8 μm). All sections are observed at microscope Olympus BH-2 equipped with a Leica DCF480 digital camera and the software IM50.

4.8 Injections

Injections were carried out on 1- to 2-cell-stage embryos (with Eppendorf FemtoJet Micromanipulator 5171; Fig. 4.2); the dye tracer rhodamine dextran was co-injected as a control. To repress *ccdc80* and *ccdc80-l1* mRNA translation we designed two ATG-targeting morpholino (Gene Tools, LLC) having this sequence

ccdc80-MO 5'-AACCAAGCATATACCGTGCCCTCAT-3'

ccdc80-l1-MO 5'-TTGTACCTGTAGATTTTTCATTGCA-3'

Morpholinos were dissolved in Danieau's solution (58 mM NaCl; 0,7 mM KCl; 0,4 mM $MgSO_4 \cdot H_2O$; 0,6 mM $Ca(NO_3)_2$; 5 mM Hepes pH 7.2) at 2 mM concentration and stored at –80°C.

Embryos were microinjected at the 1–4 cells stage and Rodamin dextran (Molecular Probes) was usually co-injected as a tracer. As a negative control we injected standard control morpholino (ctrl-MO) that targets human *a-globin* gene. This oligo has not been reported to have other targets or generate any phenotypes in any known test system except human β-thalessemic hematopoetic cells.

For the *in vivo* test of the specificity of *ccdc80*-MO, 300 pg per embryo of the pCS2+-ccdc80-GFP sensor plasmid have been coinjected with 12 ng of ccdc80-MO or ctrl-MO, respectively. The presence/absence of the GFP signal has been monitored under a fluorescent microscope from 24 to 48 hpf. ccdc80-MO cDNA fragments inserted in the *BamHI* site were obtained using the following complementary oligos:

ccdc80-MO FF : 5' gatcATGAGGGCACGGTATATGCTTGGTTCA 3'

ccdc80-MO rev : 5' gatcTGAACCAAGCATATACCGTGCCCTCAT 3'

For the *in vivo* test of the efficiency of *ccdc80-l1*-MO, 425 pg per embryo of the pCS2+-*ccdc80-l1*-GFP sensor plasmid have been injected alone or co-injected with 12 ng of *ccdc80-l1*-MO. *ccdc80-l1*-MO cDNA fragments inserted in the *BamHI* site were obtained using the following complementary oligos:

ccdc80-l1-MO FF 5' gatcTTGTACCTGTAGATTTTTCATTGCACA 3'

ccdc80-l1-MO REV 5' gatcTGTGCAATGAAAAATCTACAGGTACAA 3'

Overexpression of ccdc80 was obtained through the injection of 400 pg/embryo of the *ccdc80* full-length sequence, synthesized from the pCS2+/*ccdc80* plasmid. *shh* mRNA was has been kindly provided by Paolo Sordino laboratory (300 pg/embryo of mRNA were used). To control for unspecific effects, each overexpression experiment was performed in parallel with injection of the same amount of EGFP mRNA, which encodes for the enhanced green fluorescent protein.

For the *in vivo* test of the specificity of *ccdc80-l1*-MO-mediated knockdown, the rescue of morphants phenotype was obtained co-injecting 12 ng/embryo of *ccdc80-l1*-MO together with 400 pg/embryo of *ccdc80*-encoding mRNA.

Figure 4.2: Microinjection apparatus.

4.9 Cyclopamine treatment

Embryos were exposed to 15 µM cyclopamine (purchased from SIGMA-ALDRICH) from 50% epiboly stage up to fixation in PFA at 15 somites stage. Cyclopamine was dissolved in embryo medium and 0.5% ethanol. Controls consisted of corresponding incubations in 0.5% ethanol in embryo medium.

4.10 Statistical analysis

Statistical analysis was performed with Student's t-test using GraphPad PRISM version 5.0 (GraphPad, San Diego, California). A p value <0.001 indicates a statistically significant effect.

Results

5.1 Identification of *ccdc80* homologs in the genome of zebrafish

Blast analysis of the ENSEMBL zebrafish assembly version 9 (Zv9) using human CCDC80 protein sequence as a bait returned three positive hits: the first corresponds to Ccdc80, that shows the highest levels of identity and similarity with human CCDC80 (51.6% and 65.2%, respectively). The other homologs are encoded by a gene on chromosome 9 (nucleotide position: 35,060,460-35,084,513) and a gene on chromosome 21 (nucleotide position: 18,662,129-18,669,986). The homolog sequence on chromosome 6 is translated in a protein showing 44.4% of identity and 59.3% of similarity with human CCDC80. This sequence was named Ccdc80-like1 (Ccdc80-l1). The last homolog protein show 27% of identity and 44.9% of similarity with human CCDC80, and was named Ccdc80-like2 (Ccdc80-l2). We then performed alignments between the three homologs: Ccdc80 share the 51.4% of identity and 64.4% of similarity with Ccdc80-l1 and the 30.4% of identity and the 47.4% of similarity with Ccdc80-l2. Ccdc80-l1 and Ccdc80-l2 share the 29.1% of identity and the 46.9% of similarity (Tab. 1). Analysis of chromosomal organization of the three *ccdc80* zebrafish homologs across vertebrates revealed that only *ccdc80* is synthenic with other vertebrates (Fig. 5.1), suggesting that it might be their ortholog. *ccdc80-l1* and *ccdc80-l2* might be paralogs derived from an intra-species duplication.

	Human CCDC80		Zebrafish Ccdc80		Zebrafish Ccdc80-like1		Zebrafish Ccdc80-like2	
	Identity	Similarity	Identity	Similarity	Identity	Similarity	Identity	Similarity
Zebrafish Ccdc80	51,6%	65,2%	/	/	51,4%	64,4%	30,4%	47,4%
Zebrafish Ccdc80-like1	44,4%	59,3%	51,4%	64,4%	/	/	29,1%	46,9%
Zebrafish Ccdc80-like2	27%	44,9%	30,4%	47,4%	29,1%	46,9%	/	/

Table 5.1: percentages of identity and similarity between zebrafish and human CCDC80 homologs. The table shows the scores obtained after alignments between the aminoacidic sequences of zebrafish and human CCDC80 homologs. Alignments were performed with Stretcher-P tool.

The chromosomal organization of *ccdc80-l1* across vertebrate species revealed the absence of synteny, whereas conserved synteny was observed between the chromosome region hosting zebrafish *ccdc80* and human CCDC80 *loci*. These observation led us to refer to zebrafish *ccdc80* as the homolog of human and rat ccdc80, whereas *ccdc80-l1* is its paralog. The analysis of Ccdc80-l1 aminoacidic sequence revealed the presence of two nuclear internalization signals at amino acids 527 (RRRR) and 515 (bipartite: KKSLETFLSYFQRRRRL) (Fig. 5.1), and the absence of signal or mitochondrial targeting peptide. Ccdc80-l1 shares similar features with its paralog: the two proteins are in fact highly basic and show a threonine-rich domain in a similar position (Fig. 5.1). Moreover, three P-DUDES domain are present also in Ccdc80-l1 sequence, as in Ccdc80 (Pawlowski *et al*., 2010). The domains are located in similar positions between the two paralogs and the alignment of their sequences revealed high percentages of identity and similarity.

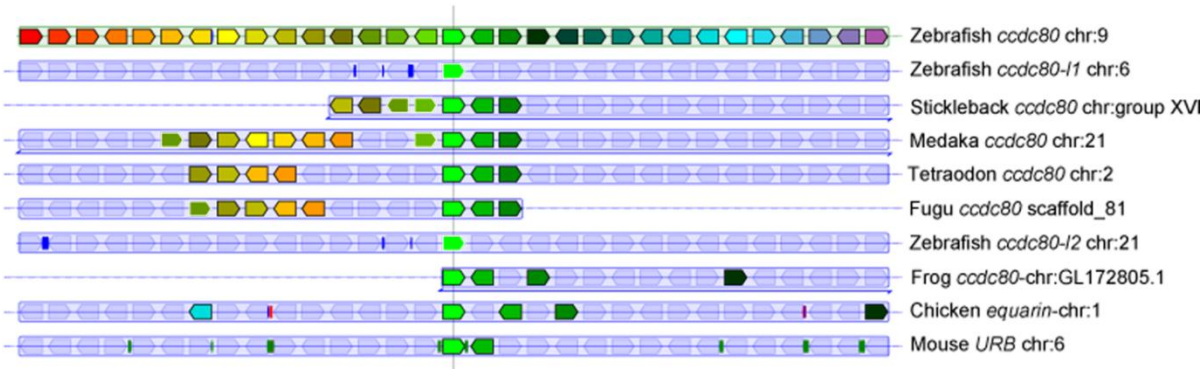

Figure 5.1: Analysis of chromosomal organization of the three *ccdc80* zebrafish homologs across vertebrates. Each *ccdc80* gene is shown as a reference locus. Genes annotated as paralogs (no surrounding line) or orthologs (with a surrounding line) by the Ensembl database share the same color, blue lines beneath individual tracks indicate that orientations of gene blocks and are inverted with respect to their genomic annotation. For zebrafish *ccdc80* (chr. 9), *ccdc80-l1* (chr. 6) and *ccdc80-l2* (chr. 21), only *ccdc80* shows notable synteny with other vertebrates. The figure was derived from the output of the Genomicus website (version 57.01).

The *in silico* translation of *ccdc80-l1* gives an 842 aminoacids protein. Its physical and chemical properties are similar to those shown by the ortholog proteins and its zebrafish paralog. In fact, *ccdc80-l1* is a highly basic protein (pI 9.55) and has a predicted molecular mass of 95,89 kDa kDa. The sequence analysis shows that it has two nuclear localization signals at amino acids 527 (RRRR) and 515 (KKSLETFLSYFQRRRRL, bipartite) (Fig. 5.2); moreover, unlike its paralog, Ccdc80-l1 has no signal peptides. These *data* suggest the nuclear localization of the protein. A threonine-rich region starting at aminoacid 298 is present (Figure 5.2). Moreover, three P-DUDES domains were detected, which boundaries were defined by on the basis of the Ccdc80-l1 motifs alignment with Ccdc80 sequence (Fig. 5.2)

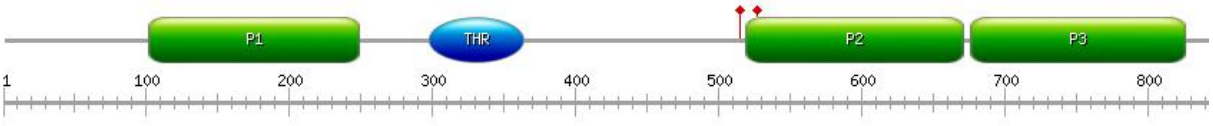

Figure 5.2: Ccdc80-l1 protein structure. The image is displayed with the software PROSITE tool MyDomains - Image Creator (Sigrist *et al.*, 2002). P1, P2, P3: P-DUDES domains; Thr: threonine-rich region; ↑: nuclear localization signal.

The alignment between the two nucleotide sequences allowed us to discriminate a small region in which homology was absent, corresponding to the first 300 bp fallowing the start

codon. In this region, we designed different primers to perform specific RT-PCR assays, and two different probes to investigate the expression patterns of the two genes.

5.2.1 *ccdc80* expression profiling

ccdc80 expression was analyzed by means of RT-PCR and WISH standard protocols with digoxigenin-UTP-labeled probes (Thisse *et al*., 1993). RT-PCR analysis on cDNA from organs of the adult fish showed that *ccdc80* is expressed in all the analyzed tissues. In particular, it is expressed in the ovary, brain, eyes and muscle (Fig. 5.3). RT-PCR on cDNA from embryos at different developmental stages showed the presence of *ccdc80* transcript from the early blastula up to 72 hpf (Fig. 5.3), indicating that it is both maternally and zygotically expressed. Spatial analysis of *ccdc80* expression was obtained from WISH assays. The gene resulted to be expressed in pre-gastrulation embryos (1-2, 8, 16 and 64 cells) and early gastrulation developmental stages (30%-70% epiboly) in a diffuse pattern (*data* not shown). From the 5-somite stage (5 s) up to 48 hpf, *ccdc80* transcript was only detected in the entire notochord (Fig. 5.3). Moreover, ccdc80 is expressed in the heart of 48 hpf embryos (Fig. 5.3).

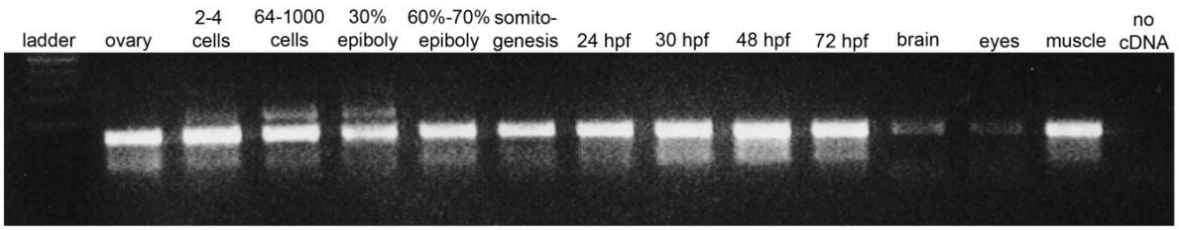

Figure 5.3: RT-PCR on different developmental stages and adult tissues. Different stages and tissues are indicated above the panel. *ccdc80* is expressed in all the analyzed adult tissues (ovary, brain, muscle) and from 2-4 cells stage to 72 hpf.

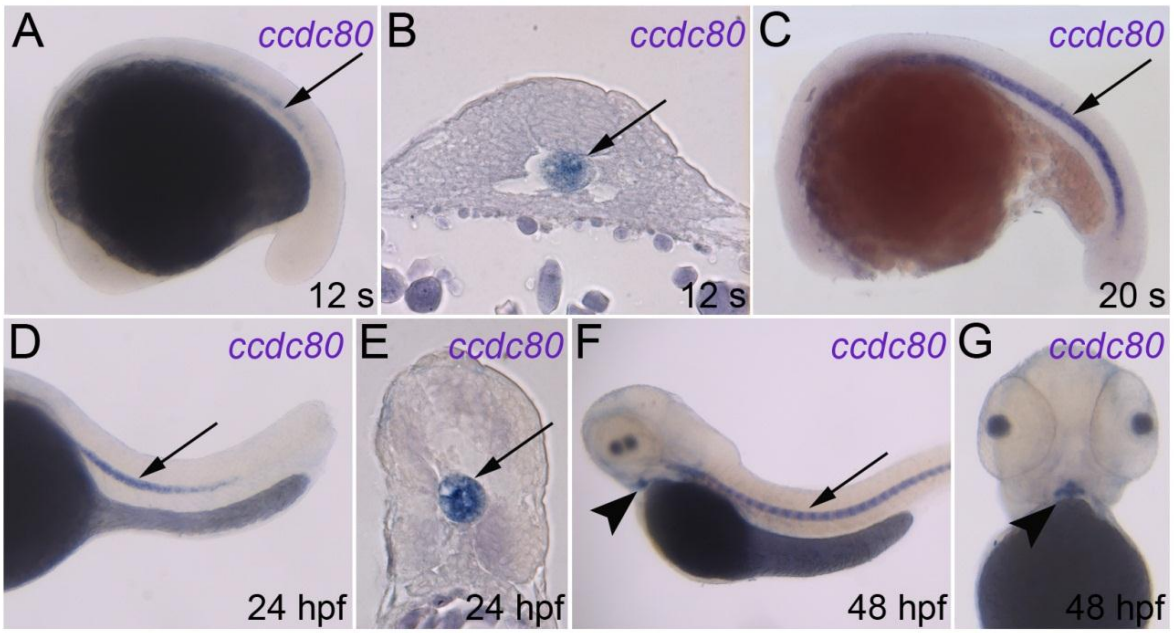

Figure 5.3: Expression pattern of *ccdc80* during zebrafish early embryogenesis. *(A-G)* WISH performed on zebrafish embryos at several stage of development. *(A-C)* Starting from somitogenesis, *ccdc80* is expressed in the notochord (*A* and *C*, arrow), as better shown by the histological section of the trunk at 12 somites stage (arrow in *B*). The same hybridization signal persists also at 24 hpf (*D* and histological section *E*, arrow) and 48 hpf (*F*, arrow). At 48 hpf, *ccdc80* is also expressed in the heart (*F* and *G*, arrowhead). *(A, C, D, F)* Later views, dorsal is up. *(B, E)* Transversal sections of the trunk, dorsal is up. *(G)* Frontal view of the head, dorsal is up.

5.2.2 *ccdc80*-loss- and gain-of-function affects somitogenesis *in vivo*

To determine the role of *ccdc80* during zebrafish development, we performed its knock-down injecting a specific antisense oligonucleotide morpholino (*ccdc80*-MO1, Gene Tools) in embryos at 1-2 cells stage. The morpholino is designed against the start site of the transcript, thus leading to a steric block that prevents the protein translation. In all the experiments, *ccdc80*-MO-injected embryos were compared to embryos at the same developmental stage, injected with the same amount of a non-specific control MO (ctrl-MO). In order to test the *in vivo* efficiency of *ccdc80*-MO1, 450 pg per embryo of the *ccdc80*-GFP sensor plasmid have been co-injected with 12 ng of *ccdc80*-MO or ctrl-MO, respectively. The presence/absence of the GFP signal was monitored under a fluorescent microscope from 24 to 48 hpf. 70% of the embryos (N=36) injected with the sensor plasmid alone displayed fluorescence (Fig. 5.4.A-B). This percentage decreased to 2% when the plasmid was co-injected with *ccdc80*-MO (N= 81) (Fig. 5.4.C-D), indicating that the morpholino specifically bounds to its target region.

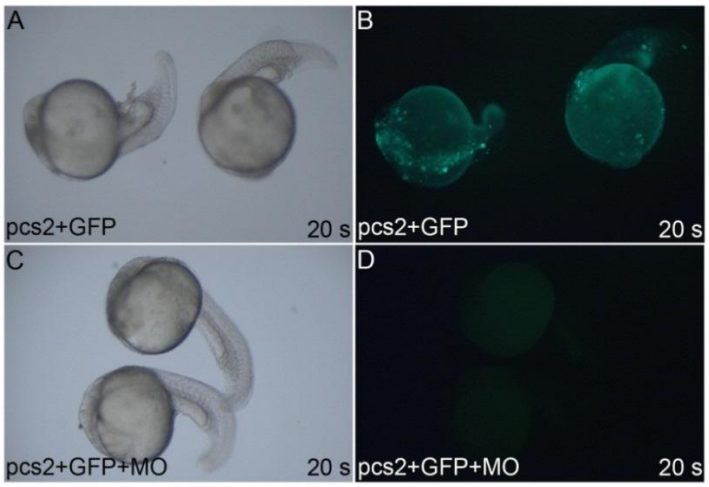

Figure 5.4: *ccdc80* morpholino is capable to inhibit the expression of the fluorescent protein GFP. *(A, B)* In the 70% of embryos injected with the *ccdc80*-GFP sensor plasmid, the presence of fluorescent GFP signal was detected (N= 20). *(C, D)* When the plasmid was injected together with the morpholino, the transcription of GFP protein was inhibited and the percentage of fluorescent embryos decreased to 2% (N=81). In *A* and *C* embryos are visualized under normal light, in *B* and *D* under fluorescent light.

The majority of *ccdc80* silenced embryos (70-80%; N=150) displayed multiple defects in the forming somites, which lost their proper morphology in comparison to control embryos. Somites were larger and disorganized when compared to somites of control embryo, or even absent (Fig. 5.5.A-B). Interestingly, the notochord, in which *ccdc80* is expressed, always appeared properly formed (Fig. 5.5.A-B). At 24 hpf, 64.5% of morphants (N=62) showed curved tails when compared to controls, although the differentiated somites seemed almost completely recovered and the embryos moved properly (Fig 5.5.D-E). A similar disruption of somitogenesis patterning was observed when gain-of-function experiments were performed, injecting *ccdc80*-mRNA. In fact, over-expressed embryos showed enlarged and disorganized somites, but also the presence of other smaller, supernumerary somites (Fig. 5.5.A, C). Taken together, these *data* suggest the involvement of *ccdc80* in somitogenesis, despite its expression in the notochord solely.

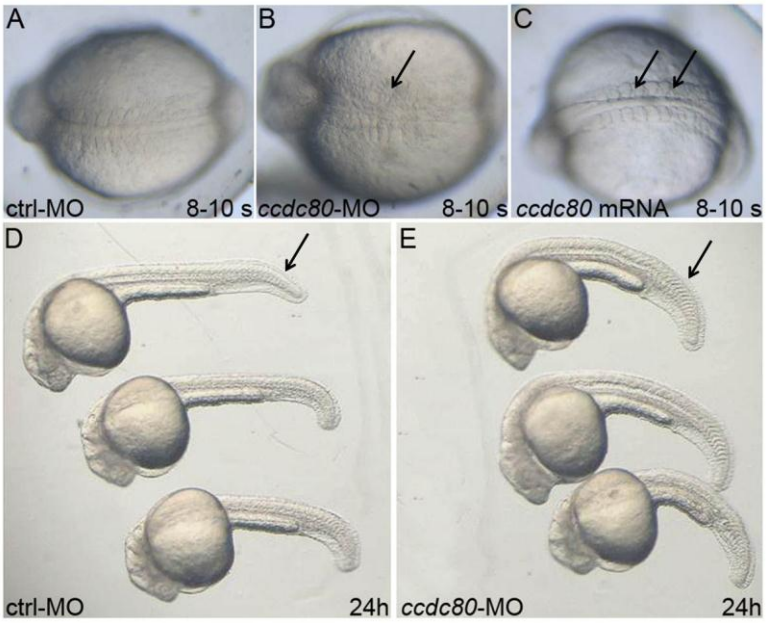

Figure 5.5: Both loss and gain of ccdc80 function affect somitogenesis *in vivo*. *(A-C)* Morphants *(B)* and over-expressed embryos *(C)* displayed enlarged and disorganized somites (arrows) in comparison to control embryos *(A)*. Smaller, supernumerary somites are observable in over-expressed embryos (arrows in *C*). *(A-C)* Dorsal views, rostral to the left; *(D-E)* lateral views, anterior to the left.

5.2.3 *ccdc80* is involved in somitogenesis, but not in the development of the notochord

To gain insight into the functional role of *ccdc80*, we analyzed the expression, in morphants and overexpressed embryos, of specific markers of different structures and developmental processes. Due to the early onset of *ccdc80* expression during crucial embryonic developmental processes, we analyzed the expression of *gsc* as a marker of epiboly at shield stage. We chose also *ntl* as a marker of the notochord and *her1* and *myod* as markers of different phases of somitogenesis, due to *ccdc80* expression in the notochord and its involvement in somitogenesis. Whereas *ntl* and *gsc* were always correctly expressed in both control embryos and morphants (Fig. 5.6.A-F), all somitogenesis markers showed striking alteration. Both in morphants and overexpressed embryos, *her1* expression resulted expanded in broader domains rather than in defined territories as in control embryos at the same developmental stages (Fig. 5.6.G-I). Furthermore, in *ccdc80*-MO- and *ccdc80*-mRNA-injected embryos, also the myogenic markers *myod* was present but disorganized (Fig. 5.6.J-L), reflecting the phenotype observed *in vivo*. Taken together, these *data* confirmed the phenotype observed *in vivo*, with *ccdc80* loss-of –function affecting somitogenesis but not the notochord development nor early embryonic development.

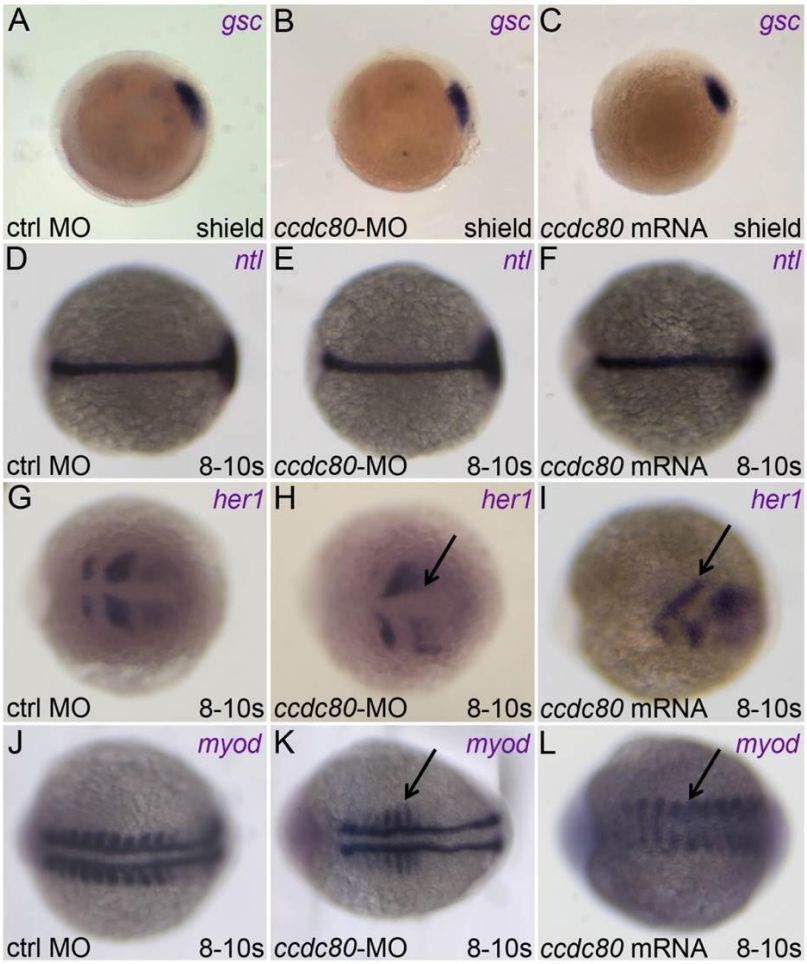

Figure 5.6: Expression pattern of different markers in loss- and gain-of-function experiments. *(A-C) gsc*, marker of epiboly, resulted correctly expressed at shield stage, both in morphants and in overexpressed embryos. *(D-F)* Also the expression pattern of *ntl*, marker of the notochord, resulted unaltered in all embryos. (G-I) *her1* expression was expanded and asymmetric in *ccdc80*-MO- and *ccdc80*-mRNA-injected embryos (arrows). *(J-L)* The expression domains of *myod* resulted highly disorganized in all embryos, reflecting the defects observed *in vivo* (arrows). *(A-C)* Lateral views, dorsal to the right. *(D-L)* Dorsal views, rostral to the left.

5.2.4 *ccdc80* is positively regulated by the Hedgehog pathway

Bearing in mind the relationship between Hedgehog pathway and notochord formation, we decided to analyze its possible interaction with *ccdc80*. The blockage of Hedgehog signaling was obtained through exposure from early cleavage stages to cyclopamine, that inhibits the Hedgehog transducer *Smoothened* (*smo*) (Barresi *et al*., 2001; Wolff *et al*., 2003). This treatment produced an inhibition of *ccdc80* expression in the notochord (Fig. 5.7.A-B). Conversely, overexpression of the synthetic *shh* mRNA at 1-to-2 cell stage, induced *ccdc80* upregulation in this structure (Fig. 5.7.A, C). These results evidenced a relationship between *ccdc80* and the Hedgehog pathway, in particular *ccdc80* seems to be an Hh downstream effector. To test

whether this might be a feed-back regulation, we verified if the modulation of *ccdc80* expression, inhibiting or inducing its protein translation, could induce any difference in *shh* expression. Both experiments did not perturb the proper *shh* transcript distribution, indicating that *ccdc80* does not regulate it. Taken together, these *data* strongly indicate *ccdc80* as a down-stream effector of *shh*, and not *vice versa*.

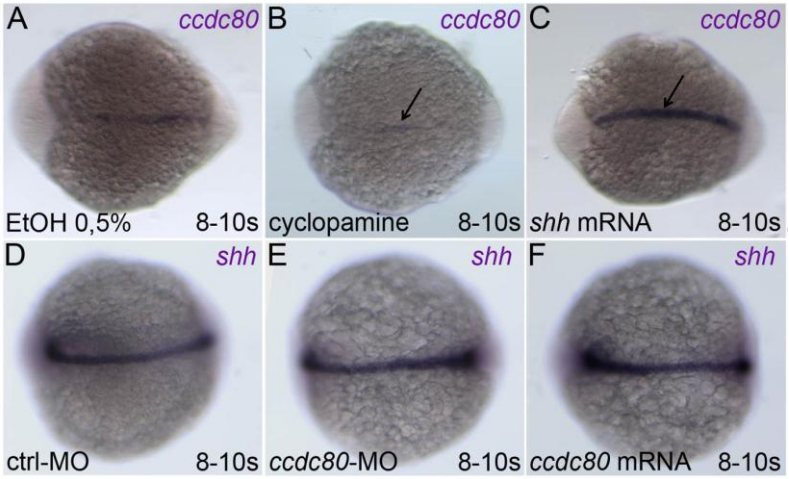

Figure 5.7: *shh* regulates, and is not regulated by, *ccdc80* expression. *(A-C)* In comparison with control embryos *(A)*, cyclopamine treatment strongly down-regulated *ccdc80* expression in the notochord *(*arrow in *B)*, whereas injection of shh mRNA led to its up-regulation *(*arrow in *C)*. *(D-F) shh* expression was not perturbed by the loss- *(E)* nor the gain-of-*ccdc80* funtion *(F)*, and remained comparable with expression in control embryos *(D)*. *(A-F)* Dorsal views, rostral on the left.

5.3.1 *ccdc80-l1* expression profiling

RT-PCR performed on cDNA extracts from different stages of embriogenesis and adult tissues, revealed the presence of *ccdc80-l1* transcript from the first stages of development up to 72 hpf (Fig.5.8.A, lanes 3-11). Hence, the gene is both maternally and zygotically expressed, as its paralog ccdc80. *ccdc80-l1* is also expressed in the ovary and muscle of the adult zebrafish (Fig. 5.8.A, lanes 2 and 12). No expression was detected in brain and eyes (*data* not shown).

ccdc80-l1 spatial and temporal expression was investigated by means of WISH from 1–2 cell stage up to 48 hpf. In early pre-gastrulation embryos (2 and 32 cells) and during gastrulation, *ccdc80-l1* expression was observed in a diffuse pattern, in all the blastomers (*data* not shown). During somitogenesis, the hybridization signal is restricted to the horizontal myoseptum (Fig.5.8.B-C). From this stage, *ccdc80-l1* expression is observed also in the cranial ganglia and dorsal dermis (Fig.5.8.B-L). At 24 hpf, the co-localization between *ccdc80-l1* transcript and the

nuclear engrailed labeling with 4D9 antibody (Hatta *et al*., 1991; Patel *et al*., 1989) evidenced *ccdc80-l1* to be expressed in muscle pioneers cells (Fig.5.8.G-H). At the same stage, the *ccdc80-l1* hybridization signal is also detectable at the level of a specific sub-population of migrating adaxial cells, that moves along the lateral axis towards the external somite (Devoto *et al*., 1996) (Fig.5.8.E-F). *ccdc80-l1* expression in adaxial cells and somites persisted at 36 hpf and 48 hpf, and at the same stages *ccdc80-l1* is also expressed in the caudal vein (Fig.5.8.I-L).

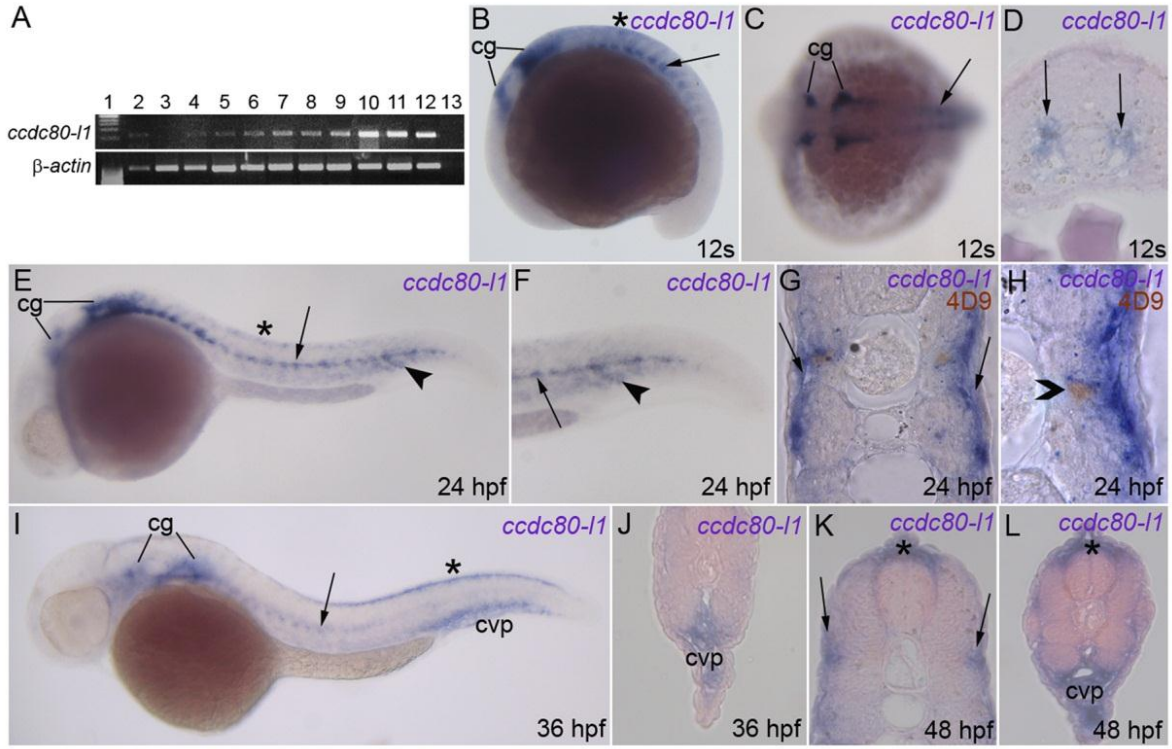

Figure 5.8: Expression of *ccdc80-l1* analyzed by RT-PCR and WISH. *(A)* RT-PCR performed on different embryonic stages and adult tissues; the expression of *ccdc80-l1* and *β-actin* are shown. Lanes are: ladder (lane 1) , ovary (lane 2), 2-4 cells stage (lane 3), 64-1000 cells stage (lane 4) 30% epiboly (lane 5), 60-70% epiboly (lane 6), somitogenesis (lane 7), 24 hpf (lane 8), 30 hpf (lane 9), 48 hpf (lane 10), 72 hpf (lane 11), adult muscle (lane 12) and negative control (lane 13) in the absence of cDNA. *(B-J)* WISH performed on zebrafish embryos at several stage of development. *(B, C)* During somitogenesis *ccdc80-l1* was expressed by cranial ganglia (cg), dorsal dermis (asterisk), adaxial cells and muscle pioneers at the level of the horizontal myoseptum (arrow). *(D) ccdc80-l1* expression in a transverse section of the trunk of an embryo at 12 somites stage (arrows). *(E-G)* At 24 hpf, the hybridization signal was detectable in cranial ganglia (cg), dermis (asterisk), adaxial cells (arrow) and ventral somites (arrowhead). *(F)* Higher magnification of the tail at 24 hpf. *(G)* Transversal section of an embryo at 24 hpf. *(H)* Transversal section showing that at 24 hpf *ccdc80-l1* hydridization signal co-localized with the nuclear labeling of 4D9 antibody, corresponding to the engrailed-positive muscle pioneers population (open arrowhead). *(I-J)* At 36 hpf, the signal of *ccdc80-l1* probe was detected in cranial ganglia (cg), migrated adaxial cells (arrow), dorsal dermis (asterisk) and caudal vein plexus region (cvp). *(K-L)* At 48 hpf, *ccdc80-l1* was detected in dorsal dermis (asterisk), external adaxial cells (arrows in *K*) and caudal vein plexus region (cvp in *L*). *(B, E, F, I)* Lateral views; dorsal is up, anterior is left; *(C)* dorsal view, anterior is left; *(D, G, H, J-L)* transversal sections, dorsal is up.

5.3.2 *ccdc80-l1* knocked-down embryos displayed impaired motility

To determine the functional role of *ccdc80-l1* during zebrafish development, the gene was specifically knocked it down by means of the injection of an antisense oligonucleotide morpholino (*ccdc80-l1*-MO, Gene Tools) designed against the start site of the transcript. In all the experiments, *ccdc80-l1*-MO-injected embryos (morphants) were compared to embryos at the same developmental stage, injected with the same amount of a control MO (ctrl-MO). For the *in vivo* test of the efficiency of *ccdc80-l1*-MO, 425 pg/embryo of the pCS2+-*ccdc80-l1*-GFP sensor plasmid have been injected alone or with 12 ng of *ccdc80-l1*-MO. The presence/absence of the GFP signal has been monitored under a fluorescent microscope starting from somitogenesis up to 48 hpf (Fig. 5.9). 70% of the embryos (N=20) injected with the sensor plasmid alone displayed fluorescence (Fig. 5.8.A-B). This percentage decreased to 51% when the plasmid was co-injected with *ccdc80-l1*-MO (N= 93) (Fig 5.9.C-D), indicating that the morpholino specifically bounds to its target region.

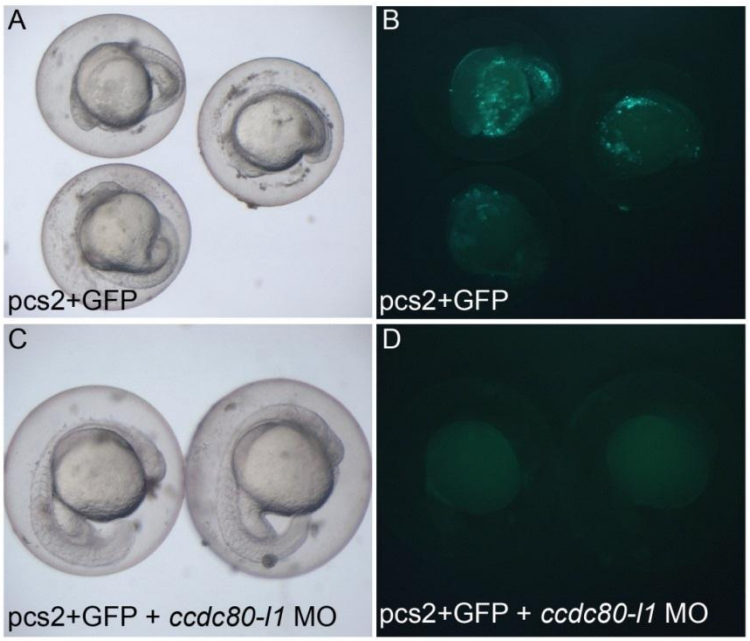

Figure 5.9: *ccdc80-l1* morpholino is capable to inhibit the expression of the fluorescent protein GFP. *(A, B)* In the 70% of embryos injected with the *ccdc80-l1*-GFP sensor plasmid, the presence of fluorescent GFP signal was detected (N= 20). *(C, D)* When the plasmid was injected together with the morpholino, the transcription of GFP protein was inhibited and the percentage of fluorescent embryos decreased to 51% (N=93). In *A* and *C* embryos are visualized under normal light, in *B* and *D* under fluorescent light.

The efficiency of *ccdc80-l1* loss-of-function was not so striking, as demonstated by the low percentage of embryos with GFP decreasement and by the high amount of morpholino we had to inject to obtain a phenotype (8 and 12 ng/embryo of *ccdc80-l1*-MO). Therefore, we designed a second morpholino against the splice site (*ccdc80-l1*-splice-MO) to confirm the specificity of *ccdc80-l1*-loss-of-function. Embryos injected with this second morpholino, still exhibited motility issues as *ccdc80-l1*-MO-injected embryos did (*data* not shown). In particular, all the knocked-down embryos showed no severe body plan alteration when observed *in vivo*, indicating the proper progression of early developmental processes such as gastrulation and segmentation (Griffin *et al*., 1995; Holley, 2007; Melby *et al*., 1996; Stickney *et al*., 2000). Moreover, we observed that morphants displayed physiological body contractions upon dechorionation at 24 hpf (Saint-Amant and Drapeau, 1998). However, at 48 hpf, almost 80% of the morphant embryos (N=37) presented abnormal escaping behavior after tactile stimulation, often resulting in body contractions on the spot or circling behavior rather than a fast escape in the opposite direction to the stimulus. The same phenotype was observed also at 5 days post fertilization (5 dpf, *data* not shown). These results indicated that *ccdc80-l1* loss-of-function affects the swimming behavior of zebrafish embryos and larvae. We were also able to rescue the *ccdc80-l1*-loss-of-function phenotype by means of the injection of the homolog *ccdc80*-full-length transcript. In fact, despite we demonstrated that *ccdc80*-loss-of-function did not affect axonal pathfinding (*data* not shown), the high degree of conservation between the two homologs allowed rescue of motility (only 42% of rescued embryos presented motility issues in comparison to the nearly 80% of *ccdc80-l1*-MO injected embryos, N=63)

5.3.3 *ccdc80-l1* loss of function does not affect somitogenesis nor muscle pioneers and adaxial cells formation

To assess whether the phenotype displayed by morphants was due to the impairment of musculature, somitogenesis and myogenesis markers were examined. The expression of *myod* and *myog* (Holley, 2007; Rescan, 2001) was not altered in *ccdc80-l1*-MO-injected embryos (Fig. 5.10.A-D). Moreover, the expression of *smyhc1*, a marker of slow-twitch fibers (Elworthy *et al*., 2008), was unaffected as well (Fig. 5.10.E-F), notwithstanding the strong expression of *ccdc80-l1* in adaxial cells and muscle pioneers, from which slow fibers develop (Wolff *et al*., 2003). In addition, at 24 hpf, myofibers were correctly organized and distributed as shown by the immunohistochemistry with anti-sarcomeric MF20 antibody (Bader *et al*.,

1982) (Fig. 5.10.G-H). Also muscle pioneers, labeled with 4D9 anti-engrailed antibody (Hatta *et al*., 1991; Patel *et al*., 1989) were correctly formed in *ccdc80-l1* morphants (Fig. 5.10.I-J). These results indicate that defects of adaxial cells, muscle pioneers or body musculature formation could not be responsible for motility issues observed in *ccdc80-l1* knocked-down embryos.

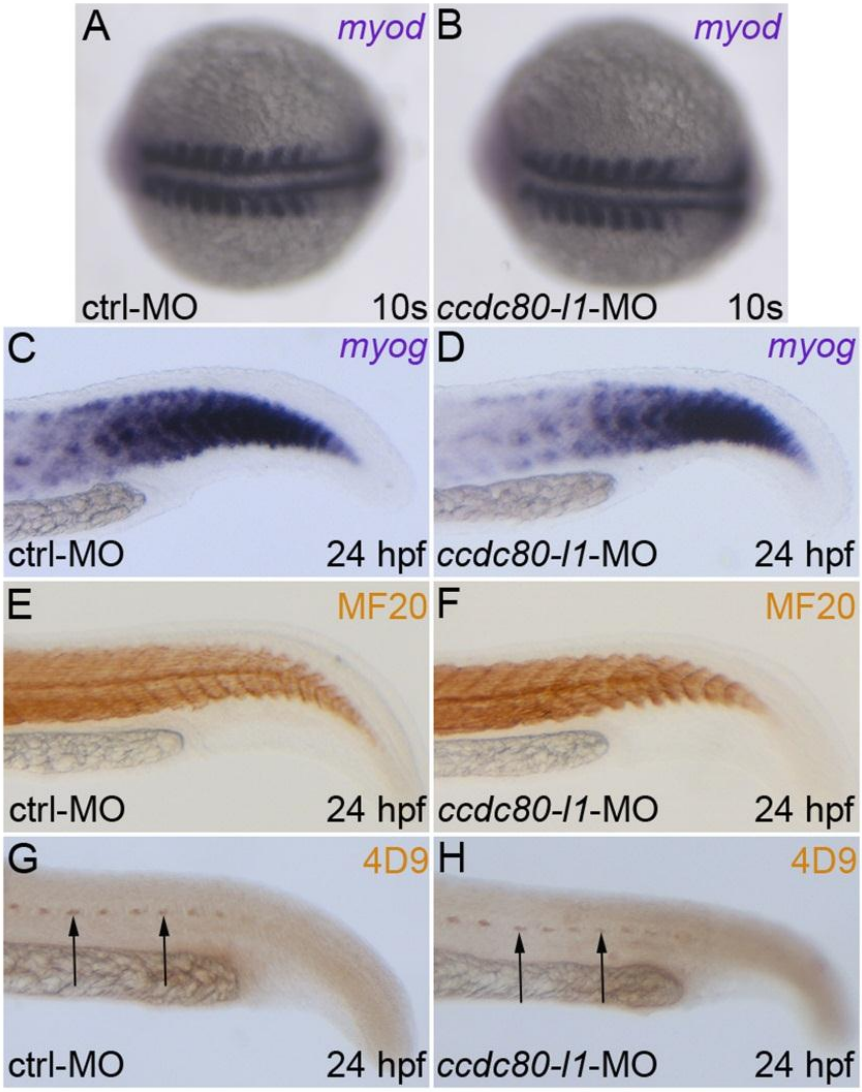

Figure 5.10: Analysis of myogenic markers expression and muscle pioneers in *ccdc80-l1* morphant embryos. *(A-D)* The myogenic markers *myod (A-B)* and *myog (C-D)* were correctly expressed both in control and morphants embryos at 10 s stage *(A, B)* and 24 hpf *(C-D)*, respectively. *(E-F) ccdc80-l1* loss of function did not perturb the expression of *smyhc1*, as morphant embryos *(F)* are indistinguishable from control embryos *(E)*. *(G-H)* The MF20 antibody staining showed that both slow and fast twitch fibers were correctly formed and organized in control *(G)* and in knocked-down embryos *(H)* at 24 hpf. *(I-J)* At the same developmental stage, muscle pioneers resulted unaffected after *ccdc80-l1* loss-of-function, as shown by the labeling with 4D9 antibody (anti-engrailed) (arrows). *(A-B)* Dorsal views, anterior is left; *(C-J)* lateral views of the tails, dorsal is up and anterior is left.

5.3.4 analysis of neurogenesis of primary motoneurons in *ccdc80-l1* morphants

Due to motility impairment of *ccdc80-l1* morphants, motoneurons development was investigated performing both WISH with PMNs molecular markers and immunohistochemistry with znp1 and zn-5 antibody against PMNs and SMNs (Fashena and Westerfield, 1999; Trevarrow *et al*., 1990). *sema3e* and *islet1* were used as markers of primary motoneurons soma at 24 and 26 hpf, respectively (Hutchinson and Eisen, 2006; Lamont *et al*., 2009). The expression patterns of both transcript in *ccdc80-l1* morphants resulted unaltered when compared to control embryos (Fig. 5.11), revealing that PMNs are present and correctly specified.

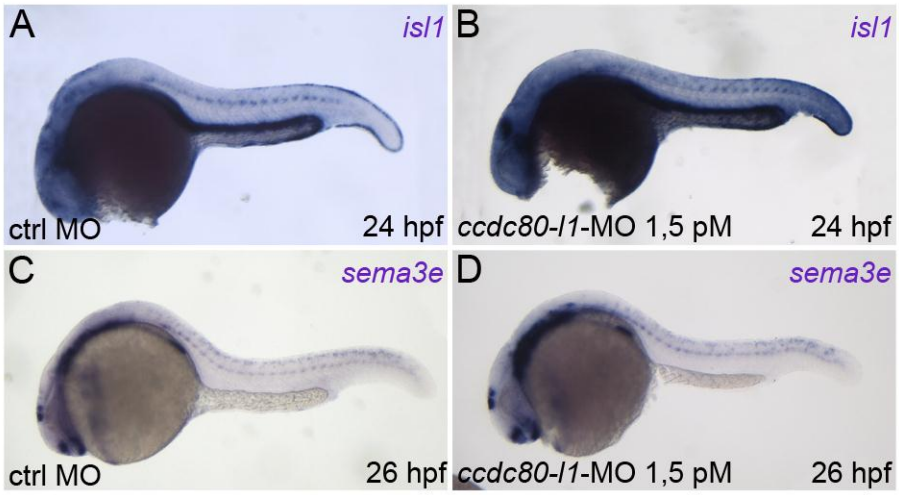

Figure 5.11: Analysis of PMNs soma markers in *ccdc80-l1* morphants. *(A-B) isl1* expression resulted unaltered by *ccdc80-l1* loss of function *(B)* in comparison with control embryos *(A)*. *(C-D)* Also *sema3e* was correctly expressed both in control *(C)* and in morphants embryos *(D)*. *(A-D)* Lateral views, rostral is left.

Axonal migration was analyzed at 48 hpf, by means of immunohistochemistry. For all embryos, we analyzed the trunk region overhanging the yolk extension; defects in at least three motoneurons were enough to consider the embryo as affected. At 48 hpf, in the 84% (N=33) of morphants injected with 12 ng/embryo of morpholino, axonal pathfinding resulted impaired. 60% of morphants displayed an overall disorganization: both dorsal and ventral motoneurons resulted mis-orientated and over-branched (Fig. 5.12.A-C). In the 9% of embryos, these defects were observed together with an opposite phenomenon, axonal stalling. In the 12% of *ccdc80-l1* only ventral axons resulted mis-orientated and over-branched, whereas in the 3% only the dorsal ones were affected (Tab. 5.2). This phenotype was dose-dependent: when 8 ng/embryo of morpholino were used, a lower percentage of embryos resulted affected (64%, N=35) (Tab. 5.2). Interestingly, at this concentration, only 27% of the knocked-down embryos displayed both ventral and dorsal defective axons, whereas in the 37% of morphants the same defects were detectable in the ventral motoneurons solely. Dorsal axons alone were never affected (Tab. 5.2). Thus, a striking reduction of CCDC80-l1 protein amount led to the affection of both ventral and dorsal motoneurons, whereas a lower dose of morpholino is sufficient for ventral axons migration impairment. In order to discriminate whereas loss-of-*ccdc80-l1*-function impaired PMNs or SMNs, we analyzed morphants phenotype also at 26 hpf and 30 hpf, by the time SMNs have just begun extending axons (Fashena and Westerfield, 1999), so most of znp1 labeling correspond to PMNs. At this stages, we replicated the same phenotype observed at 48 hpf (Fig. 5.12.D-G). Furthermore, we performed an immunohistochemistry at 48 hpf using Alcam , a specific antibody for SMNs axons (Fashena and Westerfield, 1999). We observed that also SMNs axons seems to be affected after loss-of-*ccdc80-l1*-function (Fig. 5.12.G-H). Thus, the analysis of the motoneuronal patterning in morphant embryos revealed that *ccdc80-l1* plays a role in both PMNs and SMNs axonal pathfinding. In fact, *ccdc80-l1* loss-of-function leads to defects in primary and secondary motoneurons, that often lost their proper pattern and branched excessively or stalled, indicating the lack of proper guidance toward muscle targets.

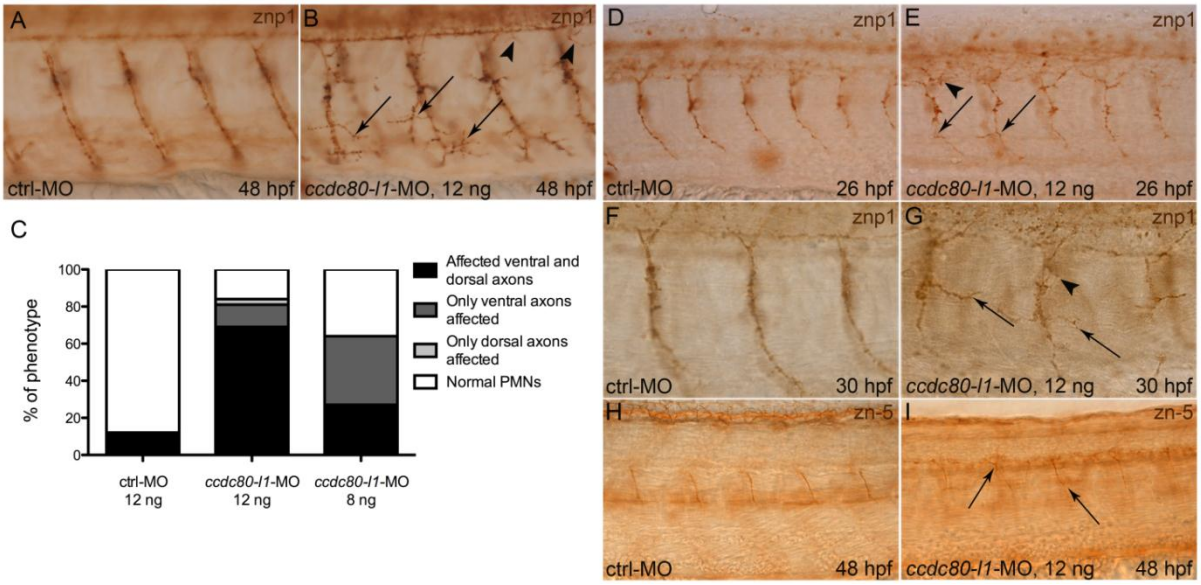

Figure 5.12: Analysis of motoneurons morphology by means of znp1-immunohistochemistry. *(A, B)* At 48 hpf, using 12 ng/embryo of morpholino, both ventral (arrows) and dorsal axons (arrowheads) were mis-orientated and over-branched in morphants *(B)* in comparison to control embryos *(A)*. *(C)* Statistical analysis showing the percentages of the different phenotypes (affected ventral axons, dorsal axons or both) occurring in control embryos and in morphants, when different doses of *ccdc80-l1*-MO were injected (12 ng/embryo and 8 ng/embryo). Using a lower dose of morpholino (8 ng/embryo), we observed that in a significant percentage of embryos only ventral axons were defective. *(D-G)* Immunohistochemistry performed at 26 hpf *(D, E)* and 30 hpf *(F, G)* confirmed that loss-of-*ccdc80-l1*-function affects both CaPs (arrows) and MiPs (arrowheads) axonal migration. *(H, I)* The same analysis performed at 48 hpf using Alcam antibody revealed that also SMNs axonal migration is impaired in morphants (arrows) *(A, B; D-I)* Lateral flat-mount preparation was applied for a better visualization of the motoneurons. Lateral views of the trunk region overhanging the yolk extension, dorsal is up and anterior is left.

Dose/type of morpholino	Total percentage of affected embryos (N)	Alteration of both CaP and MiP	Only CaP affected	Only MiP affected
ctrl-MO 12 ng	12% (N=25)	12%	0%	0%
ccdc80-l1-MO 12 ng	84% (N=33)	69%	12%	3%
ccdc80-l1-MO 8ng	64% (N=35)	27%	37%	0%

Table 5.2: The phenotype of *ccdc80-l1*-MO-injected embryos is dose-dependent. The percentage of embryos displaying axonal defects decreased from 84% to 64% when a lower dose of morpholino was used. Both CaP and MiP axonal pathfinding resulted impaired in the most part of affected embryos (69%) when 12 ng of morpholino were used. After the injection of 8 nh of *ccdc80-l1*-MO, most part of affected embryos (37%) displayed only CaP defects, whereas MiP alone were never affected.

5.3.5 Also *ccdc80-l1* expression is positively regulated by the Hedgehog pathway

Due to *ccdc80-l1* expression in adaxial cells and muscle pioneers, the existence of a *ccdc80-l1* up-stream regulation Hedgehog-mediated was investigated. We modulated *shh* activity by exposing embryos to cyclopamine. To avoid the complete loss of the territories in which *ccdc80-l1* is expressed, we chose a concentration of cyclopamine (5µM) by which muscle pioneers and adaxial cells-derived slow fibers are unaffected as already described (Wolff *et al.*, 2003) and as we demonstrated by the proper expression of their markers engrailed, *myod* and *smyhc1* respectively. (Fig. 5.13).

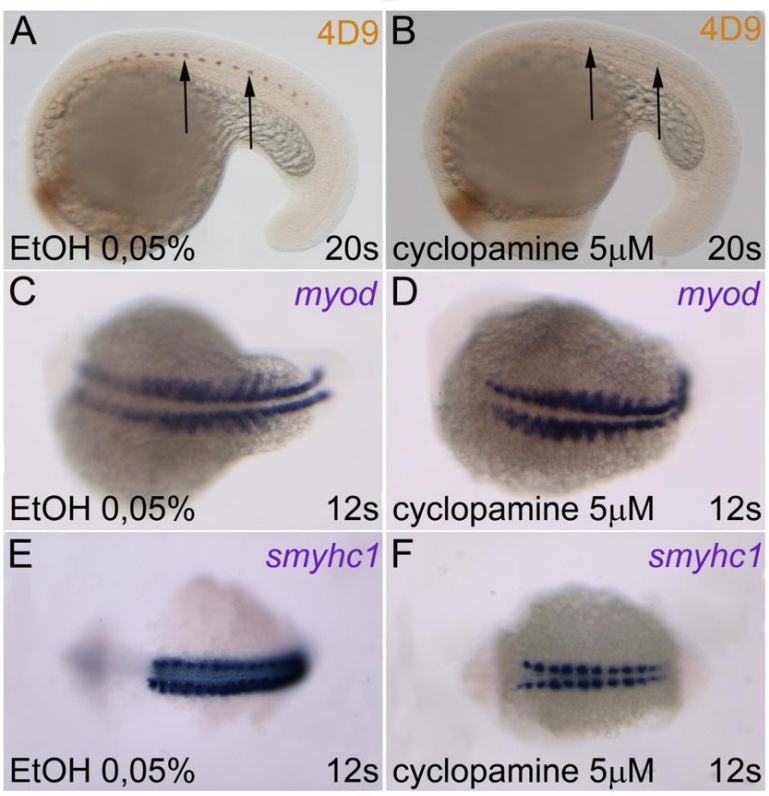

Figure 5.13: Muscle pioneers and adaxial cells are not lost after 5µM cyclopamine treatment. *(A, B)* Labeling with 4D9 antibody (anti-engrailed) showed that muscle pioneers are not missing after pharmacological inhibition of the hedgehog pathway (arrows). *(C-F)* Also adaxial cells are still present, as shown by the expression of the markers *myod (C, D)* and *smyhc1 (E, F)*. *(A, B)* Lateral views, dorsal is up. *(C-F)* Dorsal views, anterior is left.

A striking down-regulation of *ccdc80-l1* expression was observed in 72% of the treated embryos (N=32) (Fig 5.14.A-B). Interestingly, this down-regulation was detectable only at the level of myoseptum and somites, whereas the cephalic and dorsal territories in which *ccdc80-l1* is expressed were not involved. A similar down-regulation was observed in *syu* mutants,

carriers of a deletion in the gene *sonic-you* encoding for *shh* (Schauerte *et al*., 1998). *ccdc80-l1* signal in adaxial cells was extremely weak or absent in the 35% of mutants, and slightly down-regulated in the 40% of observed embryos (N=20) (Fig. 5.14.D-F). Moreover, the overexpression of *shh* by means of the injection of the full-length transcript (300 pg/embryo), led to the opposite phenotype with an increasing of *ccdc80-l1* expression in the somites of the 71% of the injected embryos (N=31) (Fig. 5.14.C). On the contrary, *ccdc80-l1* loss-of-function did not affect *shh* expression (Fig. 5.15). Therefore, these findings suggest that *ccdc80-l1* is a down-stream target of the Hedgehog pathway.

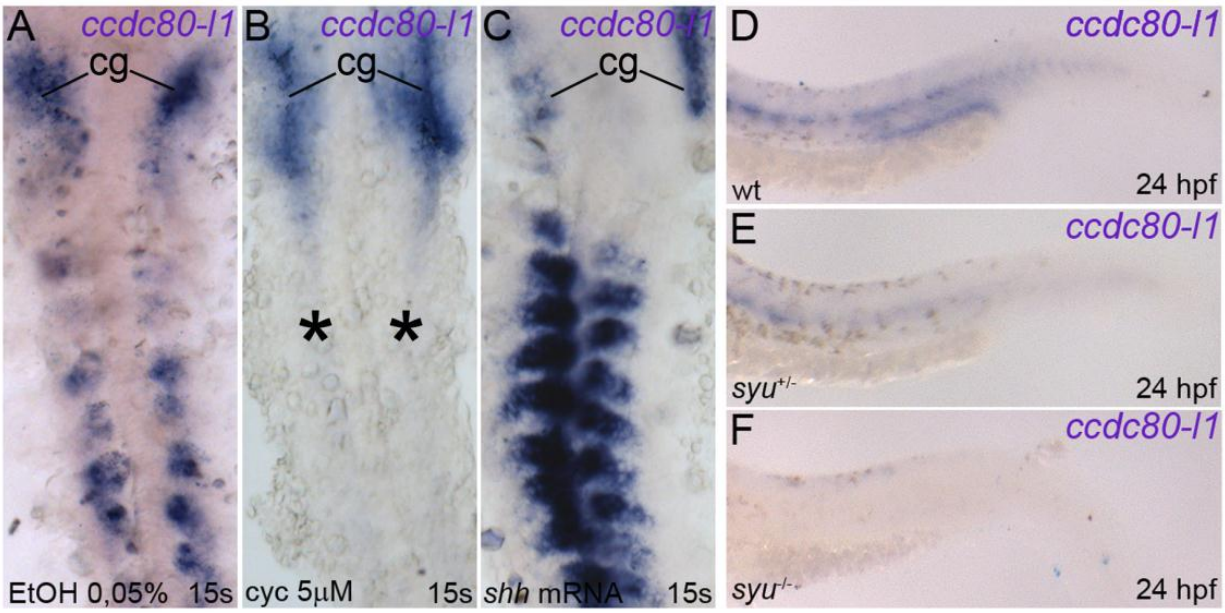

Figure 5.14: *ccdc80-l1* is positively regulated by *shh*. *(A-C) ccdc80-l1* expression in somites and myoseptum resulted strongly inhibited in embryos treated with 5 µM cyclopamine (asterisks in *B*), in comparison to control embryos at the same developmental stage *(A)*. By converse, over-expression of *shh* led to an up-regulation of *ccdc80-l1* in muscular territories *(C)*. Expression in cranial ganglia (cg) was never perturbed. *(D-F) ccdc80-l1* resulted slightly down-regulated also in the trunk of heterozygous *syu* mutants *(E)* in comparison to wild type siblings *(D)*. A strikingly down-regulation was observed in homozygous mutants *(F)*. *(A-C)* Dorsal flat-mount preparations, anterior is up. *(D-F)* Lateral views of the tails, anterior is left.

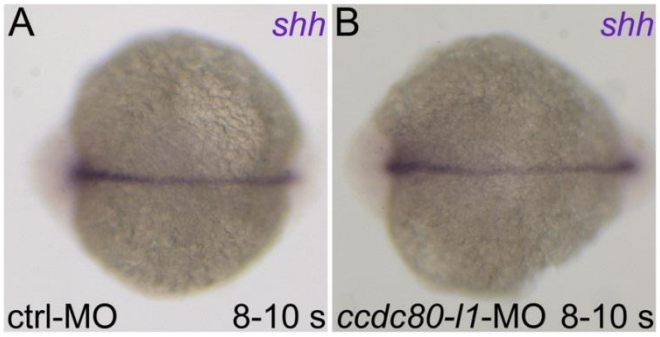

Fig 5.15: *shh* expression is not perturbed by loss-of-*ccdc80-l1*-function. *(A, B) shh* resulted correctly expressed both in control embryos *(A)* and in morphants *(B)*. *(A, B)* Dorsal views, anterior is left.

5.4.1 *ccdc80* expression is not regulated by *ccdc80-l1*, nor *vice versa*

According to our hypothesis, *ccdc80-l1* arose from a duplication of *ccdc80*, and both genes are regulated by the same Hedgehog pathway. Bearing in mind these observations, we decided to test the presence of a regulatory and/or synergic relationship between the two genes. Thus, we analyzed the expression of *ccdc80* after *ccdc80-l1* loss-of-function, and *vice versa*. The expression pattern of *ccdc80* resulted unaltered after the injection of *ccdc80-l1*-MO (Fig. 5.16), indicating that the latter is not necessary for the transcriptional activation of the former. Also *ccdc80-l1* expression resulted to be independent from *ccdc80*, given that both loss- and gain-of-*ccdc80*-function experiments did not lead to alterations of *ccdc80-l1* expression pattern and levels (Fig. 5.17)

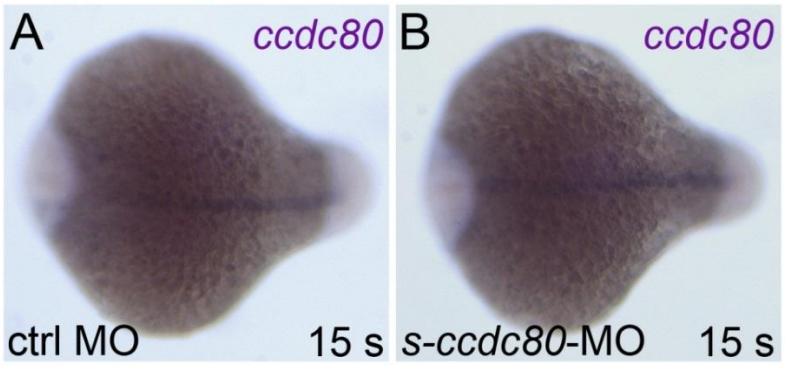

Figure 5.16: The expression pattern of *ccdc80* is unaltered after *ccdc80-l1* loss-of-function. *(A-B)* Control embryos *(A)* are indistinguishable from morphants *(B)*. *(A-B)* Dorsal views, rostral is left.

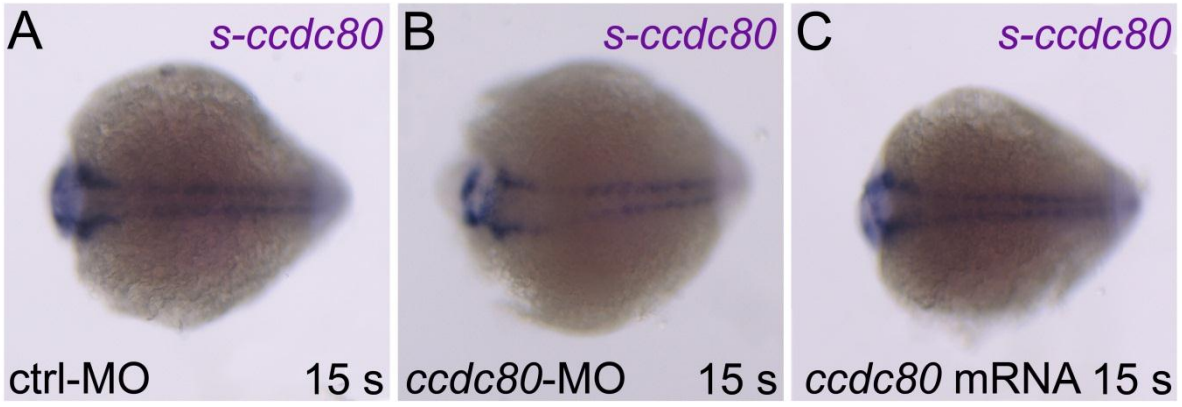

Figure 5.17: *ccdc80-l1* expression is not regulated by *ccdc80*. Expression pattern of *ccdc80-l1* is unaltered between control embryos *(A)*, *ccdc80* morphants *(B)* and *ccdc80* overexpressed embryos *(C)*. *(A-C)* Dorsal views, anterior is left.

To verify whether a synergic effect could exist between *ccdc80* and *ccdc80-l1* functions, the two morpholinos were injected together. Injected embryos were then tested at 48 hpf for their motor behavior after tactile stimulation. For both morpholinos a lower dose than what was used in the previous loss-of-function experiments was used. Hence, the aggravation of the phenotype between single- and double-injection resulted more easily assessable. 88% of uninjected embryos, used as positive controls, showed standard motor behavior: they fast escaped after touch stimuli, and just the 12% did not move. 91% of Embryos injected with 0,5 pM of *ccdc80*-MO reacted standardly when touched, whereas 9% of them showed muscle contractions on the spot or circular swimming (Tab. 5.3). Similar percentages were observed when 0,3 pM of *ccdc80-l1* was injected: the 83% of morphants showed touch evoked swimming whether the 17% reacted aberrantly, with muscle contraction on the spot or circular swimming. When the two morpholinos were co-injected, there was no aggravation of this phenotype, nor the increase of the percentage of affected embryos: standard motor behavior was observed in the 90% of double morphants, whether the 10% showed aberrant swimming (Tab. 5.3). These results indicate that *ccdc80* and *ccdc80-l1* do not act synergically for zebrafish embryo motility.

	Standard motor behavior	Aberrant motor behavior	Total number of embryos
Uninjected embryos	88%	12%	25
ccdc80-MO 0,5 pM	91%	9%	35
s-ccdc80-MO 0,3 pM	83%	17%	44
Co-injected embryos	90%	10%	37

Table 5.3: *ccdc80* and *ccdc80-l1* do not co-operate nor act synergically. Standard motor behavior after tactile stimulation was observed in similar percentages in all treated embryos as in controls. Also the percentages of affected embryos were comparable between single injections and the double injection, and were not significantly different from the positive control (uninjected embryos).

Discussion
and
future perspectives

6.1 *ccdc80* and zebrafish somitogenesis

Somitogenesis is the process by which the vertebrate trunk is divided into a series of segments termed somites. In zebrafish, somites bud off sequentially, in an anterior to posterior fashion from the unsegmented presomitic mesoderm. This complex process requires a segmentation clock that comprises oscillations in gene expression in individual cells within the PSM. These oscillations are synchronized between adjacent cells such that stripes of gene expression are formed and move in a posterior to anterior direction through the PSM. The coordination of this mechanism is guaranteed by several molecular pathway, such as Notch, Fgf and Bmp pathways (Ishimatsu *et al*., 2010; Lewis and Ozbudak, 2007; Patterson *et al*., 2010). A pivotal role is played by the Hedgehog signaling, by means of secreted molecules by the notochord (Lewis *et al*., 1999; Wolff *et al*., 2003). In fact, mutants lacking the notochord show often somitogenesis defects (reviewed by Stickney *et al*., 2000), and modulation of Shh protein affects the proper formation of somites and then muscular structures (reviewed by Ingham and Kim, 2005). *ccdc80* is expressed in the notochord by the time somites are formed and specified. Its function is not fundamental for notochord development, as injection of *ccdc80* morpholino or mRNA does not lead to the impairment of medial structures. Moreover, despite its zygotic expression, *ccdc80* is not required for embrionic proper development during early stages. By converse, both morphants and overexpressed embryos displayed severe somitogenesis defects. These observation suggest that *ccdc80* could be a potential signal secreted by the notochord. Ccdc80 protein show a signal peptide, besides nuclear localization signals, suggesting that it could be both secreted and internalized. Investigation on its cellular localization in zebrafish is still needed, whereas several studies already indicated human, rat, mouse and chicken homologs of Ccdc80 as secreted proteins (Bommer *et al*., 2005; Ferragud *et al*., 2011; Liu *et al*., 2004; Mu *et al*., 2003; Visconti *et al*., 2003). Analysis of the expression patterns of different somitogenesis markers, both on morphants and overexpressed embryos, confirmed that somites lost their proper pattern. In particular, synchronization of molecular clock oscillations seemed to be lost after both loss- and gain-of-*ccdc80*-function, given that the earliest marker we analyzed, *her1*, clearly resulted asymmetric and disorganized. Consequently, the expression pattern of *myod*, the marker of the last step of somitogenesis, resulted strikingly altered. Thus, *ccdc80* may play a role in somitogenesis from the earliest phases, impairing subsequent stages. Nevertheless, the phenotype displayed by morphants seemed to be recovered later in development, and motility is not impaired at 24 hpf, even if the gross morphology of the embryos is slightly affected (curved tails). Hence, *ccdc80* function may be relevant but not necessary for somites formation; this is consistent with the plenty of pathways that regulate

this process and the complexity of positive and negative feedback loops involved (Mara and Holley, 2007).

In support of the hypothesis of Ccdc80 secretion by the notochord, interaction with the Hedgehog pathway was demonstrated. Expression of *ccdc80* resulted directly regulated by the levels of Shh protein, and the opposite phenomenon was never observed. These findings strongly indicate *ccdc80* as a down-stream effector of *shh*: its expression is promoted by *shh* in the notochord, and the protein is then released in the surrounding tissues, playing a role in somitogenesis. The identification of potential targets is in progress: our collaborators in Modena verified the interaction *in vitro* with *gadd45β1* and *gadd45β2* proteins, which are known to be involved in somitogenesis, even if their function is not well known yet (Kawahara *et al*., 2005). Preliminary *data in vivo*, suggest that *ccdc80* positively regulates *gadd45β2* and negatively regulates *gadd45β1*. Given that the two genes are expressed in somites, whereas *ccdc80* is expressed in the notochord, the regulative interaction among the three proteins could be a further evidence of the secretion of *ccdc80* from the notochord in the somites.

Human CCDC80 is highly expressed in skeletal muscle and heart, suggesting the importance of its function in this tissues (Visconti *et al*., 2003; Raymond *et al*., 2010). In zebrafish, the role of *ccdc80* in muscle formation was demonstrated, and also the potential role of *ccdc80* in heart development has been investigated. Preliminary *data* suggest that loss-of-*ccdc80*-function leads to heart defects such as lack of looping, dilatation of the atrium and the atrium-ventricular valve. However, *ccdc80* overexpression did not cause heart defects (unpublished *data*). In human, *CCDC80* was found to be up-regulated in myocardial samples from patients affected by dilated cardiomyopathy (Barth *et al*., 2006), suggesting the evolutionary conservation of *ccdc80* function between zebrafish and human as regards heart development. Zebrafish *ccdc80* could have similar functions also with respect to homologs of the other vertebrates. In fact, the potential involvement in eye development as in chick (Mu *et al*., 2003) or in energy metabolism and skeletogenesis as in mice (Aoki *et al*., 2002; Tremblay *et al*., 2009) has not been investigated yet and could be a future prospective.

6.2 *ccdc80-l1* and axonal pathfinding

The genetic program underlying axon guidance is not completely defined. Adaxial cells and muscle pioneers are both involved in axonal outgrowth and pathfinding (Melancon *et al*., 1997; Zeller and Granato, 1999), even if little is known about the specific proteins and molecular mechanisms acting in this process. *ccdc80-l1* is expressed during embryonic

development in muscle pioneers and adaxial cells. *ccdc80-l1*-MO-injected embryos displayed physiological body contractions upon dechorionation at 24 hpf; at 48 hpf embryos were still able to move, but tactile stimuli induced an abnormal escaping behavior. Both musculature and nervous system are responsible for embryonic motility and touch response and are the basis of spontaneous motor output that occurs in the developing zebrafish embryo ever since 18 hpf (Menelaou *et al*., 2008). Nevertheless, musculature defects were unlikely the basis of the observed phenotype. Indeed, there was no difference between the expression pattern of myogenic markers in morphants and control embryos. Moreover, muscle fibers resulted correctly formed and distributed by the end of somitogenesis. The territories in which *ccdc80-l1* is expressed were unaffected as well: in fact, adaxial cells and muscle pioneers showed no defects. These findings revealed that *ccdc80-l1* function is not necessary for the specification and further differentiation of myogenic cell populations, suggesting that the motility issues displayed by morphants at 48 hpf could be due to an impairment of neurogenesis.

The analysis of motoneuronal development in morphant embryos revealed that *ccdc80-l1* plays a role in motoneurons axonal pathfinding. In fact, *ccdc80-l1* loss-of-function did not prevent the formation of PM and axon projection, but led to an overall disorganization of PM. CaP and MiP resulted mis-orientated and over-branched in a high percentage of embryos, whereas a smaller fraction of morphants displayed also the simultaneous presence of its opposite phenomenon, axonal stalling. However, the growth cones are still able to exit the spinal cord, most of them reach the muscle pioneers along the common pathway, and axonal extensions develop without altering the target choice: in fact, CaP and MiP still projected their axons ventrally and dorsally, respectively. These *data* are consistent with the proper development of muscle pioneers, which provide a choice point for motor growth cones. Axonal over-branching and stalling were detected in the CaP solely in a significant percentage of embryos, especially when a lower dose of morpholino was used. Moreover, the impairment of axonal migration was more severe in CaP then in MiP, even when both PM were affected simultaneously. These *data* suggest that *ccdc80-l1* may have a differential role as regards the development of CaP and MiP. This is consistent with the asymmetric distribution of *ccdc80-l1* transcript in the somites: indeed, the *ccdc80-l1* transcript is present in the ventral portion of somites, innervated by CaP, and not in their dorsal portion, innervated by MiP. The same motility issues displayed at 48 hpf were observed also at 5 dpf, when secondary motoneurons are already formed (Eisen, 1991). Indeed, *ccdc80-l1* loss-of-function led also to the mis-expression of SMNs marker zn-5. This is not surprising, as the growth cones of SMNs require the axons of PMNs for proper pathfinding (Eisen, 1991). In conclusion, *ccdc80-l1* loss-of-function prevents the proper development of the peripheral

nervous system, that lacks a proper guidance toward muscle target: axons do not fallow a single direction-pathway but stall or extend towards any direction, leading to an over-branched and non-functional nervous network. Hence, embryos are able to move and to respond to tactile stimuli, but the coordination of muscle contractions is impaired, and motor behavior is affected.

The Hedgehog signaling is fundamental for both axon guidance and adaxial cells and muscle pioneers formation (Charron and Tessier-Lavigne, 2005; Wolff *et al*., 2003), and it is known to play a pivotal role in the specification of both primary and secondary motoneurons (Beattie *et al*., 1997; Lewis and Eisen, 2001). Indeed, mutants for different molecules involved in this pathway displayed axonal defects, including random axonal migration or stalling (Chen *et al*., 2001; Schauerte *et al*., 1998). PM target choice was never impaired after *ccdc80-l1* loss-of-function, still axonal migration resulted aberrant. Furthermore, *ccdc80-l1* expression resulted strikingly down-regulated after exposure to 5 μM of cyclopamine in the body musculature of the zebrafish embryo. This modulation was observed only in muscles and not in other territories in which *s-ccc80* is expressed (cranial ganglia and dorsal dermis). Moreover, the overexpression of *shh* led to an up-regulation of *ccdc80-l1* expression. These findings strongly suggest the existence of a specific regulation of *ccdc80-l1* Hedgehog-mediated as regards its function in motoneuronal development. Interestingly, the opposite effect was not observed: *ccdc80-l1* loss-of-function did not affect the expression of *shh*. These findings strongly indicate *ccdc80-l1* as a down-stream effector of the Hedgehog pathway for what concern axonal pathfinding. Further analysis on the predicted Ccdc80-l1 protein sequence and its cellular distribution will help to understand the molecular process underlying its functioning. Moreover, investigation on possible targets is still needed. Indeed, other cues contribute to proper pathway navigation in zebrafish. For instance, the semaphorin and netrin families are both involved in attracting and/or repelling growth cones from a variety of organisms (Lauderdale *et al*., 1997; Tessier-Lavigne and Goodman, 1996), and the possibility of an interaction with *ccdc80-l1* has not been investigated yet. Nevertheless, results from *ccdc80-l1* functional study provided further insights into motoneurons development, a complex mechanism that requires the action of several different molecules. Moreover, these findings may shed light on the involvement of the Hedgehog pathway in this process.

6.3 Interaction between the two homologs

Zebrafish is the only vertebrate in which paralogs of *ccdc80* are present (Pawlowsky *et al*., 2010). Gene duplication is very common in this species, and often paralogs adopt different

functions (Postlethwait *et al*., 2011). Even if *ccdc80* and *ccdc80-l1* resulted to be regulated by the same pathway, in particular by *shh*, they displayed different expression patterns and very distinct roles during embryonic development. In fact, *ccdc80* seems to be secreted by the notochord and to regulate somitogenesis, whereas *s-ccd80* is involved in axonal pathfinding of primary motoneurons. The two paralogs do not cooperate neither: results from motility test on embryos injected with the two morpholinos together clearly showed that there is no synergic effect, since double and single morphants respond to touch stimuli in the same manner. Moreover, *ccdc80* do not regulate *ccdc80-l1* expression, and there is no evidence of the reverse phenomenon. Hence, *ccdc80* and *ccdc80-l1* could derive from an ancestor gene, and despite the high percentage of identity and similarity between the two sequences, during evolution they acquired very different roles. Moreover, also the molecular mechanism underlying their functions may be different, since Ccdc80, but not Ccdc80-l1, display a signal peptide besides nuclear localization signals, suggesting it could be secreted. However, the presence of three conserved P-DUDES domains in both proteins may indicate the conservation of similar biological functions. Nevertheless, both genes are involved in key processes for early motility, that is fundamental for escape predators and to provide nourishment, and then for embryonic viability in the external environment.

References

Aoki, K., Sun, Y. J., Aoki, S., Wada, K. and Wada, E. (2002). Cloning, expression, and mapping of a gene that is upregulated in adipose tissue of mice deficient in bombesin receptor subtype-3. *Biochem Biophys Res Commun* **290**, 1282-8.

Bader, D., Masaki, T. and Fischman, D. A. (1982). Immunochemical analysis of myosin heavy chain during avian myogenesis in vivo and in vitro. *J Cell Biol* **95**, 763-70.

Barresi, M. J., D'Angelo, J. A., Hernandez, L. P. and Devoto, S. H. (2001). Distinct mechanisms regulate slow-muscle development. *Curr Biol* **11**, 1432-8.

Barth, A. S., Kuner, R., Buness, A., Ruschhaupt, M., Merk, S., Zwermann, L., Kaab, S., Kreuzer, E., Steinbeck, G., Mansmann, U. et al. (2006). Identification of a common gene expression signature in dilated cardiomyopathy across independent microarray studies. *J Am Coll Cardiol* **48**, 1610-7.

Beattie, C. E. (2000). Control of motor axon guidance in the zebrafish embryo. *Brain Res Bull* **53**, 489-500.

Beattie, C. E., Hatta, K., Halpern, M. E., Liu, H., Eisen, J. S. and Kimmel, C. B. (1997). Temporal separation in the specification of primary and secondary motoneurons in zebrafish. *Dev Biol* **187**, 171-82.

Blagden, C. S., Currie, P. D., Ingham, P. W. and Hughes, S. M. (1997). Notochord induction of zebrafish slow muscle mediated by Sonic hedgehog. *Genes Dev* **11**, 2163-75.

Bommer, G. T., Jager, C., Durr, E. M., Baehs, S., Eichhorst, S. T., Brabletz, T., Hu, G., Frohlich, T., Arnold, G., Kress, D. C. et al. (2005). DRO1, a gene down-regulated by oncogenes, mediates growth inhibition in colon and pancreatic cancer cells. *J Biol Chem* **280**, 7962-75.

Charron, F. and Tessier-Lavigne, M. (2005). Novel brain wiring functions for classical morphogens: a role as graded positional cues in axon guidance. *Development* **132**, 2251-62.

Chen, W., Burgess, S. and Hopkins, N. (2001). Analysis of the zebrafish smoothened mutant reveals conserved and divergent functions of hedgehog activity. *Development* **128**, 2385-96.

Della Noce I. Identification and functional characterization of the *CL2* (*URB*) gene during embryonic development in zebrafish (*Danio rerio*). Ph.D. thesis (2009).

Devoto, S. H., Melancon, E., Eisen, J. S. and Westerfield, M. (1996). Identification of separate slow and fast muscle precursor cells in vivo, prior to somite formation. *Development* **122**, 3371-80.

Downes, G. B. and Granato, M. (2006). Supraspinal input is dispensable to generate glycine-mediated locomotive behaviors in the zebrafish embryo. *J Neurobiol* **66**, 437-51.

Durbin, L., Sordino, P., Barrios, A., Gering, M., Thisse, C., Thisse, B., Brennan, C., Green, A., Wilson, S. and Holder, N. (2000). Anteroposterior patterning is required within segments for somite boundary formation in developing zebrafish. *Development* **127**, 1703-13.

Echeverri, K. and Oates, A. C. (2007). Coordination of symmetric cyclic gene expression during somitogenesis by Suppressor of Hairless involves regulation of retinoic acid catabolism. *Dev Biol* **301**, 388-403.

Eisen, J. S. (1991). Motoneuronal development in the embryonic zebrafish. *Development* **Suppl 2**, 141-7.

Eisen, J. S. (1999). Patterning motoneurons in the vertebrate nervous system. *Trends Neurosci* **22**, 321-6.

Elworthy, S., Hargrave, M., Knight, R., Mebus, K. and Ingham, P. W. (2008). Expression of multiple slow myosin heavy chain genes reveals a diversity of zebrafish slow twitch muscle fibres with differing requirements for Hedgehog and Prdm1 activity. *Development* **135**, 2115-26.

Ericson, J., Morton, S., Kawakami, A., Roelink, H. and Jessell, T. M. (1996). Two critical periods of Sonic Hedgehog signaling required for the specification of motor neuron identity. *Cell* **87**, 661-73.

Fashena, D. and Westerfield, M. (1999). Secondary motoneuron axons localize DM-GRASP on their fasciculated segments. *J Comp Neurol* **406**, 415-24.

Felsenfeld, A. L., Curry, M. and Kimmel, C. B. (1991). The fub-1 mutation blocks initial myofibril formation in zebrafish muscle pioneer cells. *Dev Biol* **148**, 23-30.

Ferragud, J., Avivar-Valderas, A., Pla, A., De Las Rivas, J. and de Mora, J. F. (2011). Transcriptional repression of the tumor suppressor DRO1 by AIB1. *FEBS Lett* **585**, 3041-6.

Gasteiger, E., Hoogland, C., Gattiker, A., Duvaud, S., Wilkins, M.R., Appel, R.D., Bairoch, A. (2005). Protein Identification and Analysis Tools on the ExPASy Server. In: John M. Walker (ed.), *The Proteomics Protocols Handbook*, Humana Press; pp. 571-607.

Granato, M., van Eeden, F. J., Schach, U., Trowe, T., Brand, M., Furutani-Seiki, M., Haffter, P., Hammerschmidt, M., Heisenberg, C. P., Jiang, Y. J. et al. (1996). Genes controlling and mediating locomotion behavior of the zebrafish embryo and larva. *Development* **123**, 399-413.

Griffin, K., Patient, R. and Holder, N. (1995). Analysis of FGF function in normal and no tail zebrafish embryos reveals separate mechanisms for formation of the trunk and the tail. *Development* **121**, 2983-94.

Haffter, P., Granato, M., Brand, M., Mullins, M. C., Hammerschmidt, M., Kane, D. A., Odenthal, J., van Eeden, F. J., Jiang, Y. J., Heisenberg, C. P. et al. (1996). The identification of genes with unique and essential functions in the development of the zebrafish, Danio rerio. *Development* **123**, 1-36.

Haffter, P. and Nusslein-Volhard, C. (1996). Large scale genetics in a small vertebrate, the zebrafish. *Int J Dev Biol* **40**, 221-7.

Haslett, J. N., Sanoudou, D., Kho, A. T., Han, M., Bennett, R. R., Kohane, I. S., Beggs, A. H. and Kunkel, L. M. (2003). Gene expression profiling of Duchenne muscular dystrophy skeletal muscle. *Neurogenetics* **4**, 163-71.

Hatta, K., Bremiller, R., Westerfield, M. and Kimmel, C. B. (1991). Diversity of expression of engrailed-like antigens in zebrafish. *Development* **112**, 821-32.

Hirata, H., Carta, E., Yamanaka, I., Harvey, R. J. and Kuwada, J. Y. (2009). Defective glycinergic synaptic transmission in zebrafish motility mutants. *Front Mol Neurosci* **2**, 26.
Holley, S. A. (2007). The genetics and embryology of zebrafish metamerism. *Dev Dyn* **236**, 1422-49.

Hutchinson, S. A. and Eisen, J. S. (2006). Islet1 and Islet2 have equivalent abilities to promote motoneuron formation and to specify motoneuron subtype identity. *Development* **133**, 2137-47.

Ingham, P. W. and Kim, H. R. (2005). Hedgehog signalling and the specification of muscle cell identity in the zebrafish embryo. *Exp Cell Res* **306**, 336-42.

Ishimatsu, K., Takamatsu, A. and Takeda, H. (2010). Emergence of traveling waves in the zebrafish segmentation clock. *Development* **137**, 1595-9.

Jowett, T. and Lettice, L. (1994). Whole-mount in situ hybridizations on zebrafish embryos using a mixture of digoxigenin- and fluorescein-labelled probes. *Trends Genet* **10**, 73-4.

Kawahara, A., Che, Y. S., Hanaoka, R., Takeda, H. and Dawid, I. B. (2005). Zebrafish GADD45beta genes are involved in somite segmentation. *Proc Natl Acad Sci U S A* **102**, 361-6.

Kimmel, C. B., Ballard, W. W., Kimmel, S. R., Ullmann, B. and Schilling, T. F. (1995). Stages of embryonic development of the zebrafish. *Dev Dyn* **203**, 253-310.

Lamont, R. E., Lamont, E. J. and Childs, S. J. (2009). Antagonistic interactions among Plexins regulate the timing of intersegmental vessel formation. *Dev Biol* **331**, 199-209.

Lauderdale, J. D., Davis, N. M. and Kuwada, J. Y. (1997). Axon tracts correlate with netrin-1a expression in the zebrafish embryo. *Mol Cell Neurosci* **9**, 293-313.

Lewis, J. and Ozbudak, E. M. (2007). Deciphering the somite segmentation clock: beyond mutants and morphants. *Dev Dyn* **236**, 1410-5.
Lewis, K. E., Currie, P. D., Roy, S., Schauerte, H., Haffter, P. and Ingham, P. W. (1999). Control of muscle cell-type specification in the zebrafish embryo by Hedgehog signalling. *Dev Biol* **216**, 469-80.
Lewis, K. E. and Eisen, J. S. (2001). Hedgehog signaling is required for primary motoneuron induction in zebrafish. *Development* **128**, 3485-95.

Liu, D. W. and Westerfield, M. (1990). The formation of terminal fields in the absence of competitive interactions among primary motoneurons in the zebrafish. *J Neurosci* **10**, 3947-59.

Liu, Y., Monticone, M., Tonachini, L., Mastrogiacomo, M., Marigo, V., Cancedda, R. and Castagnola, P. (2004). URB expression in human bone marrow stromal cells and during mouse development. *Biochem Biophys Res Commun* **322**, 497-507.

Mara, A. and Holley, S. A. (2007). Oscillators and the emergence of tissue organization during zebrafish somitogenesis. *Trends Cell Biol* **17**, 593-9.

Melancon, E., Liu, D. W., Westerfield, M. and Eisen, J. S. (1997). Pathfinding by identified zebrafish motoneurons in the absence of muscle pioneers. *J Neurosci* **17**, 7796-804.

Melby, A. E., Warga, R. M. and Kimmel, C. B. (1996). Specification of cell fates at the dorsal margin of the zebrafish gastrula. *Development* **122**, 2225-37.

Menelaou, E., Husbands, E. E., Pollet, R. G., Coutts, C. A., Ali, D. W. and Svoboda, K. R. (2008). Embryonic motor activity and implications for regulating motoneuron axonal pathfinding in zebrafish. *Eur J Neurosci* **28**, 1080-96.

Mu, H., Ohta, K., Kuriyama, S., Shimada, N., Tanihara, H., Yasuda, K. and Tanaka, H. (2003). Equarin, a novel soluble molecule expressed with polarity at chick embryonic lens equator, is involved in eye formation. *Mech Dev* **120**, 143-55.

Myers, E. W. and Miller, W. (1988). Optimal alignments in linear space. *Comput Appl Biosci* **4**, 11-7.

Myers, P. Z., Eisen, J. S. and Westerfield, M. (1986). Development and axonal outgrowth of identified motoneurons in the zebrafish. *J Neurosci* **6,** 2278-89.

Nakai, K. and Horton, P. (1999). PSORT: a program for detecting sorting signals in proteins and predicting their subcellular localization. *Trends Biochem Sci* **24**, 34-6.

Oates, A. C., Mueller, C. and Ho, R. K. (2005). Cooperative function of deltaC and her7 in anterior segment formation. *Dev Biol* **280**, 133-49.

Pawlowski, K., Muszewska, A., Lenart, A., Szczepinska, T., Godzik, A. and Grynberg, M. (2010). A widespread peroxiredoxin-like domain present in tumor suppression- and progression-implicated proteins. *BMC Genomics* **11**, 590.

Patel, N. H., Martin-Blanco, E., Coleman, K. G., Poole, S. J., Ellis, M. C., Kornberg, T. B. and Goodman, C. S. (1989). Expression of engrailed proteins in arthropods, annelids, and chordates. *Cell* **58**, 955-68.

Patterson, S. E., Bird, N. C. and Devoto, S. H. (2010). BMP regulation of myogenesis in zebrafish. *Dev Dyn* **239**, 806-17.

Pfaff, S. and Kintner, C. (1998). Neuronal diversification: development of motor neuron subtypes. *Curr Opin Neurobiol* **8**, 27-36.

Pfaff, S. L., Mendelsohn, M., Stewart, C. L., Edlund, T. and Jessell, T. M. (1996). Requirement for LIM homeobox gene Isl1 in motor neuron generation reveals a motor neuron-dependent step in interneuron differentiation. *Cell* **84**, 309-20.

Pietri, T., Manalo, E., Ryan, J., Saint-Amant, L. and Washbourne, P. (2009). Glutamate drives the touch response through a rostral loop in the spinal cord of zebrafish embryos. *Dev Neurobiol* **69**, 780-95.

Pike, S. H., Melancon, E. F. and Eisen, J. S. (1992). Pathfinding by zebrafish motoneurons in the absence of normal pioneer axons. *Development* **114**, 825-31.

Postlethwait, J. H., Woods, I. G., Ngo-Hazelett, P., Yan, Y. L., Kelly, P. D., Chu, F., Huang, H., Hill-Force, A. and Talbot, W. S. (2000). Zebrafish comparative genomics and the origins of vertebrate chromosomes. *Genome Res* **10**, 1890-902.

Raymond, F., Metairon, S., Kussmann, M., Colomer, J., Nascimento, A., Mormeneo, E., Garcia-Martinez, C. and Gomez-Foix, A. M. (2010). Comparative gene expression profiling between human cultured myotubes and skeletal muscle tissue. *BMC Genomics* **11**, 125.

Rescan, P. Y. (2001). Regulation and functions of myogenic regulatory factors in lower vertebrates. *Comp Biochem Physiol B Biochem Mol Biol* **130**, 1-12.

Roos, M., Schachner, M. and Bernhardt, R. R. (1999). Zebrafish semaphorin Z1b inhibits growing motor axons in vivo. *Mech Dev* **87**, 103-17.

Saint-Amant, L. and Drapeau, P. (1998). Time course of the development of motor behaviors in the zebrafish embryo. *J Neurobiol* **37**, 622-32.

Sato-Maeda, M., Tawarayama, H., Obinata, M., Kuwada, J. Y. and Shoji, W. (2006). Sema3a1 guides spinal motor axons in a cell- and stage-specific manner in zebrafish. *Development* **133**, 937-47.

Sawada, A., Fritz, A., Jiang, Y. J., Yamamoto, A., Yamasu, K., Kuroiwa, A., Saga, Y. and Takeda, H. (2000). Zebrafish Mesp family genes, mesp-a and mesp-b are segmentally expressed in the presomitic mesoderm, and Mesp-b confers the anterior identity to the developing somites. *Development* **127**, 1691-702.

Schauerte, H. E., van Eeden, F. J., Fricke, C., Odenthal, J., Strahle, U. and Haffter, P. (1998). Sonic hedgehog is not required for the induction of medial floor plate cells in the zebrafish. *Development* **125**, 2983-93.

Sigrist, C. J., Cerutti, L., Hulo, N., Gattiker, A., Falquet, L., Pagni, M., Bairoch, A. and Bucher, P. (2002). PROSITE: a documented database using patterns and profiles as motif descriptors. *Brief Bioinform* **3**, 265-74.

Stemple, D. L. (2005). Structure and function of the notochord: an essential organ for chordate development. *Development* **132**, 2503-12.

Stevenson, E. J., Koncarevic, A., Giresi, P. G., Jackman, R. W. and Kandarian, S. C. (2005). Transcriptional profile of a myotube starvation model of atrophy. *J Appl Physiol* **98**, 1396-406.

Stickney, H. L., Barresi, M. J. and Devoto, S. H. (2000). Somite development in zebrafish. *Dev Dyn* **219**, 287-303.

Takke, C. and Campos-Ortega, J. A. (1999). her1, a zebrafish pair-rule like gene, acts downstream of notch signalling to control somite development. *Development* **126**, 3005-14.

Tessier-Lavigne, M. and Goodman, C. S. (1996). The molecular biology of axon guidance. *Science* **274**, 1123-33.

Thisse, C., Thisse, B., Schilling, T. F. and Postlethwait, J. H. (1993). Structure of the zebrafish snail1 gene and its expression in wild-type, spadetail and no tail mutant embryos. *Development* **119**, 1203-15.

Timothy, L, Bailey and Charles Elkan. (1994). Fitting a mixture model by expectation maximization to discover motifs in biopolymers, *Proceedings of the Second International Conference on Intelligent Systems for Molecular Biology*. 1994, pp. 28-36, AAAI Press, Menlo Park, California.

Timothy, L, Bailey and Michael Gribskov. (1998). Combining evidence using p-values: application to sequence homology searches. *Bioinformatics*, **14**: 48-54.
Tremblay, F., Revett, T., Huard, C., Zhang, Y., Tobin, J. F., Martinez, R. V. and Gimeno, R. E. (2009). Bidirectional modulation of adipogenesis by the secreted protein Ccdc80/DRO1/URB. *J Biol Chem* **284**, 8136-47.

Trevarrow, B., Marks, D. L. and Kimmel, C. B. (1990). Organization of hindbrain segments in the zebrafish embryo. *Neuron* **4**, 669-79.

Tseng, B. S., Zhao, P., Pattison, J. S., Gordon, S. E., Granchelli, J. A., Madsen, R. W., Folk, L. C., Hoffman, E. P. and Booth, F. W. (2002). Regenerated mdx mouse skeletal muscle shows differential mRNA expression. *J Appl Physiol* **93**, 537-45.

van Eeden, F. J., Granato, M., Schach, U., Brand, M., Furutani-Seiki, M., Haffter, P., Hammerschmidt, M., Heisenberg, C. P., Jiang, Y. J., Kane, D. A. et al. (1996). Mutations affecting somite formation and patterning in the zebrafish, Danio rerio. *Development* **123**, 153-64.

Visconti, R., Schepis, F., Iuliano, R., Pierantoni, G. M., Zhang, L., Carlomagno, F., Battaglia, C., Martelli, M. L., Trapasso, F., Santoro, M. et al. (2003). Cloning and molecular characterization of a novel gene strongly induced by the adenovirus E1A gene in rat thyroid cells. *Oncogene* **22**, 1087-97.
Westerfield, M., McMurray, J. V. and Eisen, J. S. (1986). Identified motoneurons and their innervation of axial muscles in the zebrafish. *J Neurosci* **6**, 2267-77.

Wilson, L., Yang, Q., Szustakowski, J. D., Gullicksen, P. S. and Halse, R. (2007). Pyruvate induces mitochondrial biogenesis by a PGC-1 alpha-independent mechanism. *Am J Physiol Cell Physiol* **292**, C1599-605.

Wolff, C., Roy, S. and Ingham, P. W. (2003). Multiple muscle cell identities induced by distinct levels and timing of hedgehog activity in the zebrafish embryo. *Curr Biol* **13**, 1169-81.

Zhang, L., Kendrick, C., Julich, D. and Holley, S. A. (2008). Cell cycle progression is required for zebrafish somite morphogenesis but not segmentation clock function. *Development* **135**, 2065-70.

Zeller, J. and Granato, M. (1999). The zebrafish diwanka gene controls an early step of motor growth cone migration. *Development* **126**, 3461-72.

Part II

Manuscript

ccdc80-l1 Is Involved in Axon Pathfinding of Zebrafish Motoneurons.

Brusegan C.[1], Pistocchi A.[1, 2,*], Frassine A.[1], Della Noce I.[3], Schepis F.[3,*], Cotelli F.[1,*]

[1]Dipartimento di Biologia, Università degli Studi di Milano, via Celoria 26, 20133 Milan, Italy

[2]Dipartimento di Medicina Rigenerativa, DiBiT, Istituto Scientifico San Raffaele, via Olgettina 60, 20132 Milan, Italy

[3] Dipartimento di Medicina, Università di Modena e Reggio Emilia, via Università 4, 41121 Modena, Italy

[*]Corresponding authors: franco.cotelli@unimi.it, anna.pistocchi@guest.unimi.it, filippo.schepis@unimore.it,

Submitted to PlosOne on July 14th, 2011

Status: under revision

Abstract

Axon pathfinding is a subfield of neural development by which neurons send out axons to reach the correct targets. In particular, motoneurons extend their axons toward skeletal muscles, leading to spontaneous motor activity. In this study, we identified the zebrafish Ccdc80 and Ccdc80-like1 (Ccdc80-l1) proteins *in silico* on the basis of their high aminoacidic sequence identity with the human CCDC80 (Coiled-Coil Domain Containing 80). We focused on *ccdc80-l1* gene that is expressed in nervous and non-nervous tissues, in particular in territories correlated with axonal migration, such as adaxial cells and muscle pioneers. Loss of *ccdc80-l1* in zebrafish embryos induced motility issues, although somitogenesis and myogenesis were not impaired. Our results strongly suggest that *ccdc80-l1* is involved in axon guidance of primary and secondary motoneurons populations, but not in their proper formation. *ccdc80-l1* has a differential role as regards the development of ventral and dorsal motoneurons, and this is consistent with the asymmetric distribution of the transcript. The axonal migration defects observed in *ccdc80-l1* loss-of-function embryos are similar to the phenotype of several mutants with altered *Hedgehog* activity. Indeed, we reported that *ccdc80-l1* expression is positively regulated by the Hedgehog pathway in adaxial cells and muscle pioneers. These findings strongly indicate *ccdc80-l1* as a down-stream effector of the Hedgehog pathway.

Introduction

The development of a functional vertebrate nervous system requires elaboration of a large number of diverse cell types. At embryonic stages, the nervous system is a complex network of growing axons, whose growth cones navigate in response to guidance cues. Among them, motoneuron axons migrate toward skeletal muscles, and form synaptic contacts [1]. Zebrafish embryos exhibit spontaneous contractions of the musculature ever since 18–19 hours post fertilization (hpf) when removed from their protective chorion [2]. These movements are due to the early-developing primary motoneurons (PMNs), that innervate the myotome with nonoverlapping arbors. In zebrafish, PMNs are present in each somitic hemisegment and are identified by their specific axonal pathway and soma position within the spinal cord: caudal primary motoneurons, middle primary motoneurons and rostral primary motoneurons (CaPs, MiPs and RoPs, respectively) [3,4,5]. PMNs extend their axons out of the spinal cord at about 16-17 hpf, following a common pathway: their growth cones project ventrally along the medial surface of the myotome and pause at the horizontal myoseptum, which separates dorsal and ventral myotomes. Here, they specifically interact

with muscle pioneers [6,7], a subset of two to six cells for each somite early differentiating into slow muscle fibers [8,9]. CaPs are responsible for pioneering the common pathway before projecting the axons that innervate the ventral myotome [10]. Among PMNs, they show the largest and most extensive branching pattern [5]. MiPs sprout a collateral axon to innervate dorsal myotome, while the first ventral process extending along the common pathway is retracted by 48 hpf [7]. RoPs innervate the middle region of the muscle segment, sprouting laterally after pausing at the myoseptum [6]. Therefore, muscle pioneers represent a choice point from which motoneurons select their specific pathway, although the ablation of this cell population leads to abnormal motor axonal extension without altering the target choice [7]. Secondary motoneurons (SMNs) growth cones extend later from spinal cord, beginning at 22 hpf and following the paths pioneered by the primary axons [11,12].

Axonal pathfinding is dependent on attractive and repulsive stimuli coming from both nervous and non-nervous surrounding tissues [1,13]. For instance, *shh* induction by notochord and floorplate patterns both primary and secondary motoneurons [14]. Indeed, mutants lacking both the notochord and the floorplate (*cyc*$^{-}$*;flh*$^{-}$) [14] or mutants in the Hedgehog pathway, such as *smoothened* (*smo*), present disorganized, reduced or absent PMNs and axons. [15]. Moreover, in *sonic-you* mutants (*syu*) CaPs and MiPs axons run along the neural tube horizontally instead of ventrally and dorsally, while axons of the secondary motoneurons fail to branch and instead cease to extend or grow further ventrally in an abnormal pattern [16].

Also muscular tissues can pattern axonal migration: muscular adaxial cells are able to rescue motor axon defects in *diwanka* mutants, showing that this myotomal population plays a pivotal role in axonal migration [17]. Furthermore, molecules expressed in the somites such as the semaphorin proteins Z1b and Sema3A1 are involved in repelling axonal migration [10,18]. On the contrary, *netrin-1a* is expressed by adaxial cells and muscle pioneers besides ventral spinal cord, and seems to guide axonal growth through a chemoattractive function [19]. The manipulation of the proper expression of these molecules, both knocking-down and inducing ectopic expression, induces axons to follow aberrant pathways, branch excessively or stall [17,18,19].

The *Coiled-Coil-Domain Containing 80* (*Ccdc80*) gene, also named *DRO1* in human (*Down-Regulated by Oncogene 1*), *URB* in mouse (*Up-Regulated in BRS-3 deficient mice*), *CL2* in rat (*Clone 2*), and *equarin* in chicken, has been recently suggested to be involved in different functions among vertebrates. *Ccdc80* was first isolated in mice, where it is up-regulated in adipose tissue of obese BRS-3-deficient animals [20]. Moreover, *Ccdc80* is highly expressed in mice white adipose tissue and its silencing inhibits adipocytes differentiation [21],

suggesting a role in the regulation of body weight and energy metabolism. *Ccdc80* is also expressed in mouse developing cartilage, suggesting a role during skeletogenesis [22]

Human *CCDC80* is almost ubiquitously expressed, with the highest levels in heart and skeletal muscles [23,24]. Furthermore, human *CCDC80* can be considered a potential tumor suppressor gene [25]. In fact, it is strikingly down-regulated in thyroid neoplastic cell lines and tissues, as well as in colon and pancreatic cancer cell lines and in most colorectal cancer specimens [26], while its ectopic expression in these cell lines results in substantial inhibition of growth properties.

The CCDC80 protein is highly conserved among vertebrates, and contains multiple signals of cellular compartmentalization and post-translational modifications. In particular, it has a N-terminus leader peptide for extracellular export and many nuclear localization signals [25]. In different studies, the CCDC80 protein has been identified in a N-glycosylated form and was suggested to be secreted. Rat, mouse and human CCDC80 show three P-DUDES domains (Procaryotes- *DRO1-URB-DRS-Equarin-SRPUL*) which in human are correlated with a tumor suppressor role [27].

In silico analysis using human CCDC80 sequence as a bait, led to the identification of three zebrafish homologs of CCDC80. Two homologs, that we named Ccdc80 and Ccdc80-like1 (Ccdc80-l1), showed high levels of aminoacid identity with the human CCDC80. We performed the molecular cloning of *ccdc80* and *ccdc80-l1* in zebrafish and analyzed their expression pattern during embryonic development. During somitogenesis *ccdc80* is expressed in the notochord (manuscript in preparation), while *ccdc80-l1* is expressed in muscle pioneers and adaxial cells. Both these regions are responsible for axon guidance, therefore we decided to investigate the role of *ccdc80* and *ccdc80-l1* in this process. While loss-of-*ccdc80*-function did not impair motoneurons development, we demonstrated the *ccdc80-l1* involvement in the proper axonal pathfinding, especially in ventral axons guidance. Indeed, *ccdc80-l1* knocked-down embryos exhibited motility issues although analysis on body musculature showed that somitogenesis and myogenesis occurred properly. Furthermore, the analysis of *ccdc80-l1* up-stream regulation revealed that the Hedgehog pathway modulates its expression in territories involved in axonal guidance.

Materials and methods

Zebrafish lines and maintenance

Current italian national rules: no approval needs to be given for research on zebrafish embryos. Zebrafish were raised and maintained according to established techniques [28], approved by the veterinarian (OVSAC) and the animal use committee (IACUC) at the University of Oregon, in agreement with local and national sanitary regulations. Embryos were collected by natural spawning, staged according to Kimmel [29], and raised at 28°C in fish water (Instant Ocean, 0.1% methylene blue) in Petri dishes [30].

Sequence analysis

Zebrafish chromosome 6 region hosting the *ccdc80-l1* gene was identified through *in silico* search of the ENSEMBL zebrafish assembly version 9 (Zv9) using human CCDC80 aminoacidic sequence as a bait. The alignments between aminoacid sequences were performed with the software program StrecherP. Analysis on synteny was performed with the program Genomicus version 57.01.

RT-PCR

Total RNA from 11 samples (an average of 30 embryos per sample) corresponding to 9 different developmental stage embryos (2-4 cells, 64-1000 cells, 30% epiboly, 60%-70% epiboly, somitogenesis, 24 hpf and 72 hpf) and 2 adult organs (ovary and muscle) was extracted with the TOTALLY RNA isolation kit (Ambion), treated with RQ1 RNase-Free DNase (Promega) and oligo (dT)-reverse transcribed using Super- Script II RT (Invitrogen), according to manufacturers' instructions. The following primers were used for PCR reactions: *ccdc80-l1*_forward 5'- ACCACAATGGAGCAAACACA -3' and *ccdc80-l1*_reverse 5'-GGTTTAGCTCTCCCCTTTGG -3'. PCR products were loaded and resolved onto 2% agarose gels.

In situ hybridization and immunohistochemistry

Whole-mount *in situ* hybridization (WISH), was carried out as described [31] on embryos fixed for 2 hours in 4% paraformaldehyde in PBS, then rinsed with PBS-Tween (PBT), dehydrated in 100% methanol and stored at –20°C until processed [32]. Antisense riboprobes were previously *in vitro* labelled with modified nucleotides (digoxigenin, Roche). *myod* and *myog* probes were prepared as described by Schnapp and collegues [33]. *smyhc1* probe has been kindly provided by Ingham laboratory. The following primers were used for PCR reactions to clone the probes: *ccdc80-l1* sense 5'- ACCACAATGGAGCAAACACA -3' and

ccdc80-l1 antisense 5′- GGTTTAGCTCTCCCCTTTGG -3′. For immunohistochemistry, embryos were fixed in 4% paraformaldehyde overnight at 4°C or 2 hours at RT, washed several times in PBT and blocked in 5% BSA in PBT for 1 hour at room temperature. Primary antibody incubation was done overnight at 4°C, followed by several washes in PBT and incubation of secondary antibody for 1 hour at room temperature. Primary antibodies are MF20 (mouse anti-sarcomeric) and 4D9 (mouse anti-engrailed/invected) purchased from Developmental Studies Hybridoma Bank, znp1 (mouse anti-*syt2b*) and zn-5 (mouse anti-*alcama*) purchased from Zebrafish International Resource Center (ZIRC). Secondary antibody is EnVision+ System- HRP Labelled Polymer anti-mouse (Dako). Images of embryos and sections were acquired using a microscope equipped with a digital camera with LAS Leica imaging software (Leica, Wetzlar, Germany). Images were processed using the Adobe Photoshop software. For histological sections, stained embryos were re-fixed in 4% paraformaldehyde, dehydrated and stored in methanol, wax embedded, and sectioned (5–8 μm).

Injections

Injections were carried out on 1- to 2-cell-stage embryos (with Eppendorf FemtoJet Micromanipulator 5171); the dye tracer rhodamine dextran was co-injected as a control. To repress *ccdc80-l1* mRNA translation we designed an ATG-targeting morpholino, *ccdc80-l1*-MO: 5′- TTGTACCTGTAGATTTTTCATTGCA-3′ and a splice-site morpholino, *ccdc80-l1*-splice- 5′- TGATACAATACATACTATGAGGCGT -3′ (Gene Tools, LLC). As a negative control we injected a standard control morpholino oligonucleotide (ctrl-MO). Morpholinos were injected in 1x Danieau buffer (pH 7.6) as suggested by Nasevicius and Ekker [34]. For the *in vivo* test of the efficiency of *ccdc80-l1*-MO, 425 pg/embryo of the pCS2+-*ccdc80-l1*-GFP sensor plasmid have been injected alone or co-injected with 12 ng/embryo of *ccdc80-l1*-MO. The presence/absence of the GFP signal has been monitored under a fluorescent microscope starting from somitogenesis up to 48 hpf. *ccdc80-l1*-MO cDNA fragments inserted in the *BamHI* site were obtained using the following complementary oligos: *ccdc80-l1*-MO sense 5′- gatcTTGTACCTGTAGATTTTTCATTGCACA -3′ and *ccdc80-l1*-MO antisense 5′ – gatcTGTGCAATGAAAAATCTACAGGTACAA- 3′.

For the *in vivo* test of the specificity of morpholino-mediated knockdown, the rescue of morphants phenotype was obtained co-injecting 12 ng/embryo of *ccdc80-l1*-MO together with 400 pg/embryo of *ccdc80*-encoding mRNA.

Over-expression of *shh* was obtained microinjecting 300 pg/embryo of *shh* mRNA, kindly provided by Sordino laboratory.

Statistical analysis

Statistical analysis was performed with Student's t-test using GraphPad PRISM version 5.0 (GraphPad, San Diego, California). A p value <0.001 indicates a statistically significant effect.

Cyclopamine treatment

Embryos were exposed to 5 μM cyclopamine (purchased from SIGMA-ALDRICH) from 50% epiboly stage up to fixation in PFA at 15 somites stage. Cyclopamine was dissolved in embryo medium and 0.5% ethanol. Controls consisted of corresponding incubations in 0.05% ethanol in embryo medium.

Results

Identification of *Ccdc80* homologs in the genome of zebrafish.

Blast analysis of the ENSEMBL zebrafish assembly version 9 (Zv9) using human CCDC80 as a bait returned three positive hits, corresponding to three proteins encoded by genes on different chromosomes: the first on chromosome 9 (nucleotide position: 35,060,460-35,084,513) that we named *ccdc80*, the second on chromosome 6 (nucleotide position: 16,322,724-16,342,517) that we named *ccdc80-like1* (*ccdc80-l1*), and the third on chromosome 21 (nucleotide position: 18,662,129-18,669,986), that we named *ccdc80-like2* (*ccdc80-l2*). The alignment of the predicted protein sequences in zebrafish with the human CCDC80, revealed that Ccdc80 presented the highest degree of aminoacid identity with human CCDC80 (51.6%), while Ccdc80-l1 and Ccdc80-l2 presented less identity (44.4% and 27% respectively) (Tab. 1 and suppl. Fig. 1). We then performed alignments among the three zebrafish homologs: Ccdc80 shared the 51.4% of aminoacid identity with Ccdc80-l1 and the 30.4% with Ccdc80-l2 while Ccdc80-l1 and Ccdc80-l2 shared the 29.1% of identity (Tab. 1). Moreover, analysis of chromosomal organization of the three *ccdc80* zebrafish homologs across vertebrates revealed that only *ccdc80* is synthenic with other vertebrates (Fig. 1).

	Human CCDC80		Zebrafish Ccdc80		Zebrafish Ccdc80-like1		Zebrafish Ccdc80-like2	
	Identity	Similarity	Identity	Similarity	Identity	Similarity	Identity	Similarity
Zebrafish Ccdc80	51,6%	65,2%	/	/	51,4%	64,4%	30,4%	47,4%
Zebrafish Ccdc80-like1	44,4%	59,3%	51,4%	64,4%	/	/	29,1%	46,9%
Zebrafish Ccdc80-like2	27%	44,9%	30,4%	47,4%	29,1%	46,9%	/	/

Table1: Percentages of identity and similarity among zebrafish and human CCDC80 homologs. The table shows the scores obtained after alignments between the aminoacidic sequences of zebrafish and human CCDC80 homologs. Alignments were performed with Stretcher-P tool.

```
CCDC80          MTWRMGPRFTMLLAMWLVCGSEPHPHATIRGSHGGRKVPLVSPDSSRPARFLRHTGRSRG 60
Ccdc80          MRARYMLGFGVLCLLTWAVYVSESSPTDKQAKLRLMSVRRARQNKSRQGQIIKTRASSTW 60
Ccdc80-like1    ------------MTLTWIQASDLDYPKTDRGNAQLQPNTFVNKYTKDVQTNRRLSGLSTS 48
Ccdc80-like2    ---------------------------------------------MSRLWILLILMINSPV 16
                                                             .          *

CCDC80          IERSTLEEPNLQPLQRRRSVPVLRLARPTEPPARSDINGAAVRPEQRPAARGSPREMIRD 120
Ccdc80          INDKRQQMQGDEGVQFRRNVQSRKVLAQRRPAQGGTRNPIQQDDGTPGARARVSRMPSSA 120
Ccdc80-like1    GNTHILRKPQND--QENSRPPARRVLKGQRP-------ALFRKPSVNDSIPAQETSLGAA 99
Ccdc80-like2    LSAKAGKKKHQAKNKSDLTIPKEDAGVHESP---------------------------- 47
                 .    .      :              *

CCDC80          EGSSARSRMLRFPSGSSSPNILASFAGKNRVWVISAP-HASEGYYRLMMSLLKDDVYCEL 179
Ccdc80          GSPNLLASFAGKNRLLVISAPHDSDGYYRLMMSLLKP-EVYCELAERHVHQIVMFHQEGE 179
Ccdc80-like1    SSINILAGFAGKNRVLIISAPNESDGYYRLMMNLLKP-DVYCEMADRHMQQIIMFHEKGK 158
Ccdc80-like2    SESDFLADFAGKHRLWVISAPSHNDNYLRMMEKQIQESEGLNCRLAERDTLIVTIIQNAL 107
                   .  : :         .    .    . :       .           :

CCDC80          AERHIQQIVLFHQAGEEGGKVRRITSEGQILEQPLDPSLIPKLMSFLKLEKGKFGMVLLK 239
Ccdc80          LGGKIRRITNEGKVMEEPLDTALIPRLMTFLKLEKGKFGMVLLKKTLQVEERYPYPVRLE 239
Ccdc80-like1    MGGKVRRVSNQGSLVEEPLDPALVPRLMGFLKLEDGKFGMVLLRKTLQIEERYPYPVQLE 218
Ccdc80-like2    MEGKIQRTTLQGEANVEAMDSEMVSKLLHHIELEDQTFSMLILKKNMRVSERFPYPVRVE 167
                   ::::     .   *  .   :.     ::       :  * . :::.:     * ::

CCDC80          KTLQVEERYPYPVRLEAMYEVIDQGPIRRIEKIRQKGFVQKCKASGVEGQVVAEGNDGGG 299
Ccdc80          AMYEVIDQSPMRKMEKVRQKGFVQKCKGAGVEGQVVEGVLTTDSQVDPPTERRKEIRKPI 299
Ccdc80-like1    AIYETIDQTPMRRLEKARHKGFVQKCKTAGIEGQVVQSAGSNTVGLQPQVNTAVHTR--- 275
Ccdc80-like2    AILEVIDQLPVRKLEKVARKGSPIKCKITKKRIVVK------------------------ 203
                   :. :: *     :.  :           .

CCDC80          GAGRPSLGSEKKKEDPRRAQVPPTRESRVKVLRKLAATAPALPQPPSTPRATTLPPAPAT 359
Ccdc80          RRPTTTTTPAPTRPTTTTTTTKATTTTTTRPPTTTRSTTTTTTTTTTTTTRPTTTTTRTTT 359
Ccdc80-like1    -RQRVRPVPQPTQMTQAQISSALTTTKTTTTLKTTTTKPPTTTTQPATTITITTTTAPTT 334
Ccdc80-like2    -------------------KQGSSKRRTFSPQRQTNTTSIVLTQKIRLDKKETLRNKVQ 243
                                  :    .        ...                 .

CCDC80          TVTRSTSRAVTVAARPMTTTAFPTTQRPWTPSPSHRPPTTTEVITARRPSVSENLYPPSR 419
Ccdc80          TPRTTRANTTPQWIPAHKTTAEPYYYNRRDRYQTTSPPTDSARYRDNHTSKKEYNHRHTN 419
Ccdc80-like1    TILPSTTTTVTTVVPTTMEQTHPDTTR--TTTPNEKTQNSHPVTSNLRKQPQEKYLVPTQ 392
Ccdc80-like2    DILSGRSRFVIRKATGGSGNGKPSDKGGSGSSKNEKSKLDSKKKASDGDRNKEPVKEVKN 303
                      :  .           *          .  .             .*     ..

CCDC80          KDQHRERPQTTRRPSKATSLESFTNAPPTTISEPS-TRAAG---PGRFRDNRMDRREHGH 475
Ccdc80          TIPTQHKPTKVRPTKKKNGDKDISNAYEEKYDVGV-PTDAY---PEEKEEEIVPTKRGKG 475
Ccdc80-like1    KMPIAVLPTHRSAQKPKNKLPAVKHGWREKLSQHTRERDALRPTAEKPETELMTSPKGRA 452
Ccdc80-like2    VLEADKKLAGVKSKSDRLN-------------------------EEYKEEQTVDHSGSK 337
                               .                                . . :

CCDC80          RDPNVVPGPPKPAKEKPPKKKAQDK-ILSNEYEEKYDLSRPTASQLEDELQVGNVP--LK 532
Ccdc80          KTDKKKKKDKTDKLSKKDKAERRGK-DGKGGKKNGKKVPKILEKEDYQKPTKRPPP--PP 532
Ccdc80-like1    KPDSADRGKKTDRPEKPLKKIPAGKKDPKVTKETNISIQNKNTAQKPNAFEEGAVVDQTT 512
Ccdc80-like2    KKDKGKDGKKKKGKGGRRKSQREAD---------------------------------D 363
                :  .      .       *     .

CCDC80          KAKESKKHEKLEKPEKEKKKKMKNENADKLLKSEKQMKKSEKKSKQEKEKSKKKKGGKTE 592
Ccdc80          PPKGTLATFLDYFESRRRLILITSPTEENSMYIQQRDEYLEHVCEMAIRKVTIITIFGTF 592
Ccdc80-like1    NPKKSLETFLSYFQRRRRLIVITAPDEQNHMYSEQRDEYLEQVCDMALRKISIISIFGPL 572
Ccdc80-like2    KKKGALKDFMQNLKGRRRLLVISSPSDVSSHHIKQRDDNELHSCEFSQRKISVLSIMGSE 423
                  * :          :.:   :.     .    ::: .   : ..   .* .  .   .

CCDC80          QDGYQKPTNKHFTQSPKKSVADLLGSFEGKRRLLLITAPKAENNMYVQQRDEYLES--FC 650
Ccdc80          RNSTMKIDHYQLEKDKPMKGLRQEDLENQDLIMELRKEYGMTYNDFYVVLTDLDMK--AK 650
Ccdc80-like1    TNSTMKIEHYQTEQDKPLRGLPDSDLINQDLITAFRKQFGMIDNDFNMVLTDFDMK--VK 630
Ccdc80-like2    HNPTLHIQHYQQDSEPPQASLP-EKFRNSELIGEIRREYRLDPKNFSMVLTDYDLRPNLN 482
                 :   :  : :  ..           : .    :        : :     :

CCDC80          KMATRKISVITIFGPVNNSTMKIDHFQLDNEKPMRVVDDEDLVDQRLISELRKEYGMTYN 710
Ccdc80          QYYEVPIAMKAVFDYIDTFSSRIREMEQQKRDGVTCKKEDKPRSLENFLSRFRWRRRLFV 710
Ccdc80-like1    QRYEVPIVMKAMFDYIDTLSTRIKEIEQQRKLGAMCKKEDKSRSLEDFLSRFRWRRRLFI 690
Ccdc80-like2    RVFNKPTAPSDLLDYIDSFSSRQSEKEEERKSPSPCSKAETN-NQENSLLRFISKRRLLI 541
                :          ::. ::. : :  . : :..      . :   . .

CCDC80          DFFMVLTDVDLRVKQYYEVPITMKSVFDLIDTFQSRIKDMEKQKKEGIVCKEDKKQSLEN 770
Ccdc80          ISAPNDEEWAYQQQLYALTSQACNLGLRHVSVLKLVGTDLLDMGGVLELYPINGSATVER 770
Ccdc80-like1    ISTPSDEEWAYQQQLYAINSQACNLGLRHMSLLKLLGKTLDDMSGVLELYPINGSSSVDR 750
Ccdc80-like2    ISAPNPDDYSFHQQLQAVNGQECPLGIRHFALLKIVGTGS-TASGTVEFFPLNGKSQPEK 600
                       :   : :           :  .  ::   .          .   : .   :.

CCDC80          FLSRFRWRRRLLVISAPNDEDWAYSQQLSALSGQACNFGLRHITILKLLGVGEEVGGVLE 830
Ccdc80          EGISATLVRDIRNYFQISPEYFSMLLVGKDGNVKSWYPSPMWSMAIIYDLIDSMQLRRQE 830
Ccdc80-like1    EALSASLVQDIRNYFQISLEYFSMLLVGKDGNVKSWYPSPMWSMSIIYELVDSMQLRRQE 810
Ccdc80-like2    ETLSQDMVESLRNQLKINREYFTMLVVGKDGDVKAWFTSPMWSLGSIYDLVDSLELRQQE 660
                        . :      . * ::     .  . ::   .           :.     *

CCDC80          LFPINGSSVVEREDVPAHLVKDIRNYFQVSPEYFSMLLVGKDGNVKSWYPSPMWSMVIVY 890
Ccdc80          MAIQQSLGMRCPEDEYGGYGYHHHEGYQEGYHQGYGY----------------------- 867
Ccdc80-like1    MAIQQSLGMRCPDHDYT-----HHDGYHEAYHQGYAY----------------------- 842
Ccdc80-like2    HKLQQTLGIRCVDENTG-----TYHGYTEETEDSYLYHRSED----------------- 697
                   :  .:   :.          . :    .

CCDC80          DLIDSMQLRRQEMAIQQSLGMRCPEDEYAGYGYHSYHQGYQDGYQDDYRHHESYHHGYPY 950
Ccdc80          ------------------------------------------------------------
Ccdc80-like1    ------------------------------------------------------------
Ccdc80-like2    ------------------------------------------------------------
```

Supplementary Figure S1: Alignment among human CCDC80 and the three zebrafish homologs. *= identical aminoacids; : = conservative substitution; . = non-conservative substitution.

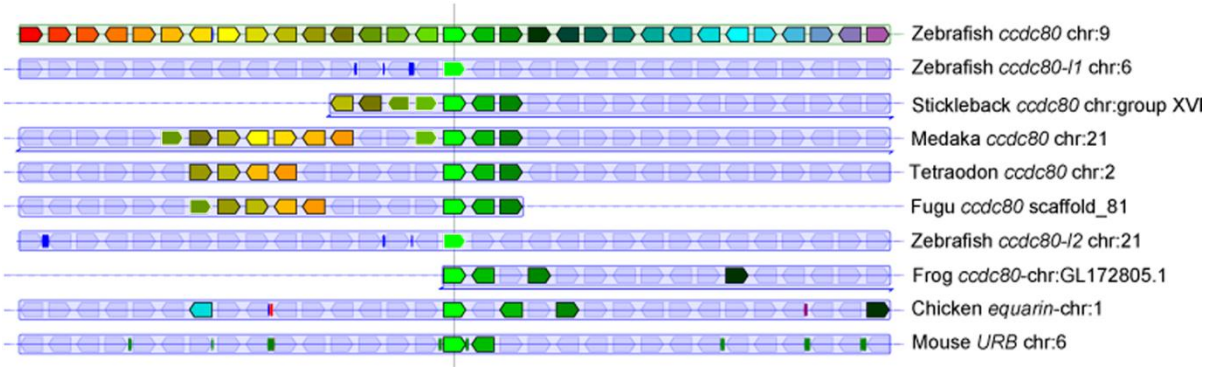

Figure 1: Analysis of chromosomal organization of the three *ccdc80* zebrafish homologs across vertebrates. Each *ccdc80* gene is shown as a reference locus. Genes annotated as paralogs (no surrounding line) or orthologs (with a surrounding line) by the Ensembl database share the same color, blue lines beneath individual tracks indicate that orientations of gene blocks and are inverted with respect to their genomic annotation. For zebrafish *ccdc80* (chr. 9), *ccdc80-l1* (chr. 6) and *ccdc80-l2* (chr. 21), only *ccdc80* shows notable synteny with other vertebrates. The figure was derived from the output of the Genomicus website (version 57.01).

ccdc80-l1 is expressed in muscle pioneers and adaxial cells of the zebrafish embryo

Characterization of *ccdc80-l1* expression, using RT-PCR, revealed that *ccdc80-l1* transcript is present from the first stages of development up to 72 hpf, thus including maternal and zygotic transcription (Fig. 2A). *ccdc80-l1* is also expressed in the ovary and muscle of the adult zebrafish (Fig. 2A). During somitogenesis, the hybridization signal is restricted to the horizontal myoseptum (Fig. 2B-D). From this stage, *ccdc80-l1* expression is observed also in the cranial ganglia and dorsal dermis (Fig. 2B, 2C, 2E, 2I, 2K-L and data not shown). At 24 hpf, *ccdc80-l1* is detectable in a specific sub-population of migrating adaxial cells, that moves along the lateral axis towards the external somite [35] (Fig. 2E-G). Moreover, *ccdc80-l1* is expressed in muscle pioneers, as shown by the co-localization between *ccdc80-l1* and engrailed [36,37] (Fig. 2H). *ccdc80-l1* expression in adaxial cells persisted at 36 hpf and 48 hpf (Fig. 2I, 2K). At the same stages *ccdc80-l1* is also expressed in the caudal vein plexus region (Fig. 2I, 2J, 2L).

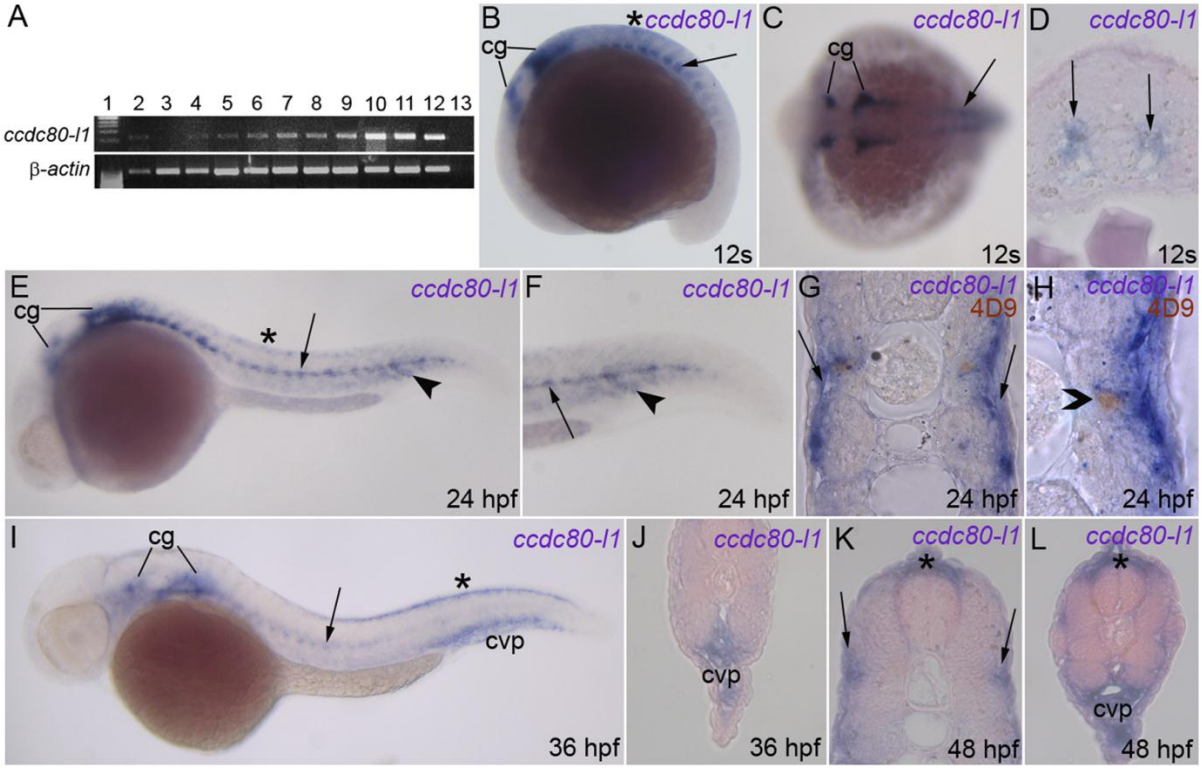

Figure 2: Expression of *ccdc80-l1* analyzed by RT-PCR and WISH. *(A)* RT-PCR performed on different embryonic stages and adult tissues; the expression of *ccdc80-l1* and *β-actin* are shown. Lanes are: ladder (lane 1) , ovary (lane 2), 2-4 cells stage (lane 3), 64-1000 cells stage (lane 4), 30% epiboly (lane 5), 60-70% epiboly (lane 6), somitogenesis (lane 7), 24 hpf (lane 8), 30 hpf (lane 9), 48 hpf (lane 10), 72 hpf (lane 11), adult muscle (lane 12) and negative control (lane 13) in the absence of cDNA. *(B-J)* WISH performed on zebrafish embryos at several stage of development. *(B, C)* During somitogenesis *ccdc80-l1* was expressed by cranial ganglia (cg), dorsal dermis (asterisk), adaxial cells and muscle pioneers at the level of the horizontal myoseptum (arrow). *(D) ccdc80-l1* expression in a transverse section of the trunk of an embryo at 12 somites stage (arrows). *(E-H)* At 24 hpf, the hybridization signal was detectable in cranial ganglia (cg), dermis (asterisk), adaxial cells (arrow) and ventral somites (arrowhead). *(F)* Higher magnification of the tail at 24 hpf. *(G)* Transversal section of an embryo at 24 hpf. *(H)* Transversal section showing that at 24 hpf *ccdc80-l1* hydridization signal co-localized with the nuclear labeling of 4D9 antibody, corresponding to the engrailed-positive muscle pioneers population (open arrowhead). *(I, J)* At 36 hpf, the signal of *ccdc80-l1* probe was detected in cranial ganglia (cg), migrated adaxial cells (arrow), dorsal dermis (asterisk) and caudal vein plexus region (cvp). *(K, L)* At 48 hpf, *ccdc80-l1* was detected in dorsal dermis (asterisk), external adaxial cells (arrows in *K*) and caudal vein plexus region (cvp in *L*). *(B, E, F, I)* Lateral views; dorsal is up, anterior is left; *(C)* dorsal view, anterior is left; *(D,G, H, J-L)* transversal sections, dorsal is up.

ccdc80-l1 knocked-down embryos displayed impaired motility

To determine the functional role of *ccdc80-l1* during zebrafish development, we specifically knocked it down by means of the injection of an antisense oligonucleotide morpholino (*ccdc80-l1*-MO, Gene Tools) designed against the start site of the transcript. In all the experiments, *ccdc80-l1*-MO-injected embryos (morphants) were compared to embryos at the same developmental stage, injected with the same amount of a control MO (ctrl-MO). For the

in vivo test of the efficiency of *ccdc80-l1*-MO, 425 pg/embryo of the pCS2+-*ccdc80-l1*-GFP sensor plasmid has been injected alone or with 12 ng/embryo of *ccdc80-l1*-MO. The presence/absence of the GFP signal has been monitored under a fluorescent microscope starting from somitogenesis up to 48 hpf (Suppl. Fig. S2). 70% of the embryos (N=20) injected with the sensor plasmid alone displayed fluorescence. This percentage decreased to 51% when the plasmid was co-injected with *ccdc80-l1*-MO (N=93), indicating that the morpholino specifically bound to its target region. The efficiency of *ccdc80-l1* loss-of-function was not so striking, as demonstated by the low percentage of embryos with GFP decreasement and by the high amount of morpholino we had to inject to obtain a phenotype (8 and 12 ng/embryo of *ccdc80-l1*-MO). Therefore, we designed a second morpholino against the splice site (*ccdc80-l1*-splice-MO) to confirm the specificity of *ccdc80-l1*-loss-of-function. Embryos injected with this second morpholino, still exhibited motility issues as *ccdc80-l1*-MO-injected embryos did (data not shown). In particular, all the knocked-down embryos showed no severe body plan alteration when observed *in vivo*, indicating the proper progression of early developmental processes such as gastrulation and segmentation [38,39,40,41]. Moreover, we observed that morphants displayed physiological body contractions upon dechorionation at 24 hpf [42]. However, at 48 hpf, almost 80% of the morphant embryos (N=37) presented abnormal escaping behavior after tactile stimulation, often resulting in body contractions on the spot or circling behavior rather than a fast escape in the opposite direction to the stimulus (Supplementary Video S1-S2). The same phenotype was observed also at 5 days post fertilization (5 dpf, data not shown). These results indicated that *ccdc80-l1* loss-of-function affects the swimming behavior of zebrafish embryos and larvae. We were also able to rescue the *ccdc80-l1*-loss-of-function phenotype by means of the injection of the homolog *ccdc80*-full-length transcript. In fact, despite we demonstrated that *ccdc80*-loss-of-function did not affect axonal pathfinding (data not shown), the high degree of conservation between the two homologs allowed rescue of motility (only 42% of rescued embryos presented motility issues in comparison to the nearly 80% of *ccdc80-l1*-MO injected embryos, N=63)

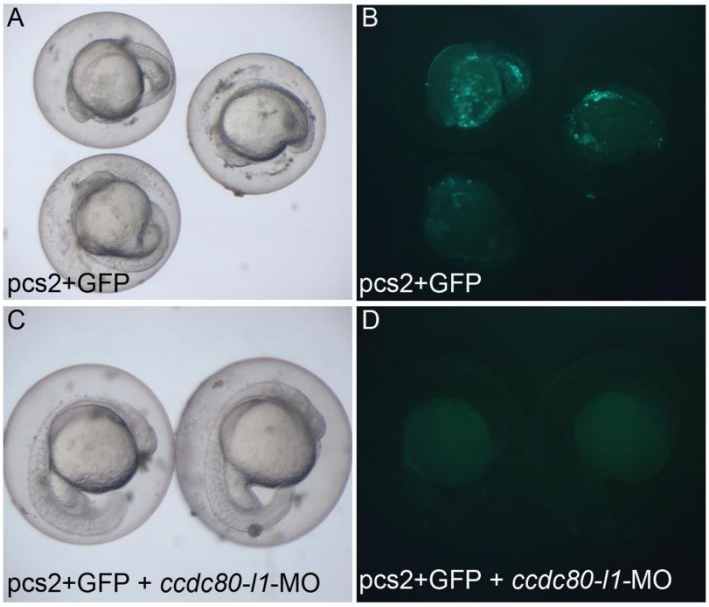

Supplementary Figure S2: *ccdc80-l1* morpholino is capable to inhibit the expression of the fluorescent protein GFP. This assay was performed in order to verify the *in vivo* efficiency of *ccdc80-l1*-MO. *(A, B)* In the 70% of embryos injected with the *ccdc80-l1*-GFP sensor plasmid, the presence of fluorescent GFP signal was detected (N= 20). *(C, D)* When the plasmid was injected together with the morpholino, the transcription of GFP protein was inhibited and the percentage of fluorescent embryos decreased to 51% (N=93). In *A* and *C* embryos are visualized under normal light, in *B* and *D* under fluorescent light.

ccdc80-l1 loss of function does not affect somitogenesis nor muscle pioneers and adaxial cells formation

To assess whether the phenotype displayed by morphants was due to the impairment of musculature, we examined somitogenesis and myogenesis markers. The expression of *myod* and *myog* [39,43] was not altered in *ccdc80-l1*-MO-injected embryos (Fig. 3A-D). Moreover, the expression of *smyhc1*, a marker of slow-twitch fibers [44], was unaffected as well, notwithstanding the strong expression of *ccdc80-l1* in adaxial cells and muscle pioneers, from which slow fibers develop [9] (Suppl. Fig. S3A, S3B). In addition, at 24 hpf, myofibers were correctly organized and distributed as shown by the immunohistochemistry with anti-sarcomeric MF20 antibody [45] (Fig. 3E, 3F). Also muscle pioneers, labeled with 4D9 anti-engrailed antibody [36,37] were correctly formed in *ccdc80-l1* morphants (Fig. 3G-H). These results led us to exclude that defects of adaxial cells, muscle pioneers or body musculature formation were responsible for motility issues observed in *ccdc80-l1* knocked-down embryos.

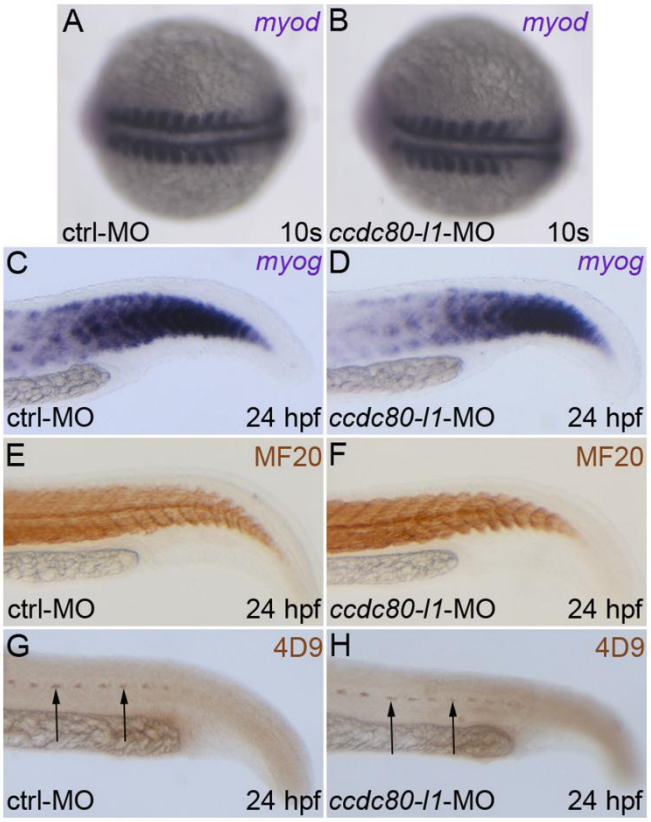

Figure 3: Analysis of myogenic markers expression and muscle pioneers in *ccdc80-l1* morphant embryos. *(A-D)* The myogenic markers *myod (A, B)* and *myog (C, D)* were correctly expressed both in control and morphants embryos at 10 s stage *(A, B)* and 24 hpf *(C, D)*, respectively. *(E, F)* The MF20 antibody staining showed that both slow and fast twitch fibers were correctly formed and distributed in control and in knocked-down embryos at 24 hpf. *(G, H)* At the same developmental stage, muscle pioneers resulted unaffected after *ccdc80-l1* loss-of-function, as shown by the labeling with 4D9 antibody (anti-engrailed) (arrows). *(A, B)* Dorsal views, anterior is left; *(C-H)* lateral views of the tails, dorsal is up and anterior is left.

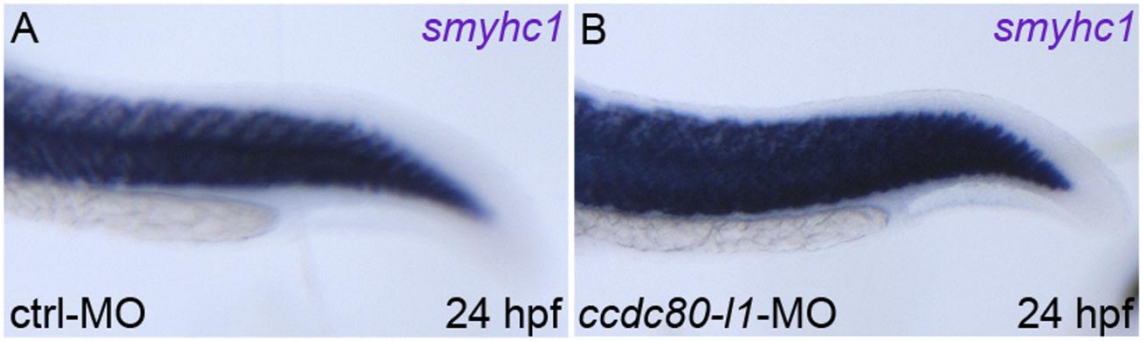

Supplementary Figure S3: The expression pattern of the slow-myosin marker *smyhc1* is unaffected in *ccdc80-l1* knocked-down embryos. *(A, B)* Loss-of-*ccdc80-l1*-function did not perturb the expression of *smyhc1*, as morphant embryos *(B)* are indistinguishable from control embryos *(A)*. Lateral views of the tails, dorsal is up, anterior is left.

Proper pathfinding and branching of axons are affected in *ccdc80-l1*-MO-injected embryos

Segmentally repeated motoneurons connect nervous system to somites, as their growth cones exit the spinal cord during embryogenesis and migrate to their appropriate muscle targets, allowing movement [3,5]. Due to motility impairment of *ccdc80-l1* morphants, we investigated the morphology of motoneurons performing immunohistochemistry with znp1 (*syt2b*) antibody [46]. For all embryos, we analyzed the trunk region overhanging the yolk extension; defects in at least three motoneurons were enough to consider the embryo as affected. At 48 hpf, in the 84% (N=33) of morphants injected with 12 ng/embryo of morpholino, axonal pathfinding resulted impaired. 60% of morphants displayed an overall disorganization of both dorsal and ventral motoneurons, that resulted mis-orientated and over-branched (Fig. 4A, 4B). In the 9% of embryos, these defects were observed together with an opposite phenomenon, axonal stalling. In the 12% of morphants only ventral axons resulted mis-orientated and over-branched, whereas in the 3% only the dorsal ones were affected. This phenotype was dose-dependent: when 8 ng/embryo of morpholino were used, a lower percentage of embryos resulted affected (64%, N=35). Interestingly, at this concentration, only 27% of the knocked-down embryos displayed both ventral and dorsal defective axons, whereas in the 37% of morphants the same defects were detectable in the ventral motoneurons solely (Fig. 4C). Dorsal axons alone were never affected (Tab. 2 and Suppl. Fig. S4). Thus, a striking reduction of Ccdc80-l1 protein amount led to the affection of both ventral and dorsal motoneurons, whereas a lower dose of morpholino is sufficient for ventral axons migration impairment. In order to discriminate whereas loss-of-*ccdc80-l1*-function impaired PMNs or SMNs, we analyzed the phenotype of morphants also at 26 hpf and 30 hpf, by the time SMNs have just begun extending axons [47], so most of znp1 labeling correspond to PMNs. At this stages, we replicated the same phenotype observed at 48 hpf (Fig. 4D-G and Tab. 3). Furthermore, by performing an immunohistochemistry at 48 hpf using the specific antibody for SMNs (zn-5, anti-*alcama*) [47], we observed that also SMNs axons seems to be affected after loss-of-*ccdc80-l1*-function (Fig. 4H, 4I). Thus, the analysis of the motoneuronal patterning in morphant embryos revealed the lack of proper guidance toward muscle targets , suggesting *ccdc80-l1* involvement in axonal pathfinding of both PMNs and SMNs.

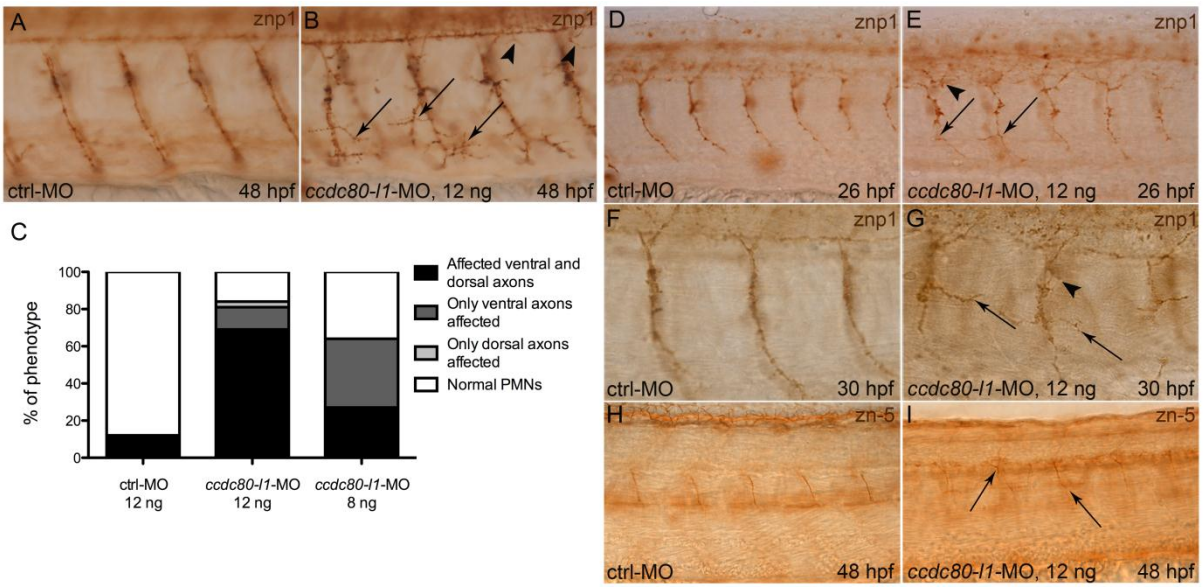

Figure 4: Analysis of motoneurons morphology by means of znp1- and zn-5-immunohistochemistry. *(A, B)* At 48 hpf, using 12 ng/embryo of morpholino, both ventral (arrows) and dorsal axons (arrowheads) were mis-orientated and over-branched in morphants *(B)* in comparison to control embryos *(A)*. *(C)* Statistical analysis showing the percentages of the different phenotypes (affected ventral axons, dorsal axons or both) occurring in control embryos and in morphants, when different doses of *ccdc80-l1*-MO were injected (12 ng/embryo and 8 ng/embryo). Using a lower dose of morpholino (8 ng/embryo), we observed that in a significant percentage of embryos only ventral axons were defective. *(D-G)* Immunohistochemistry performed at 26 hpf *(D, E)* and 30 hpf *(F, G)* confirmed that loss-of-*ccdc80-l1*-function affects both CaPs (arrows) and MiPs (arrowheads) axonal migration. *(H, I)* The same analysis performed at 48 hpf using zn-5 antibody revealed that also SMNs axonal migration is impaired in morphants (arrows in *I*) in comparison to control embryos *(H)*. *(A, B; D-I)* Lateral flat-mount preparation was applied for a better visualization of the motoneurons. Lateral views of the trunk region overhanging the yolk extension, dorsal is up and anterior is left.

Dose/type of morpholino	Total percentage of affected embryos (N)	Alteration of both ventral and dorsal axons	Only defective ventral axons	Only defective dorsal axons
ctrl-MO 12 ng	12% (N=25)	12%	0%	0%
ccdc80-l1-MO 12 ng	84% (N=33)	69%	12%	3%
ccdc80-l1-MO 8 ng	64% (N=35)	27%	37%	0%

Table 2: The phenotype of *ccdc80-l1*-MO-injected embryos is dose-dependent. The percentage of embryos displaying axonal defects decreased from 84% to 64% when a lower dose of morpholino was used. Both ventral and dorsal axonal pathfinding resulted impaired in the 69% of affected embryos when 12 ng/embryo of morpholino were used. After the injection of the lower dose of *ccdc80-l1*-MO (8 ng/embryo), 27% of affected embryos showed alteration of both ventral and dorsal axons, whereas the 37% displayed only ventral defective axons and dorsal axons alone were never affected.

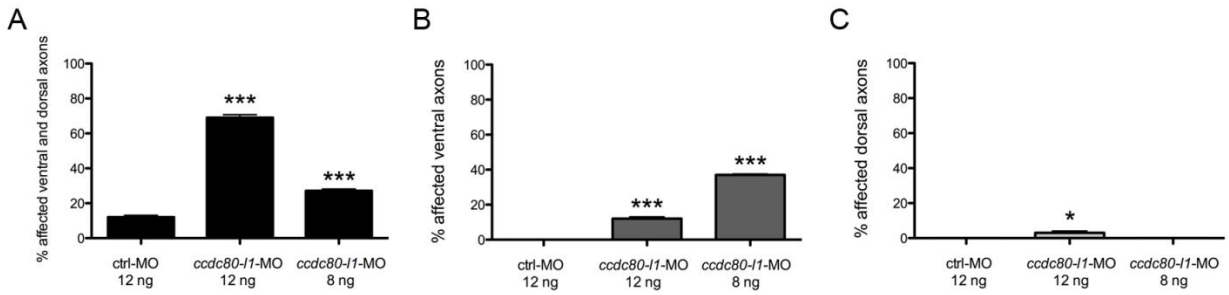

Supplementary Figure S4: Statistical analysis of three distinct defects observed after loss-of-*ccdc80-l1*-function. *(A-C)* The graphics show the occurrence of three axonal migration defects in control embryos and morphants when two doses of *ccdc80-l1*-MO are used: both dorsal and ventral defective axons *(A)*, only ventral defective axons *(B)* and only dorsal defective axons *(C)*. The last phenotype was not statistically significant. *** p<0.001 vs ctrl-MO. * p<0.05 vs ctrl-MO.

Developmental stage/dose of morpholino	Total percentage of affected embryos (N)	Alteration of both CaPs and MiPs	Only CaPs affected	Only MiPs affected
26hpf/*ccdc80-l1*-MO 12 ng	54,5% (N=33)	40%	11%	3,5%
30hpf/*ccdc80-l1*-MO 12 ng	62% (N=35)	33%	24,5%	4,5%

Table 3: Loss-of-*ccdc80-l1*-function impairs PMNs axonal migration. Embryos injected with 12 ng/embryo of *ccdc80-l1*-MO were observed also at 26 hpf and 30 hpf. At these stages, affected embryos were 54,5% and 62%, respectively. The percentages of the different phenotypes are listed.

ccdc80-l1 expression is positively regulated by the Hedgehog pathway

Both muscle and motoneurons induction is finely regulated by levels and range of *shh* expression [9,48,49]. Due to *ccdc80-l1* expression in adaxial cells and muscle pioneers, we decided to investigate the existence of a *ccdc80-l1* up-stream regulation Hedgehog-mediated. We modulated *shh* activity by exposing embryos to cyclopamine, that inhibits the *Hedgehog* transducer Smoothened (smo) [9,50]. To avoid the complete loss of the territories in which *ccdc80-l1* is expressed, we chose a concentration of cyclopamine (5 μM) by which muscle pioneers and adaxial cells-derived slow fibers are unaffected, as already described [9] and as we demonstrated by the proper expression of their markers engrailed, *myod* and *smyhc1* respectively. (Suppl. Fig. S5). A striking down-regulation of *ccdc80-l1* expression was observed in 72% of the treated embryos in comparison to controls (N=32) (Fig. 5A, 5B). Interestingly, this down-regulation was detectable only at the level of myoseptum and somites, whereas the cephalic territories in which *ccdc80-l1* is expressed were not involved. A

similar down-regulation was observed in *syu* mutants, carriers of a deletion in the gene *sonic-you* encoding for *shh* (Fig. 5D-F) [16]. *ccdc80-l1* signal in adaxial cells was extremely weak or absent in the 35% of mutants, and slightly down-regulated in the 40% of observed embryos (N=20). Moreover, the overexpression of *shh* by means of the injection of the full-length transcript (300 pg/embryo), led to the opposite phenotype with an increasing of *ccdc80-l1* expression in the somites of the 71% of the injected embryos (N=31) (Fig. 5C). On the contrary, *ccdc80-l1* loss-of-function did not affect *shh* expression (Suppl. Fig. S6). Therefore, these findings suggest that *ccdc80-l1* is a down-stream target of the Hedgehog pathway.

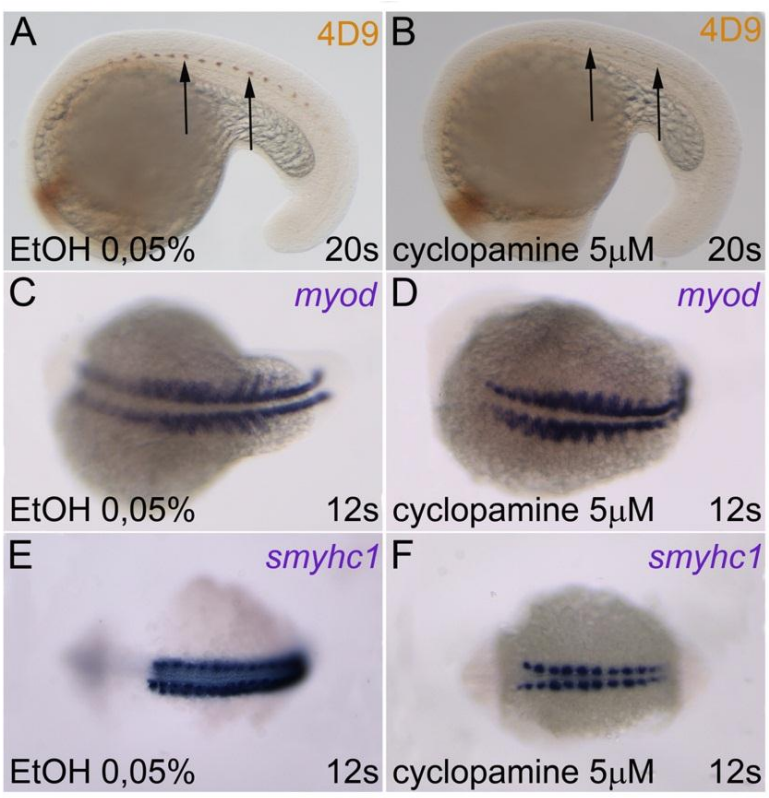

Supplementary Figure S5: Muscle pioneers and adaxial cells are present after 5µM cyclopamine treatment. *(A, B)* Labeling with 4D9 antibody (anti-engrailed) showed that muscle pioneers are not missing after pharmacological inhibition of the Hedgehog pathway (arrows). *(C-F)* Also adaxial cells are still present, as shown by the expression of the markers *myod (C, D)* and *smyhc1 (E, F)*. *(A, B)* Lateral views, dorsal is up. *(C-F)* Dorsal views, anterior is left.

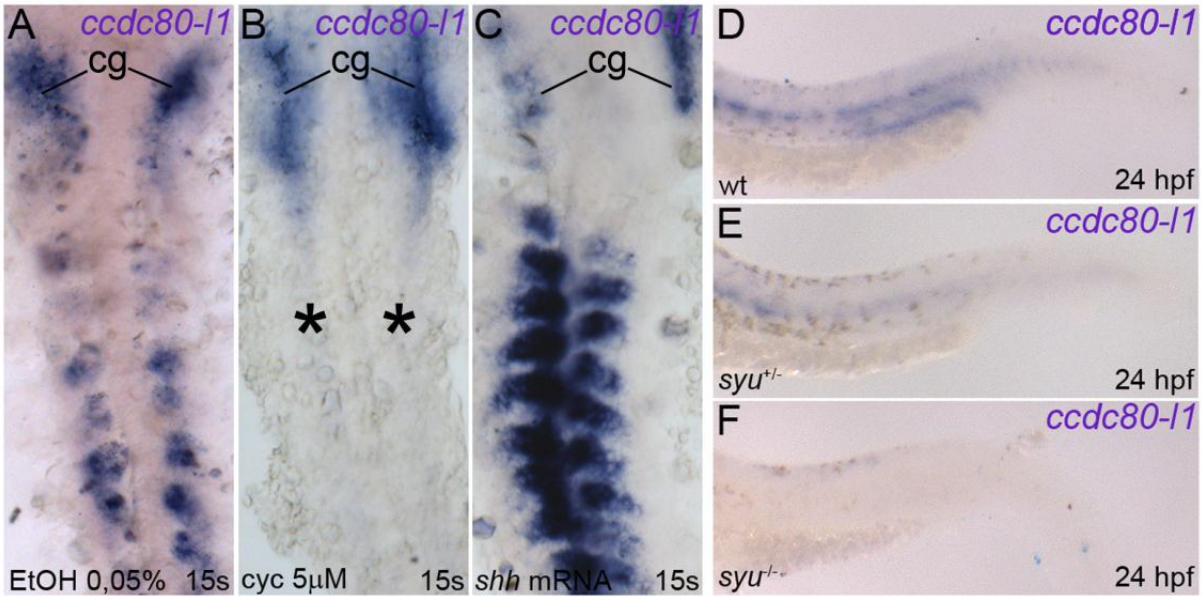

Figure 5: *ccdc80-l1* is positively regulated by *shh*. *(A-C) ccdc80-l1* expression in somites and myoseptum resulted strongly inhibited in embryos treated with 5 µM cyclopamine (asterisks in *B*), in comparison to control embryos at the same developmental stage *(A)*. By converse, over-expression of *shh* led to an up-regulation of *ccdc80-l1* in muscular territories *(C)*. Expression in cranial ganglia (cg) was never perturbed. *(D-F) ccdc80-l1* resulted slightly down-regulated in the muscles of heterozygous *syu*$^{+/-}$ mutants *(E)* in comparison to wild type siblings *(D)*. A strikingly down-regulation was observed in homozygous *syu*$^{-/-}$ mutants *(F)*. *(A-C)* Dorsal flat-mount preparations, anterior is up. *(D-F)* Lateral views of the tails, anterior is left.

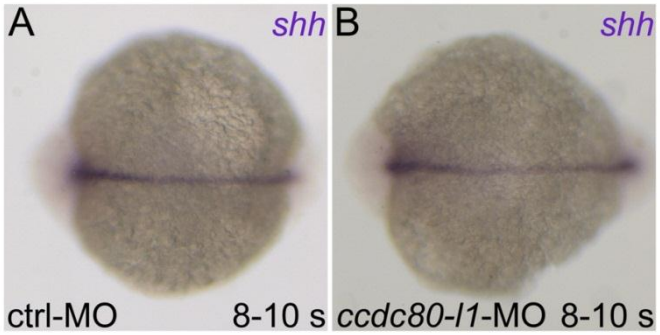

Supplementary Figure S6: *shh* expression is not perturbed by loss-of-*ccdc80-l1*-function. *(A, B) shh* resulted correctly expressed both in control embryos *(A)* and in morphants *(B)*. *(A, B)* Dorsal views, anterior is left.

Discussion

The genetic program underlying axon guidance is not completely defined. Adaxial cells and muscle pioneers are both involved in axonal outgrowth and pathfinding [7,17], even if little is known about the specific proteins and molecular mechanisms acting in this process. *ccdc80-l1*, the novel gene we recently identified in zebrafish, is expressed during embryonic

development in muscle pioneers and adaxial cells. Ccdc80-l1 was identified, together with its homolog Ccdc80, on the basis of its high aminoacid identity with human CCDC80. However, zebrafish *ccdc80* and *ccdc80-l1* do not share the same expression pattern and seems to play different roles. In fact, only *ccdc80-l1*-MO-injected embryos displayed an abnormal escaping behavior after tactile stimulation at 48 hpf. Both musculature and nervous system are responsible for embryonic motility and touch response and are the basis of spontaneous motor output that occurs in the developing zebrafish embryo ever since 18 hpf [2]. Nevertheless, musculature defects were unlikely the basis of the observed phenotype. Indeed, there was no difference between the expression pattern of myogenic markers in morphants and control embryos. Moreover, muscle fibers resulted correctly formed and distributed by the end of somitogenesis. The territories in which *ccdc80-l1* is expressed were unaffected as well: in fact, adaxial cells and muscle pioneers showed no defects. These findings revealed that *ccdc80-l1* function is not necessary for the specification and further differentiation of myogenic cell populations, suggesting that the motility issues displayed by morphants at 48 hpf could be due to an impairment of neuronal development.

The analysis of motoneuronal development in morphant embryos revealed that *ccdc80-l1* plays a role in motoneurons axonal pathfinding. In fact, *ccdc80-l1* loss-of-function did not prevent the formation of PMNs and axon projection, but led to an overall disorganization of PMNs. CaPs and MiPs resulted over-branched in a high percentage of embryos, whereas a smaller fraction of morphants displayed also the simultaneous presence of its opposite phenomenon, axonal stalling. Axonal over-branching and stalling were detected in the CaPs solely in a significant percentage of embryos, especially when a lower dose of morpholino was used. Moreover, the impairment of axonal migration was more severe in CaPs then in MiPs, even when both PMNs were affected simultaneously. These data suggest that *ccdc80-l1* may have a differential role as regards the development of CaPs and MiPs. This is consistent with the asymmetric distribution of *ccdc80-l1* transcript in the somites: indeed, the *ccdc80-l1* transcript is present in the ventral portion of somites, innervated by CaPs, and not in their dorsal portion, innervated by MiPs. The same motility issues displayed at 48 hpf were observed also at 5 dpf, when secondary motoneurons are already formed. Therefore, *ccdc80-l1* plays a role also in guidance of SMNs, as shown by the mis-expression of their marker zn-5. This is not surprising, as the growth cones of SMNs require the axons of PMNs for proper pathfinding [6]. We concluded that the *ccdc80-l1* loss-of-function prevents the proper development of the peripheral nervous system, that lacks a proper guidance toward muscle target: axons do not fallow a single direction-pathway but stall or extend towards any direction, leading to an over-branched and non-functional nervous network. Hence, embryos

are able to move and to respond to tactile stimuli, but the coordination of muscle contractions is impaired, and motor behavior is affected.

Axon outgrowth is influenced by many factors, for instance different molecules (netrins, semaphorins, slits) with chemotropic functions (reviewed in [51]) and components of the extracellular matrix (ECM) [52,53]. In fact, the growth cone shares many features with the motile structures of migrating cells, including actin polymerization at the leading edge, dynamic interactions between cell-surface adhesion receptors and components of the extracellular matrix (ECM), and generation of traction forces in the cytoskeleton applied to ECM through adhesion sites [54,55]. In *ccdc80-l1* knocked-down embryos, the growth cones are still able to exit the spinal cord and reach the muscle pioneers along the common pathway. Moreover, axonal extensions developed without altering the target choice: in fact, CaPs and MiPs still project their axons ventrally and dorsally, respectively. These data are consistent with the proper development of muscle pioneers, which provide a choice point for motor growth cones. However, further defects occur during axon pathfinding. It has been recently reported that DRO1/CCDC80 is a Golgi-associated-protein [56]. Moreover, the *in silico* prediction of the Ccdc80 protein structure (String 9.0) suggests its interaction with fibronectin, a component of the ECM. If this is the case also for its homolog *ccdc80-l1*, its loss-of-function might interfere with the proper axon migration by influencing the secretion of guidance molecules or by altering interactions with ECM proteins such as fibronectin. Further analysis on the predicted Ccdc80-l1 protein sequence and its interaction with other proteins will be necessary to understand the molecular process underlying *ccdc80-l1* functioning. Moreover, investigation on possible targets is still needed. For instance, it is to explore the possibility of an interaction with the semaphorin and netrin families, both involved in attracting and/or repelling growth cones from a variety of organisms [13,19]. Nevertheless, our results provide further insights into motoneurons development, a complex mechanism that requires the action of several different molecules. Moreover, we suggest that *ccdc80-l1* may act as a down-stream effector of *shh*. The Hedgehog family consists of secreted morphogens fundamental for both axon guidance and formation of adaxial cells and muscle pioneers [9,57]. The Hedgehog signaling is known to play a pivotal role in the specification of both primary and secondary motoneurons [14,49]. Indeed, mutants for different molecules involved in this pathway displayed axonal defects, including random axonal migration or stalling [15,16]. PMNs target choice was never impaired after *ccdc80-l1* loss-of-function, still axonal migration resulted aberrant. Furthermore, *ccdc80-l1* expression resulted strikingly down-regulated after exposure to 5 μM of cyclopamine and up-regulated after over-expression of *shh*. This modulation was observed only in muscles and not in other territories

in which *s-ccc80* is expressed (cranial ganglia and dorsal dermis). These findings strongly suggest the existence of a specific regulation Hedgehog-mediated of *ccdc80-l1,* as regards its function in motoneuronal development. Moreover, these findings may shed light on the involvement of the Hedgehog pathway in this process.

Author Contributions

Conceived and designed the experiments: CB AP FC. Performed the experiments: CB AP AF. Analyzed the data: CB AP FC. Wrote the paper: CB AP. Contributed to experimental design: IDN FS. Provided helpful suggestions and supervised the paper drafting: IDN FS. Supervised the research project and supervised paper drafting: FC.

Acknowledgments

We thank P. Ingham and S. Elworthy for providing the *smych1* plasmid; P. Sordino for the *shh* full-length construct and for the zn-5 antibody and E. Foglia for statistical analysis.

References

1. Beattie CE (2000) Control of motor axon guidance in the zebrafish embryo. Brain Res Bull 53: 489-500.
2. Menelaou E, Husbands EE, Pollet RG, Coutts CA, Ali DW, et al. (2008) Embryonic motor activity and implications for regulating motoneuron axonal pathfinding in zebrafish. Eur J Neurosci 28: 1080-1096.
3. Eisen JS (1999) Patterning motoneurons in the vertebrate nervous system. Trends Neurosci 22: 321-326.
4. Liu DW, Westerfield M (1990) The formation of terminal fields in the absence of competitive interactions among primary motoneurons in the zebrafish. J Neurosci 10: 3947-3959.
5. Westerfield M, McMurray JV, Eisen JS (1986) Identified motoneurons and their innervation of axial muscles in the zebrafish. J Neurosci 6: 2267-2277.
6. Eisen JS (1991) Motoneuronal development in the embryonic zebrafish. Development Suppl 2: 141-147.
7. Melancon E, Liu DW, Westerfield M, Eisen JS (1997) Pathfinding by identified zebrafish motoneurons in the absence of muscle pioneers. J Neurosci 17: 7796-7804.
8. Felsenfeld AL, Curry M, Kimmel CB (1991) The fub-1 mutation blocks initial myofibril formation in zebrafish muscle pioneer cells. Dev Biol 148: 23-30.

9. Wolff C, Roy S, Ingham PW (2003) Multiple muscle cell identities induced by distinct levels and timing of hedgehog activity in the zebrafish embryo. Curr Biol 13: 1169-1181.

10. Sato-Maeda M, Tawarayama H, Obinata M, Kuwada JY, Shoji W (2006) Sema3a1 guides spinal motor axons in a cell- and stage-specific manner in zebrafish. Development 133: 937-947.

11. Myers PZ, Eisen JS, Westerfield M (1986) Development and axonal outgrowth of identified motoneurons in the zebrafish. J Neurosci 6: 2278-2289.

12. Pike SH, Melancon EF, Eisen JS (1992) Pathfinding by zebrafish motoneurons in the absence of normal pioneer axons. Development 114: 825-831.

13. Tessier-Lavigne M, Goodman CS (1996) The molecular biology of axon guidance. Science 274: 1123-1133.

14. Beattie CE, Hatta K, Halpern ME, Liu H, Eisen JS, et al. (1997) Temporal separation in the specification of primary and secondary motoneurons in zebrafish. Dev Biol 187: 171-182.

15. Chen W, Burgess S, Hopkins N (2001) Analysis of the zebrafish smoothened mutant reveals conserved and divergent functions of hedgehog activity. Development 128: 2385-2396.

16. Schauerte HE, van Eeden FJ, Fricke C, Odenthal J, Strahle U, et al. (1998) Sonic hedgehog is not required for the induction of medial floor plate cells in the zebrafish. Development 125: 2983-2993.

17. Zeller J, Granato M (1999) The zebrafish diwanka gene controls an early step of motor growth cone migration. Development 126: 3461-3472.

18. Roos M, Schachner M, Bernhardt RR (1999) Zebrafish semaphorin Z1b inhibits growing motor axons in vivo. Mech Dev 87: 103-117.

19. Lauderdale JD, Davis NM, Kuwada JY (1997) Axon tracts correlate with netrin-1a expression in the zebrafish embryo. Mol Cell Neurosci 9: 293-313.

20. Aoki K, Sun YJ, Aoki S, Wada K, Wada E (2002) Cloning, expression, and mapping of a gene that is upregulated in adipose tissue of mice deficient in bombesin receptor subtype-3. Biochem Biophys Res Commun 290: 1282-1288.

21. Tremblay F, Revett T, Huard C, Zhang Y, Tobin JF, et al. (2009) Bidirectional modulation of adipogenesis by the secreted protein Ccdc80/DRO1/URB. J Biol Chem 284: 8136-8147.

22. Liu Y, Monticone M, Tonachini L, Mastrogiacomo M, Marigo V, et al. (2004) URB expression in human bone marrow stromal cells and during mouse development. Biochem Biophys Res Commun 322: 497-507.

23. Haslett JN, Sanoudou D, Kho AT, Han M, Bennett RR, et al. (2003) Gene expression profiling of Duchenne muscular dystrophy skeletal muscle. Neurogenetics 4: 163-171.

24. Tseng BS, Zhao P, Pattison JS, Gordon SE, Granchelli JA, et al. (2002) Regenerated mdx mouse skeletal muscle shows differential mRNA expression. J Appl Physiol 93: 537-545.

25. Visconti R, Schepis F, Iuliano R, Pierantoni GM, Zhang L, et al. (2003) Cloning and molecular characterization of a novel gene strongly induced by the adenovirus E1A gene in rat thyroid cells. Oncogene 22: 1087-1097.

26. Bommer GT, Jager C, Durr EM, Baehs S, Eichhorst ST, et al. (2005) DRO1, a gene down-regulated by oncogenes, mediates growth inhibition in colon and pancreatic cancer cells. J Biol Chem 280: 7962-7975.

27. Pawlowski K, Muszewska A, Lenart A, Szczepinska T, Godzik A, et al. A widespread peroxiredoxin-like domain present in tumor suppression- and progression-implicated proteins. BMC Genomics 11: 590.

28. Westerfield M, editor (2000) The Zebrafish Book. A guide for the laboratory use of zebrafish (Danio rerio): Eugene: University of Oregon Press.

29. Kimmel CB, Ballard WW, Kimmel SR, Ullmann B, Schilling TF (1995) Stages of embryonic development of the zebrafish. Dev Dyn 203: 253-310.

30. Haffter P, Nusslein-Volhard C (1996) Large scale genetics in a small vertebrate, the zebrafish. Int J Dev Biol 40: 221-227.

31. Thisse C, Thisse B, Schilling TF, Postlethwait JH (1993) Structure of the zebrafish snail1 gene and its expression in wild-type, spadetail and no tail mutant embryos. Development 119: 1203-1215.

32. Jowett T, Lettice L (1994) Whole-mount in situ hybridizations on zebrafish embryos using a mixture of digoxigenin- and fluorescein-labelled probes. Trends Genet 10: 73-74.

33. Schnapp E, Pistocchi AS, Karampetsou E, Foglia E, Lamia CL, et al. (2009) Induced early expression of mrf4 but not myog rescues myogenesis in the myod/myf5 double-morphant zebrafish embryo. J Cell Sci 122: 481-488.

34. Nasevicius A, Ekker SC (2000) Effective targeted gene 'knockdown' in zebrafish. Nat Genet 26: 216-220.

35. Devoto SH, Melancon E, Eisen JS, Westerfield M (1996) Identification of separate slow and fast muscle precursor cells in vivo, prior to somite formation. Development 122: 3371-3380.

36. Hatta K, Bremiller R, Westerfield M, Kimmel CB (1991) Diversity of expression of engrailed-like antigens in zebrafish. Development 112: 821-832.

37. Patel NH, Martin-Blanco E, Coleman KG, Poole SJ, Ellis MC, et al. (1989) Expression of engrailed proteins in arthropods, annelids, and chordates. Cell 58: 955-968.

38. Griffin K, Patient R, Holder N (1995) Analysis of FGF function in normal and no tail zebrafish embryos reveals separate mechanisms for formation of the trunk and the tail. Development 121: 2983-2994.

39. Holley SA (2007) The genetics and embryology of zebrafish metamerism. Dev Dyn 236: 1422-1449.

40. Melby AE, Warga RM, Kimmel CB (1996) Specification of cell fates at the dorsal margin of the zebrafish gastrula. Development 122: 2225-2237.

41. Stickney HL, Barresi MJ, Devoto SH (2000) Somite development in zebrafish. Dev Dyn 219: 287-303.

42. Saint-Amant L, Drapeau P (1998) Time course of the development of motor behaviors in the zebrafish embryo. J Neurobiol 37: 622-632.

43. Rescan PY (2001) Regulation and functions of myogenic regulatory factors in lower vertebrates. Comp Biochem Physiol B Biochem Mol Biol 130: 1-12.

44. Elworthy S, Hargrave M, Knight R, Mebus K, Ingham PW (2008) Expression of multiple slow myosin heavy chain genes reveals a diversity of zebrafish slow twitch muscle fibres with differing requirements for Hedgehog and Prdm1 activity. Development 135: 2115-2126.

45. Bader D, Masaki T, Fischman DA (1982) Immunochemical analysis of myosin heavy chain during avian myogenesis in vivo and in vitro. J Cell Biol 95: 763-770.

46. Trevarrow B, Marks DL, Kimmel CB (1990) Organization of hindbrain segments in the zebrafish embryo. Neuron 4: 669-679.

47. Fashena D, Westerfield M (1999) Secondary motoneuron axons localize DM-GRASP on their fasciculated segments. J Comp Neurol 406: 415-424.

48. Blagden CS, Currie PD, Ingham PW, Hughes SM (1997) Notochord induction of zebrafish slow muscle mediated by Sonic hedgehog. Genes Dev 11: 2163-2175.

49. Lewis KE, Eisen JS (2001) Hedgehog signaling is required for primary motoneuron induction in zebrafish. Development 128: 3485-3495.

50. Barresi MJ, D'Angelo JA, Hernandez LP, Devoto SH (2001) Distinct mechanisms regulate slow-muscle development. Curr Biol 11: 1432-1438.

51. de Castro F (2003) Chemotropic molecules: guides for axonal pathfinding and cell migration during CNS development. News Physiol Sci 18: 130-136.

52. Gomez TM, Letourneau PC (1994) Filopodia initiate choices made by sensory neuron growth cones at laminin/fibronectin borders in vitro. J Neurosci 14: 5959-5972.

53. McKerracher L, Chamoux M, Arregui CO (1996) Role of laminin and integrin interactions in growth cone guidance. Mol Neurobiol 12: 95-116.

54. Hynes RO, Lander AD (1992) Contact and adhesive specificities in the associations, migrations, and targeting of cells and axons. Cell 68: 303-322.

55. Lauffenburger DA, Horwitz AF (1996) Cell migration: a physically integrated molecular process. Cell 84: 359-369.

56. Ferragud J, Avivar-Valderas A, Pla A, De Las Rivas J, de Mora JF Transcriptional repression of the tumor suppressor DRO1 by AIB1. FEBS Lett 585: 3041-3046.

57. Charron F, Tessier-Lavigne M (2005) Novel brain wiring functions for classical morphogens: a role as graded positional cues in axon guidance. Development 132: 2251-2262.

Part III

Appendix

EMBRYONIC DEVELOPMENT OF ZEBRAFISH

The zebrafish eggs are small (400-500 μm), with a very large yolk mass. After the fertilization, several cytoplasmic rearrangements occur, and these events lead to the segregation of the cytoplasm to the animal pole, and the yolk mass to the vegetal pole. The segmentation (cleavage) is meroblastic and relative to the cytoplasm of the animal pole only. In this way, the formation of the "blastula" is observed. The blastula starts the gastrulation period, which is characterized by different cellular movements. Kimmel *et al*., (1995), distinguished the following developmental stages: zygote period (0-$^{3}/_{4}$ hpf), cleavage period ($^{3}/_{4}$-$2^{1}/_{4}$ hpf), blastula period ($2^{1}/_{4}$-$5^{1}/_{4}$ hpf), gastrula period ($5^{1}/_{4}$-10 hpf), segmentation period (10-24 hpf), pharingula period (24-48 hpf) and hatching period (48-72 hpf).

Zygote Period

The newly fertilized egg is in the zygote period until the first cleavage occurs, about 40 minutes after fertilization. The chorion swells and lifts away from the newly fertilized egg. Fertilization also activates cytoplasmic movements, easily evident within about 10 minutes. Nonyolky cytoplasm begins to stream toward the animal pole, segregating the blastodisc from the clearer yolk granule-rich vegetal cytoplasm. This segregation continues during early cleavage stages.

Cleavage Period

After the first cleavage the blastomeres divide at about 15-minute intervals. The cytoplasmic divisions are meroblastic; they only incompletely undercut the blastodisc, and the blastomeres, or a specific subset of them according to the stage, remain interconnected by cytoplasmic bridges. The six cleavages that comprise this period frequently occur at regular orientations and are synchronous. The cleavage period ends at 64-cell stage (2 hpf).

Blastula Period

We use the term blastula to refer to the period when the blastodisc begins to look ball-like, at the 128-cell stage, or eight zygotic cell cycle, and until the time of onset of gastrulation, about cycle 14. Important processes occur during this blastula period;

the embryo enters midblastula transition (MBT), the yolk syncytial layer (YSL) forms, and epiboly begins. Epiboly continues during the gastrulation period. Three different phases can be observed.

-Early-blastula: the marginal blastomeres lie against the yolk cell and remain cytoplasmatically connected to it throughout cleavage. Beginning during cycle 10, the marginal cells undergo a collapse, releasing their cytoplasm and nuclei together into the immediately adjoining cytoplasm of the yolk cell and forming the Yolk Syncytial Layer (YSL). After the YSL forms, the enveloping layer cells (EVL) that were in the second blastodisc tier, now lie at the marginal position and they are nonsyncytial.

-Mid-blastula: the YSL nuclei continue to undergo mitotic divisions in the midblastula, but the nuclear divisions are unaccompanied by cytoplasmic ones, and the yolk remains uncleaved and syncytial. After about three cycles, and coinciding with the beginning of epiboly, the YSL divisions abruptly cease. The YSL nuclei now begin to enlarge, possibly meaning that they are actively transcribing RNA. The YSL, an organ unique to teleosts, may be extraembryonic, making no direct contribution to the body of the embryo. At first the YSL has the form of a narrow ring around the blastodisc edge, but soon it spreads underneath the blastodisc, forming a complete "internal" syncytium (I-YSL), that persists throughout embryogenesis. In this position, the I-YSL might be presumed to be playing a nutritive role. Another portion of it, the E-YSL, is transiently "external" to the blastodisc edge, and appears to be a major motor for epiboly.

-Late-blastula: epiboly beginning in the late blastula is the thinning and spreading of both the YSL and the blastodisc over the yolk cell. During the early stages of this morphogenetic movement the blastodisc thins considerably, changing from a high-piled cell mound to a cup-shaped cell multiplayer of nearly uniform thickness. This is accomplished by the streaming outward, toward the surface, of the deepest blastomeres. As they move, they mix fairly indiscriminately among more superficial cells along their way, except for the EVL and the marginal blastomeres. These nonmixing marginal blastomeres will give rise to the mesoderm, and suggest the existence of a pattern established during early development. At 30% epiboly stage,

the proper blastoderm begins to develop: it is uniform and formed by the EVL monolayer and a deep cells multilayer (Deep Enveloping Layer, DEL).

Gastrula Period

The beginning of involution defines the onset of gastrulation, and, so far as we have been able to tell, this occurs at 50%-epiboly. As a consequence, within minutes of reaching 50%-epiboly a thickened marginal region termed the "germ ring" appears, nearly simultaneously all around the blastoderm rim. Convergence movements then, nearly as rapidly, produce a local accumulation of cells at one position along the germ ring, the so-called embryonic shield. During these events, epiboly temporarily arrests, but after the shield forms, epiboly continues; the margin of the blastoderm advances around the yolk cell to cover it completely. The advance occurs at a nearly constant rate, over an additional 15% of the yolk cell each hour, and providing a useful staging index during most of gastrulation. Just as there was no blastocoele during the blastula period, there is no archenteron in the gastrula. Neither is there a blastopore; DEL cells involute at the blastoderm margin, which thus plays the role of the blastopore. Involution produces the germ ring by folding the blastoderm back upon itself. Hence, within the germ ring there are two germ layers: the upper, the epiblast, continues to feed cells into the lower, the hypoblast, throughout gastrulation. Between the two layers a fissure, termed "Brachet's cleft" is observed. Cells in the two layers are streaming in different directions. Except for the dorsal region, the epiblast cells generally stream toward the margin, and those reaching the margin move inward to enter the hypoblast. Then, as hypoblast cells, they stream away from the margin. The cells remaining in the epiblast when gastrulation ends correspond to the definitive ectoderm and will give rise to such tissues as epidermis, the central nervous system, neural crest, and sensory placodes. The hypoblast gives rise to derivatives classically ascribed to both the mesoderm and endoderm. At tail-bud stage (10 hpf), cell specifications processes are ending while cell differentiation mechanisms are turned on.

Segmentation Period

A wonderful variety of morphogenetic movements now occur, the somites develop, the rudiments of the primary organs become visible, the tail bud becomes more

prominent and the embryo elongates. The AP and DV axes are unambiguous. The first cells differentiate morphologically, and the first body movements appear. Somites develop sequentially in the trunk and tail, and provide the most useful staging index. Anterior somites develop first and posterior ones last. Pronephric kidneys appear bilaterally deep to the third somite pair. The notochord differentiates, also in an AP sequence. Some of its cells vacuolate and swell to become the structural elements of this organ, and others later form a notochord sheath, an epithelial monolayer that surrounds the organ. Endoderm develops on only the dorsal side of the embryo, beneath the axial and paraxial mesoderm. The epiblast, now exclusively ectodermal, undergoes extensive morphogenesis during the segmentation period. As gastrulation ends, the primordium of the central nervous system, the neural plate, is already fairly well delineated, because of its prominent thickness. The anterior region where the brain will form is particularly thick. Formation of the neural tube then occurs by a process known as "secondary neurulation". Secondary neurulation contrasts with "primary" neurulation, the version in vertebrates where a hollow tube forms from the neural plate by an uplifting and meeting together of neural folds. In teleosts the lumen of the neural tube, the neurocoele, forms by a late process of cavitation.

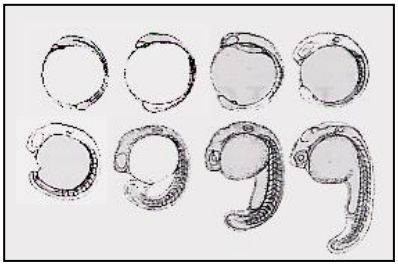

An intermediate and transient condensed primordium with no lumen, the neural keel, forms first. Because the times of neurulation and segmentation overlap so extensively the zebrafish does not have a distinct "neurula period" of development, such as occurs largely before segmentation in amphibian embryos.

Pharyngula Period

The pharyngula period (24-48 hpf) begins with the formation of the last somites (30/34 somites). At this time, the notochord is completely formed, and the brain is constituted by three lobes, which develop in an AP direction: forebrain, midbrain and hindbrain.

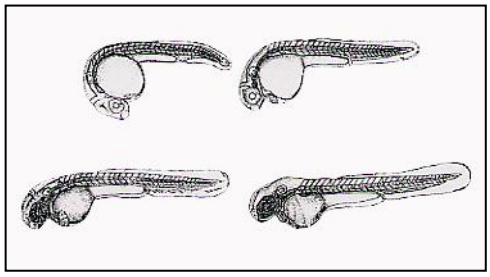

Hatching Period

During the last period, termed "hatching" (48-72 hpf), individuals within a single developing clutch hatch sporadically during the whole third day of development (at standard temperature), and occasionally later. At this time, we call these embryos "larvae"; morphogenesis of many organ rudiments is completing, and the embryo continues to grow at about the same rate.

Kimmel, C. B., Ballard, W. W., Kimmel, S. R., Ullmann, B. and Schilling, T. F. (1995). Stages of embryonic development of the zebrafish. *Dev Dyn* **203**, 253-310.